# TEMPERATURE DISTRIBUTION IN THIN PLATES WELDED UNDERWATER

James Andrews Staub

# TEMPERATURE DISTRIBUTION IN THIN PLATES WELDED UNDERWATER

by

JAMES ANDREW STAUB, JR.

A.B. MATHEMATICS, ST. VINCENT COLLEGE
(1963)

B.S.M.E., PENNSYLVANIA STATE UNIVERSITY
(1964)

SUBMITTED IN PARTIAL FULFILLMENT OF THE
REQUIREMENTS FOR THE DEGREE OF
NAVAL ENGINEER AND THE DEGREE OF
MASTER OF SCIENCE IN MECHANICAL ENGINEERING
at the
MASSACHUSETTS INSTITUTE OF TECHNOLOGY

JUNE, 1971

SIGNATURE OF AUTH

CERTIFIED BY . .

. .

ACCEPTED BY. . .

COMMITTEE ON GRADUATE STUDENTS

# TEMPERATURE DISTRIBUTION IN THIN PLATES WELDED UNDERWATER

By

JAMES ANDREW STAUB, JR.

Submitted in partial fulfillment of the requirements for the degrees of Naval Engineer and Master of Science in Mechanical Engineering at the Massachusetts Institute of Technology, June, 1971.

## ABSTRACT

During underwater (wet) welding the metal within the heat-affected-zone experiences a rapid fluctuation in temperature which results in a loss of ductility and a susceptibility to stress-corrosion cracking. The object of this study was to develop and verify a model which would predict the temperature distribution such that the metallurgical and mechanical properties of the underwater weld could be determined.

The equation of heat flow in two-dimensions with source terms was converted to its finite difference equivalent and solved by successive iterations with a digital computer. The solution incorporated all non-linear terms in the original equation and accounted for the variation of the thermal properties of the metal with temperature. The interior boundary in the temperature field was found to have a definite shape which was a function of the important welding parameters. The shape function was correlated by experiment using methods established for normal surface welding. Heat losses were assumed to occur by boiling and radiation heat transfer.

The predicted and measured temperature distributions were compared. It was found that the model predicted peak temperatures with reasonable accuracy but that comparison of cooling curves showed considerable disagreement. Since the predicted cooling curve presented a sharper slope than the measured value it was considered that the assumption of conventional boiling heat transfer processes was invalid.

Thesis Advisor: Prof. K. Masubuchi
Title: Associate Professor of Naval Architecture and Marine Engineering

ACKNOWLEDGEMENTS

The research for this study was funded by the Office of the Supervisor of Salvage, United States Navy, and the author is grateful for their interest in the subject and for their financial support.

The author also wishes to thank Professors K. Masubuchi and L. Glicksman for their advice and sustaining encouragment, and Mr. Julius Ritter for providing the facilities of his welding laboratory at the Boston Naval Shipyard. Finally, the author is indebted to Dorothy Machan for her excellent typing of the final draft.

TABLE OF CONTENTS


I ACKNOWLEDGEMENTS. . . . . .1

II ABSTRACT. . . . . .2

III LIST OF FIGURES . . . . . .6

IV LIST OF SYMBOLS . . . . . .7

V CHAPTER I . . . . . .9

A. Underwater Welding: State-Of-The-Art . . . . . 10

B. Normal Surface Welding. . . . . 12

C. Boiling Heat Transfer . . . . . 15

D. Summary of Procedure . . . . . 17

VI CHAPTER II. . . . . 19

A. Equation of Heat Flow . . . . . 21

B. Finite Difference Solution. . . . . 24

C. Boundary Conditions . . . . . 26

D. Heat Losses . . . . . 40

E. Computational Technique.. . . . . 44

VII CHAPTER III . . . . . 48

A. Experimental Equipment. . . . . 48

B. Materials . . . . . 52

C. Experimental Procedure. . . . . 54

D. Data Reduction . . . . . 61

VIII CHAPTER IV . . . . . 63

A. Results . . . . . 63

B. Conclusions . . . . . 66

C. Recommendations For Future Study. . . . . 71

IX APPENDIX

1. Transforming Heat Flow Equation To Quasi-Steady State. . . . . .72
2. Calculation Of Values For Heat Transfer (Source) Terms. . . . . .74
3. Derivation Of Pool Boundary Equations . . . . . .78
4. Normalizing The Heat Flow Equation. . . . . .81
5. Heat Flow Equation In Finite Difference Form. . . . . .83
6. Notes On The Use Of The Computer Model. . . . . .85
7. Computer Model For Temperature Distribution During Underwater Welding . . . . . .89
8. Data Reduction Programs . . . . . 127
9. Experimental Data . . . . . 144

X BIBLIOGRAPHY. . . . . 158

## LIST OF FIGURES

1-1 CHARACTERISTIC BOILING CURVE . . . . . 16

2-1 POOL CONTOUR VARIABLES . . . . . 28

2-2 DEFINITION OF A 2-D POOL . . . . . 30

2-3 MAXIMUM LENGTH VS p FOR PLATE WELDED IN AIR. . . . . 32

2-4 MAXIMUM WIDTH VS p FOR PLATE WELDED IN WATER . . . . 33

2-5 MAXIMUM WIDTH VS p FOR PLATE WELDED IN WATER . . . . 35

2-6 MAXIMUM LENGTH VS p FOR PLATE WELDED IN WATER. . . . 36

2-7 PREDICTED VS MEASURED CONTOUR OF A WELDED POOL . . . 39

2-8 MODEL OF BOILING HEAT TRANSFER PROCESS . . . . . 41

2-9 THE COMPUTATIONAL BLOCK. . . . . 46

3-1 SCHEMATIC OF EXPERIMENTAL EQUIPMENT . . . . . 49

3-2 THERMOCOUPLE LOCATIONS IN TEST SPECIMEN. . . . . 58

3-3 INSTALLATION OF A THERMOCOUPLE . . . . . 59

4-1 MEASURED AND CALCULATED TEMPERATURE CURVES . . . . . 64

4-2 MEASURED AND CALCULATED TEMPERATURE CURVES . . . . . 65

4-3 TEMPERATURE COMPARISON CURVES . . . . . 67

4-4 THEORETICAL TEMPERATURE DISTRIBUTION . . . . . 68

4-5 COOLING CURVE SLOPES . . . . . 69

## LIST OF SYMBOLS

| | |
|---|---|
| $c_p$ | SPECIFIC HEAT (BTU/lb-$^oR$) |
| E | ARC VOLTAGE (VOLTS) |
| $H_m$ | HEAT CONTENT (BTU/$FT^3$) |
| I | ARC CURRENT (AMP.) |
| $K_o, K_1$ | BESSEL FUNCTIONS |
| k | THERMAL CONDUCTIVITY (BTU/FT-HR-$^oR$) |
| L | THICKNESS OF THE WORKPIECE |
| $\ell_m$ | MAX. POOL LENGTH (IN) |
| p | LUMPED PARAMETER |
| q | HEAT FLUX RATE (BTU/$FT^2$-HR) |
| $q_c$ | CONVECTIVE HEAT LOSS |
| $q_b$ | BOILING HEAT LOSS |
| $q_r$ | RADIATIVE HEAT LOSS |
| $r_m$ | RADIAL DISTANCE TO POOL BOUNDARY (IN) |
| T | TEMPERATURE ($^oR$) |
| V | WELDING SPEED (FT/HR) |
| $y_m$ | MAX. POOL HALF-WIDTH (IN) |

GREEK LETTERS

| | |
|---|---|
| $\alpha$ | THERMAL DIFFUSIVITY (FT /HR) |
| $\partial_{min}$ | MINIMUM THERMAL DIFFUSIVITY FOR METAL |
| $\theta$ | ANGLE (DEGREES) |
| $\lambda$ | $1/(2\alpha_{Min})$ , $HR/FT^2$ |
| $\rho_L$ | MASS DENSITY OF SATURATED WATER ($lb/ft^3$) |
| $\rho_V$ | MASS DENSITY OF SATURATED VAPOR (WATER) |
| $\sigma$ | SURFACE TENSION (lb/ft) |

SUBSCRIPTS

| | |
|---|---|
| o | AMBIENT TEMPERATURE |
| M | MELTING TEMPERATURE |

SUPERSCRIPTS

| | |
|---|---|
| * | NORMALIZED QUANTITY |
| – | AVERAGE VALUE |

# CHAPTER I

## INTRODUCTION

The object of this thesis was to develop a model of an underwater welding process such that the temperature history of the metal could be predicted. Particular attention was given to temperature changes within the heat affected zone. The model was constructed with consideration for a) the variation with temperature of the thermal properties of the base metal, b) a finite heat source of predictable configuration, c) the heat losses to the liquid environment, and d) the non-linear components of the heat flow equation. Three major areas within the literature were investigated: a) underwater, b) normal surface welding, and c) boiling heat transfer.

This study was conducted in recognition of the potential benefits that could be realized if underwater welding were a viable process. Predicted trends in ocean exploration and exploitation indicate the use of large structures that could only be fabricated or repaired on site within the liquid environment. Even today, considerable savings could be realized if ship hulls, off-shore drilling platforms, buoys and salvage work were constructed or repaired without explicit dependence on the requirement that the welding operation be conducted in air. Unfortunately, underwater welds are not structurally sound due to reduced ductility, and

susceptibility to stress corrosion and hydrogen cracking.

A reasonably accurate model, one that predicts peak temperatures and cooling rates, was seen as a necessity to examine the metallurgical changes occurring in the weld zone as function of welding parameter.

## A. UNDERWATER WELDING: STATE-OF-THE-ART

Underwater welding, as a process, is best defined by considering its two subcategories: wet and dry welding. Dry underwater welding is a welding procedure in which the liquid environment is excluded from the vicinity of the workpiece by a structure such as a caisson. The structure is large enough to contain one or more workers plus the necessary welding equipment. The atmosphere within the chamber is usually at depth pressure and may, or may not, consist of life-supporting gases. This system's utility is restricted to symmetrical workpieces about which the chamber can be fitted and sealed. Hence, dry underwater welding is most used by oil companies laying undersea pipeline or repairing the submerged supporting structure on off-shore drilling rigs. Essentially, this procedure differs from normal air welding only by the pressure of the atmosphere surrounding the work.

Wet welding occurs when the liquid environment is allowed to interact directly with the joining process: the

most notable result being a rapid quenching of the liquid metal. The utility of this process is not restricted by the geometry of the workpiece, but rather by the quality of the product. No wet weld is considered safe when used in load bearing structures. The rapid quench produces a weld that has 50% of the ductility of air welds, and is subject to extreme stress corrosion cracking and hydrogen embrittlement. The object of the thesis, then, was to construct, and verify, a model that might predict the temperature cycles in a metal as it is being wet welded.

The necessity for such a model is twofold: a) considerable time and expense could be saved if current ocean structures could be repaired or fabricated in situ, and b) future projections of man's involvement with the ocean require the use of structures that can only be fabricated, by reason of their size, within the ocean environment. Currently, the most economical means of joining metal is by welding, and it would be extremely expensive if each new process, each new structural material, with their multitude of variables, had to be investigated individually by actual experimentation. Unfortunately, the state of wet welding has generally stagnated since its inception during WW II.

From its development in the 1940's until today, the most widely used wet welding process is shielded metal-arc. This is the same method used in air welding and is commonly

referred to as "covered electrode" or "stick electrode" welding. Generally, wet welding has merely borrowed whatever equipment was already developed for air welding. The only adaptation to the new environment being a coat of waterproof material for the electrode and an electrically-insulated holder. Only recently have the British begun to develop electrodes specifically designed for use under water. However, the details of the program are considered proprietary information.

The basic research conducted thus far has been an examination of the mechanical properties of the flux and the completed weld. Thus, Waugh and Eberlein[23] investigated flux coverings to determine those most suitable for underwater application.* Work at the Naval Engineering Station[26] produced some factors of safety that must be applied when wet welding. Hibshman and Jensen[8] evaluated the properties of welds in low-carbon steel, under water and in air. The data revealed that ductility was markedly reduced. As far as it is known, however, no attempt has been made, either on a theoretical or experimental basis, to determine the temperature history of the metal during the wet welding process.

## B. NORMAL SURFACE WELDING

A review of the literature for air welding, however, indicated that considerable effort has been devoted to

---

* Numbers refer to listing in Bibliography.

predicting the temperature cycles during the welding process. In 1935, Rosenthal[16] obtained an exact solution to a modified heat flow equation. He simplified his model by neglecting non-linear terms, treating the conductivity as constant, and assuming a point source. However, the resulting equation for temperature distribution contained all the important welding parameters: weld speed, heat input, plate thickness, and the thermal properties of the metal. Furthermore, the equation was in quasi-steady state form so that the location of the point source was at the origin of a stationary coordinate system. Experimental verification by Rosenthal[16] and Schmorber indicated that the model was reasonably accurate at some distance from the source of heat, but in adjacent areas (within the heat affected zone, or haz) the degree of error was unacceptably large. The primary cause for the discrepancy was due to the nature of the heat source which in actuality has a very definite shape. Nevertheless, Rosenthal's initial attempt provided the impetus which spanned a succession of attempts to include all the important variables in one well organized model.

Grosh, Hawkins, and Travant[7] investigated the effect of considering the thermal properties as a function of temperature and obtained slightly better results. Barry[3] modified Rosenthal's model by including possible heat losses to the environment but concluded that, at least for convection, the effect is negligible in comparison to the heat conducted

in the metal.

The most important attempts to derive a satisfactory model concerned those which examined the shape of the heat source. In 1952, Wells[27] proposed an equation from which the length and width of the weld pool could be determined as a function of the heat input. Subsequent experiments indicated that the relationship was reasonably accurate. Christensen, Davies, and Gjermundsen[4] examined the shape of the weld pool and its relation to a wide variety of welding conditions and associated variables. While their objective was not to formulate a model, they did present experimental data from which viable conclusions were drawn: a) pool width and length increase with heat input for a given weld speed and plate thickness, b) the pool is wider than predicted by point source theory, and c) the pool has a distinct "tear-drop" shape. These basic observations permitted the derivation of a very successful model of temperature distribution during welding.

In 1967, Pavelic[13] and Tanbakuchi[20] constructed and verified a model which combined all the disparate elements necessary to predict temperature variations in the haz. Unlike Rosenthal, they considered the variation of conductivity and diffusivity with temperature, a finite heat source, heat losses to the environment through convection and radiation, non-linearites in the heat flow equation,

and preheating of the metal from arc radiation. Their approach to the derivation of the model for a tungsten-inert-gas welding process formed the basis for this thesis.

## C. BOILING HEAT TRANSFER

The literature on boiling heat transfer was investigated selectively with respect to possible models relating to sub-cooled pool boiling on horizontal plates at a non-uniform temperature.

The complexity of the boiling process has prevented researchers from developing a single formulation covering the wide range of temperatures over which boiling will occur. Figure 1-1, reported by Rohsenow, [15] is considered to represent the regimes of boiling, each regime having a uniquely formulated model descriptive of heat transfer.

Rohsenow[15] has correlated the data of Addoms for nucleate boiling on platinum wire in water at saturation temperature. Although the data was given for a specific geometry, Rohsenow observed that the same results applied to horizontal surfaces.

Correlations in the transition regime have not been firmly developed. Jordan,[25] reporting the data of Drew and Mueller, Farber and Scorah, and Braunleh, concluded that if the data were plotted on a log-log graph, they would lie along a straight line from the critical flux (or, burnout)

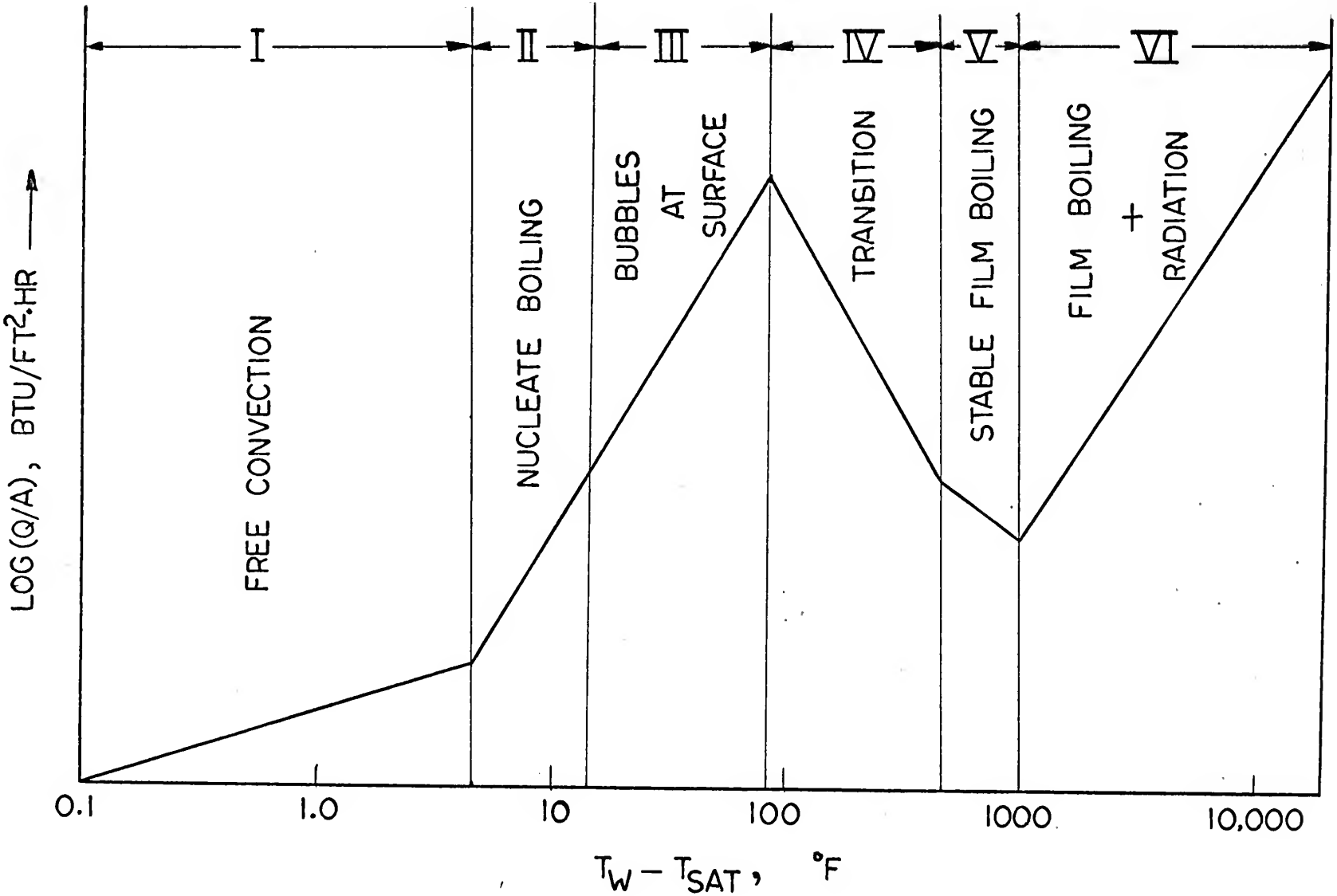
CHARACTERISTIC BOILING CURVE
I
II
III
IV
V
VI
FREE CONVECTION
NUCLEATE BOILING
BUBBLES AT SURFACE
TRANSITION
STABLE FILM BOILING
FILM BOILING + RADIATION
LOG (Q/A), BTU/FT².HR
0.1
1.0
10
100
1000
10,000
$T_W - T_{SAT}$, °F

FIGURE 1-1

to the minimum film boiling heat flux. The slope of the line varied with the surface finish: the steepest slope occurring with a mirror smooth finish.

Chang, Botushansky, and Berenson[25] developed correlations for film boiling heat flux from horizontal surfaces. Jordan[25] has reported that the Borishansky relation fits the data for pool boiling in water.

## D. SUMMARY OF PROCEDURE

The development of a model for predicting temperature changes in the heat affected zone of an underwater weld required the construction of a theoretical model followed by experimental verification. The model was to encompass the latest techniques, and should be reasonably accurate in determining peak temperatures and cooling rates.

The derivation of the model followed the approach taken by Pavelic[13] and Tanbachuchi[20] in their work for surface GTA (Gas Tungsten Arc) welding. The two-dimensional equation of heat flow with external sources was reduced to quasi-steady state form and transformed to its finite difference equivalent. The external heat sources were examined and the proper relations chosen. Then, with the help of Pavelic's results, the equation describing the shape of the molten weld pool was derived. The resulting derivation included numerical constants which were determined through experimentation.

Finally, the computer program was written. The method for laying out the finite difference grid was that developed by Tanbachuchi. His solution was refined by having the shape of pool internally generated instead of being supplied as input.

The experiment was conducted in two parts. First, the correlation constants in the pool configuration equation were determined by measuring the dimensions of molten weld pools while varying the welding parameters: Heat input and welding speed. Then, temperatures occurring during welding were determined by laying weld beads on submerged plates in which thermocouples had been installed. The results of the final experiment were compared with the values predicted by the model.

# CHAPTER II

## MATHEMATICAL MODEL AND COMPUTATIONAL TECHNIQUE

### A. PRELIMINARY OBSERVATIONS

Welding is a process of joining two or more materials together by applying sufficient quantities of heat to a local area at their interface such that melting occurs and a union is achieved. The amount of heat required is on the order of $10^4$ BTU/HR and, for structural applications, the manner of generation is by electric arc. The method for directing the arc is by an electrode which may (consumable) or may not (non-consumable) contribute metal to the finished bond. The electrode concentrates the arc and creates a small pool of molten metal which is typically "tadpole" or "raindrop" shaped when viewed in the plane perpendicular to the arc axis. As the electrode is drawn along the material a bead of weld (i.e., a chain of overlapping pools) is formed which represents the physical evidence of the interface bond.

The largest percentage of the heat developed by the arc goes into raising the temperature of the material to its melting point. The remainder is accounted for by conduction, convection, and radiation, joule heating, and pre-heating of the material in the vicinity of the arc. Pre-heating will occur in all but submerged arc processes and is due to the divergence of the arc which takes the appearance of a cone with the electrode at its apex. The central part of the

arc, or the plasma column, is responsible for the creation of the molten pool. The remainder of the arc, while not generating sufficient heat to melt the material, will cause preheating. Hence, heat may flow into the material directly from the pool and from the arc by pre-heating.

While the above heat balance has been observed in normal sruface welding, its complete relevance to the underwater welding process is less certain. Conduction and radiation have importance, but convective losses must be modified by boiling heat transfer phenomena. Joule heating losses are usually estimated to account for 1-2% of machine power and, hence, may be neglected. A search of the literature did not reveal any information on the dynamics of an arc surrounded by water so that the efeect of pre-heating could not be determined. For the experiment, it was decided that the effect, if it did exist, could be reduced to negligibility by the proper choice of electrodes. Consequently, an electrode that could be placed directly on the metal surface without shorting out was selected. These "drag" type electrodes operated in a manner such that the metal core melted faster than the flux covering the flux coat, which came in direct contact with the metal, formed a hollow barrel and prevented arc diffusion. Consequently, it was assumed that pre-heating was negligible and all heat flowed into the metal through the molten pool. Interaction with the

environment was assumed to occur by radiation and boiling heat transfer.

An approximation to the real welding process was then seen to be a boundary-value problem in two-dimensions with negative source terms. The interior boundary in the field was viewed to be formed by the contour of the molten pool; the exterior boundaries were considered as the four edges of a rectangular surface. The pool contour temperature was known to be the melting temperature of the material with the edges at ambient. Radiation and boiling heat transfer were included as the negative sources.

## B. EQUATION OF HEAT FLOW

The governing differential equations are presented in this section. In the sections to follow the equations are reduced to their finite difference equivalents, the boundaries are defined, and the relations for the source terms are determined.

The general equation of heat flow with source terms is,

$$\nabla \cdot (K\ T) + W_i = \rho c \frac{DT}{Dt} \quad ,$$

where $k, \rho$ , and c are the conductivity, density and specific heat of the material and may be a function of distance, time, and temperature. $W_i$ represents the source terms and has the units, $BTU/FT^3\text{-}HR$. In partial differential notation for two dimensions, the equation becomes,

$$\frac{\partial^2 T}{\partial x^2} + \frac{\partial^2 T}{\partial y^2} + \frac{1}{k}\frac{\partial K}{\partial T}\left[\left(\frac{\partial T}{\partial x}\right)^2 + \left(\frac{\partial T}{\partial y}\right)^2\right] + \frac{W}{k}i = \frac{\rho c}{k}\frac{\partial T}{\partial t} .$$

The equation in this form is for a coordinate system fixed to the control surface defining the temperature field. Since the interior boundary (i.e., the pool contour) moves through the field with velocity, V, the velocity of the electrode, the temperature at a given point will change with time. To eliminate the time dependence, the coordinate system was transferred to the moving boundary with the following transformation equations:

$$\acute{x} = x - Vt$$

$$\acute{t} = t$$

where $\acute{x}$ and $\acute{t}$ are coordinates in the new system. (The details of the calculation appear in Appendix 1.) With the transformation, the equation of heat flow became,

2.1

$$\frac{\partial^2 T}{\partial \acute{x}^2} + \frac{\partial^2 T}{\partial y^2} + \frac{1}{k}\frac{\partial k}{\partial T}\left[\left(\frac{\partial T}{\partial \acute{x}}\right)^2 + \left(\frac{\partial T}{\partial y}\right)^2\right] + \frac{W}{k}i = -\frac{V}{\alpha}\frac{\partial T}{\partial \acute{x}} .$$

The temperatures with respect to the new system could now be considered constant and were viewed to form isothermal contours in the plane of the field with the pool contour forming the innermost. Hence, the pool boundary could be called the isotherm of melting.

The equation was put in non-dimensional form by

defining normalizing relations. It was decided to make the exterior boundary conditions homogeneous and the conditions along the pool contour unity. Hence, the normalized temperature was defined,

$$T^* \equiv \frac{T - T_o}{T_M - T_o} \qquad 2.2$$

where $T_M$ is the melting temperature of the material (approximately 2700°F for mild steel) and $T_o$ the ambient temperature.

The normalized dimensions were defined to be,

$$x^* \equiv \frac{x}{x_o} \quad , \quad y^* \equiv \frac{y}{x_o} \quad .$$

when these definitions were substituted back into equation 2.1, it was found that $x_o$ should be defined as

$$x_o \equiv \acute{\alpha} / V \quad ,$$

where $\acute{\alpha}$ refers to a specific value of the thermal diffusivity. From a stability analysis of equation 2.1, recommended by Ames[2], it was determined that

$$\acute{\alpha} = 2\, \alpha_{Min}$$

where αMin represents the minimum thermal diffusivity for the material. Finally, the normalized dimensions became

$$x^* = \frac{XV}{2\, \alpha_{Min}} \quad , \quad y^* = \frac{YV}{2\alpha_{Min}} \qquad 2.3$$

by substitution of equations 2.2 and 2.3 into equation 2.1, the heat flow relation was obtained in non-dimensional form,

$$\frac{\partial^2 T}{\partial x^2} + \frac{\partial^2 T}{\partial y^2} + \frac{1}{k}\frac{dK}{dT}\left[\left(\frac{\partial T}{\partial x}\right) + \left(\frac{\partial T}{\partial y}\right)^2\right] + \frac{4\ \alpha Min^2}{KV^2\,(T_M - T_o)}(W)_1 = \frac{2\alpha_{Min}}{\alpha}\frac{\partial T}{\partial x} \qquad 2.4$$

where the "Star" superscript has been dropped. (See Appendix 4 for details of the derivation.)

## B. FINITE DIFFERENCE SOLUTION

Equation 2.4 was then converted to its finite difference equivalent so as to make it amenable to computer solution. Following the procedure recommended by Greenspan[6] for elliptic non-linear partial differential equations. A finite difference grid node (Figure 2-9) was defined and the bounding temperatures were approximated by a Taylor expansion about $T_o$:

$$T_1 = T_o\ (\pm)\ S_i\frac{\partial T_o}{\partial x} + \frac{S_i^2}{2}\left[+\ \frac{\partial^2 T_o}{\partial x^2}\right] + \ldots \qquad i = 1,2,3,4.$$

Now, in the limit as the $S_i$ (i.e., the grid spacing) approach zero the variation in temperature between the bounding temperatures along a given axis will represent the actual rate of change of temperature at the node. For unequal grid spacing, these changes were defined as:

$$\frac{\partial T_o}{\partial x} = a_0 T_0 + a_1 T_1 + a_2 T_2 \qquad (2\text{-}5_{a,b})$$

$$\frac{\partial\ T_o}{\partial y} = \acute{a}_0 T_o + \acute{a}_1 T_3 + \acute{a}_2 T_4$$

The weighing coefficients were found by comparison with Taylor's expansion through combination of like terms. The second partials were similarly defined

$$\frac{\partial^2 T_o}{\partial x^2} = a_3 T_0 + a_4 T_1 + a_5 T_2$$

$$\frac{\partial^2 T_o}{\partial y^2} = \acute{a}_3 T_0 + \acute{a}_4 T_3 + \acute{a}_5 T_4 \qquad (2\text{-}6_{a,b})$$

and the coefficients found from Taylor's expansion. Substitution of equations 2.5 and 2.6 into 2.4 resulted in the finite difference equivalent for the equation of heat flow:

$$T_0 = \Bigg\{ T_1 \left[\frac{2\alpha + S_2}{\alpha S_1 (S_1+S_2)}\right] + T_2 \left[\frac{2\alpha - S_1}{\alpha S_2 (S_1+S_2)}\right] + T_3 \left[\frac{2}{S_3 (S_3+S_4)}\right]$$

$$+ T_4 \left[\frac{2}{S_4 (S_3+S_4)}\right] + \frac{4\alpha^2_{Min}}{KV^2 (T_M - T_o)} [W_i]$$

$$+ \frac{1}{k}\frac{dK}{dT}\Bigg[\Bigg[\left(\frac{S_1-S_2}{S_1 S_2}\right) T_o + \left(\frac{S_2}{S_3 (S_3+S_4)}\right) T_1 + \left(\frac{S_1}{S_2 (S_1+S_2)}\right) T_2\Bigg]^2$$

$$+ \Bigg[\left(\frac{S_3-S_4}{S_3 S_4}\right) T_o + \left(\frac{S_4}{S_3 (S_3+S_4)}\right) T_3 + \left(\frac{S_3}{S_4 (S_3+S_4)}\right) T_4\Bigg]^2\Bigg]\Bigg\} \Big/ B \qquad 2.7$$

where,

$$B = \left(\frac{2}{S_1 S_2} + \frac{2}{S_3 S_4} + \left(\frac{S_2-S_1}{\alpha (S_1 S_2)}\right)\right)$$

The details of the derivation are presented in Appendix 5.

Equation 2.7 operated on a grid (i.e., an assemblage of nodes) placed over the temperature field by assigning to each node point a value consisting of the weighted "average" of the four bounding temperatures. Since the exterior points in the field were at a normalized value of zero it was decided that calculations should begin at the pool contour (T - 1) and move outward. A series of iterations over the grid were performed until the desired accuracy was obtained.

## C. THE BOUNDARY CONDITIONS

This section deals with the derivation of the equation describing the shape of the pool contour (i.e., the interior boundary in the temperature field) and a determination of the location of the exterior boundaries. The treatment of the problem follows the approach taken by Pavelic[13] in his study of the tungsten inert gas process for normal air welding. Pavelic's method for finding the shape of the pool can be summarized as follows:

1. Rosenthal's two-dimensional equation with a point source of heat is analyzed to obtain the relations predicting the maximum dimensions of the pool: length and width.
2. These theoretical relations are correlated with experimentally-obtained data.

3. The contours of actual pools are measured and a curve fitted equation is obtained. This equation is a function of the maximum pool dimensions.

Hence, for any given set of welding variables, Pavelic could predict the contour of the pool. The details of Pavelic's analysis have been summarized in Appendix 3.

It was found that the maximum theoretical dimensions of pool are

$$Y_{max} = r_m \left\{ 1 - \left[ \frac{K_o(r_m)}{K_1(r_m)} \right]^2 \right\}^{\frac{1}{2}}$$

For the maximum half width, and

$$X_{max} = 2r_m \frac{K_o(r_m)}{K_1(r_m)}$$

for the maximum length. The argument of the Bessel functions, $K_o$ and $K_1$, is the radial distance from the origin of the arbitrary coordinate system to the pool contour and was found to be a function of the lumped parameter, p:

$$p = \frac{3.415\ EI}{2\pi\ \bar{\alpha}\ L\ H_m}$$

The relationship of $x_{max}$, $Y_{max}$, and $r_m$ to the pool is presented in Figure 2.1. When plotted on a log-log graph, the pool width (= $2y_{max}$) vs p and $x_{max}$ vs p appear as a straight line and, hence, experimental data could be correlated by

# POOL CONTOUR VARIABLES

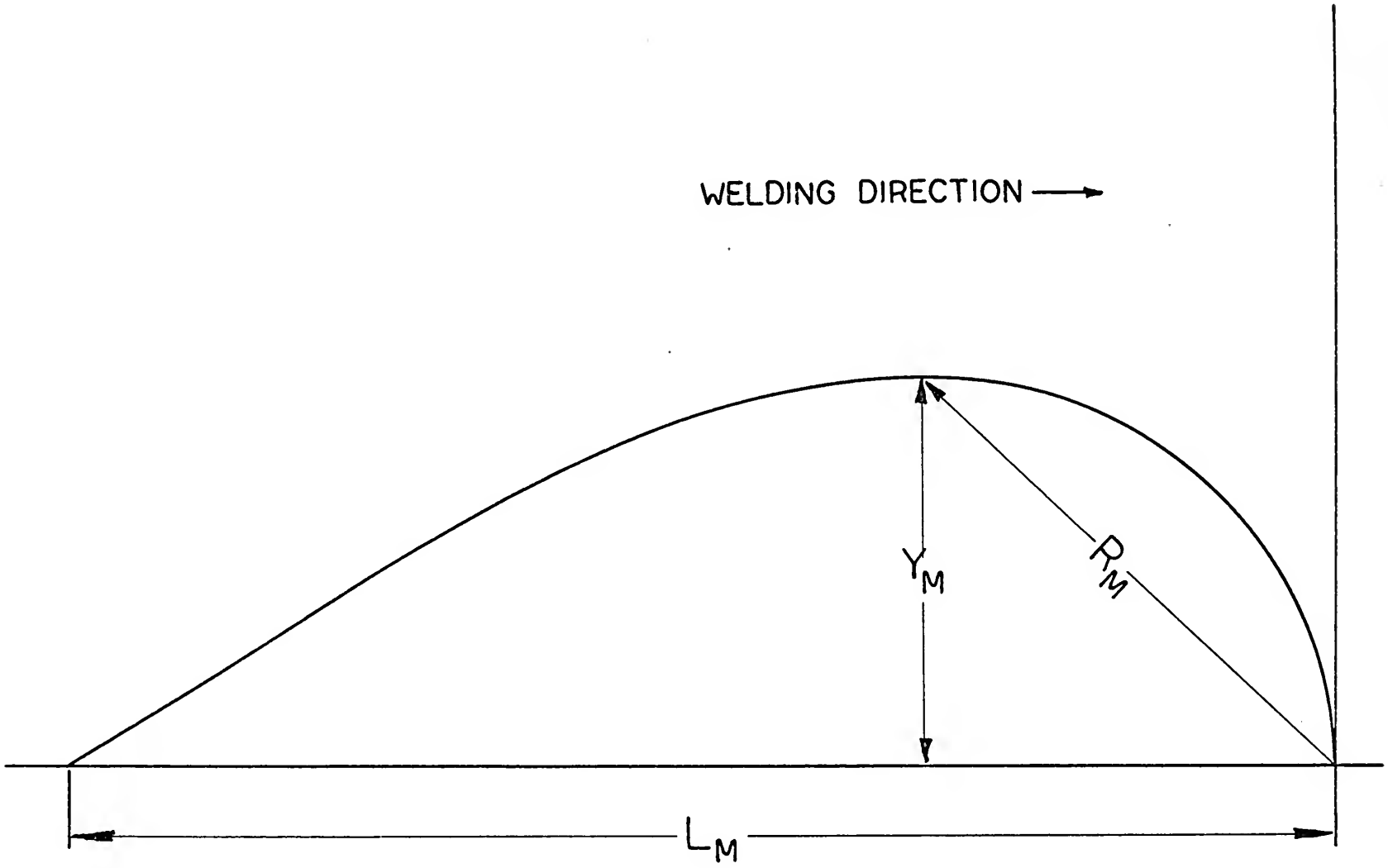


FIGURE 2-1

the relations:

$$2y_{max} = ap^b$$

$$x_{max} = cp^d$$

with a, b, c, and d becoming the correlation constants.

Experiments were conducted therefore to find values for the constants. Pools were made by welding beads on thin rectangular plates. At a predetermined point in the welding process the molten metal was ejected from the pool by a jet of high pressure air leaving a crater whose edges formed the desired contour. Only those craters nearest the ideal two-dimensional configuration were retained for measurement. An ideal 2-D crater has been defined in Figure 2.2. The maximum length and width were measured with a Bausch and Lomb microscope containing a movable micrometer table. A computer program was then written to fit a curve through the data points from which values for the correlation constants were obtained. The program with sample input is presented in Appendix 7.

Two major problems were recognized early in the attempt to produce craters for measurement: a) a search of the literature did not reveal any similar experiments conducted with stick electrodes, and b) it was very difficult to time the release of air to eject the metal during the under water welding process. Without the certainty that the metal was being ejected at the proper instant it was considered

# 2-D WELD POOL

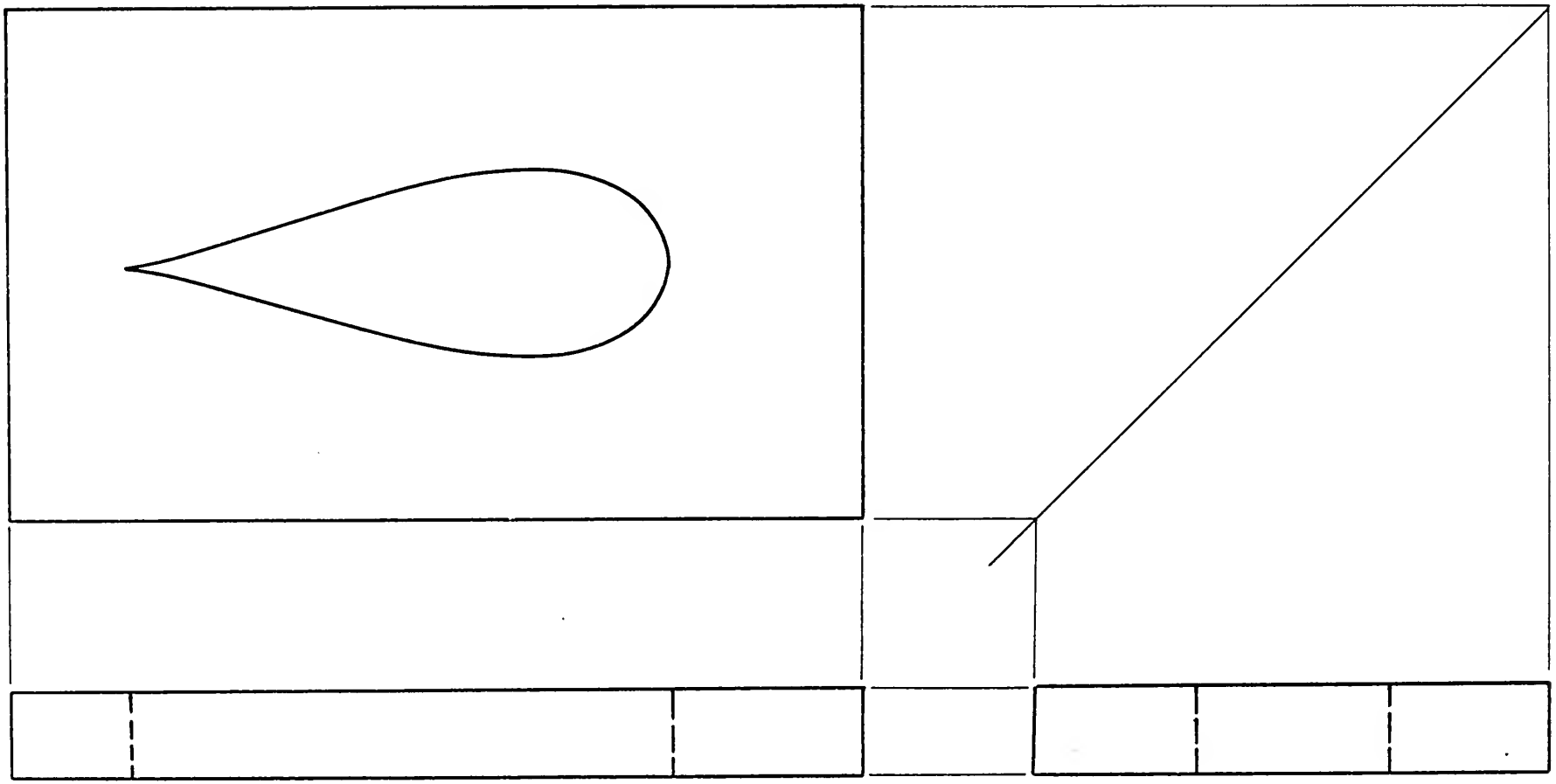

FIGURE 2-2

possible that the craters might be distorted and measurements valueless. The lack of prior experiments conducted in air denied a basis for comparison to determine if the underwater data were reasonable. Consequently, it was decided to conduct an initial series of runs in air where crater production could be closely controlled, merely to serve as a crude reference for the underwater results.

Plates of two different thicknesses, 1/8" and 1/4", were used and the data plotted as shown in Figures 2.3 and 2.4. The results for the 1/8" plate appeared to be in good agreement with the predicted relation, but those for the 1/4" plates were not. The lack of alignment was attributed to the failure to obtain two-dimensional pools in the larger specimens. The available power was insufficient to create the required configuration, and, as a result, the crater formed was only a hollow depression on the surface of the specimen. Significantly, an increase in power (ExI) would have resulted in a larger value for the lumped parameter, p, which would have shifted the data points to the right and brought them more in line with the predicted relationship. (It was noted, however, that a line drawn through the 1/4" data points was approximately parallel to the theoretical line. This relationship suggested that the penetration of the arc could also be correlated with the lumped parameter, p, so that the equation for a 3-D pool might eventually be derived. No attempt was made to do so, however.) From the plot for air welding it was observed

# MAXIMUM 2-D POOL LENGTH
# WELDED IN AIR

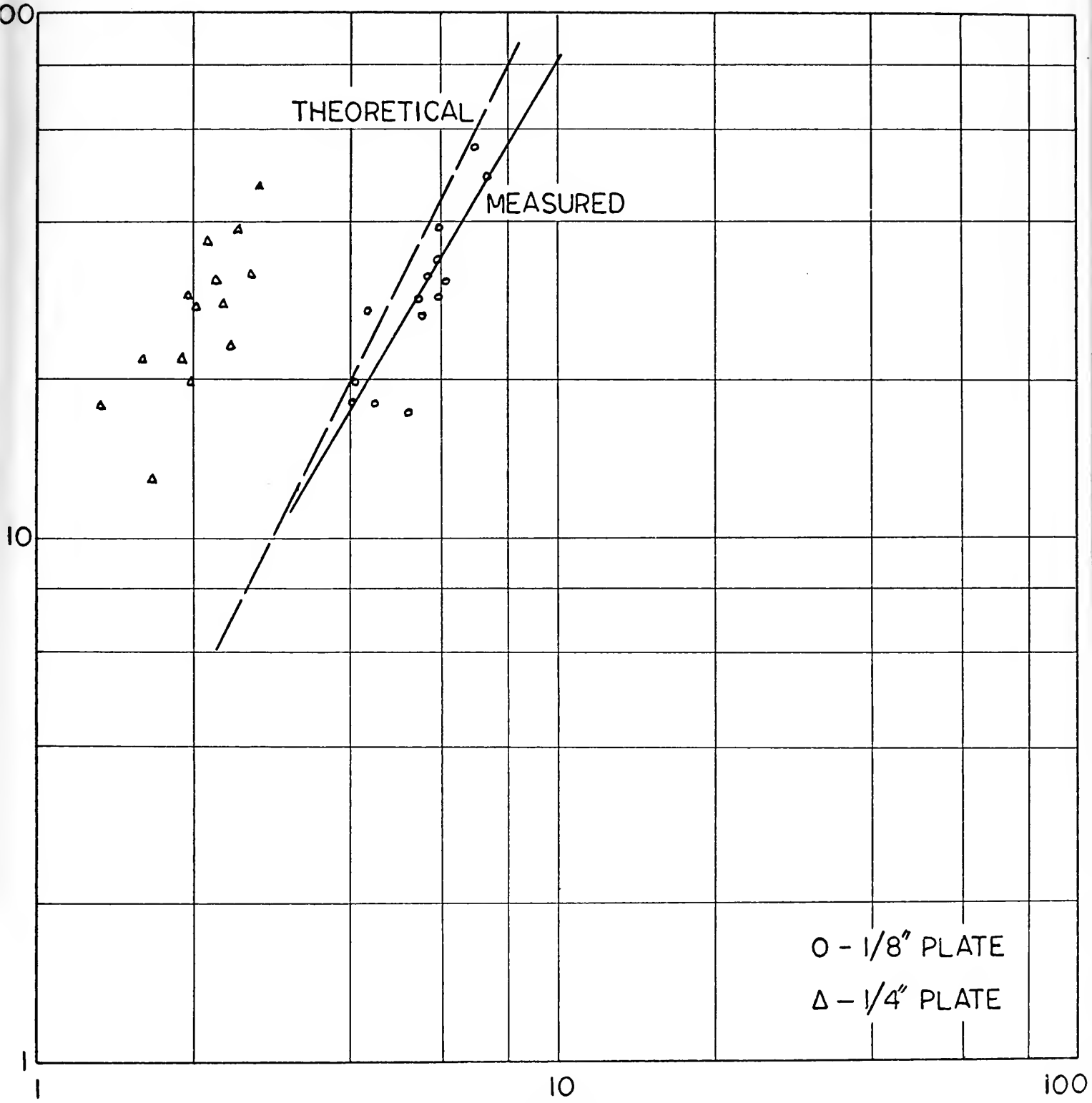


$$P = \frac{3.415EI}{2\pi\bar{a}LH_M}$$

FIGURE 2-3

# MAXIMUM 2-D POOL WIDTH WELDED IN AIR

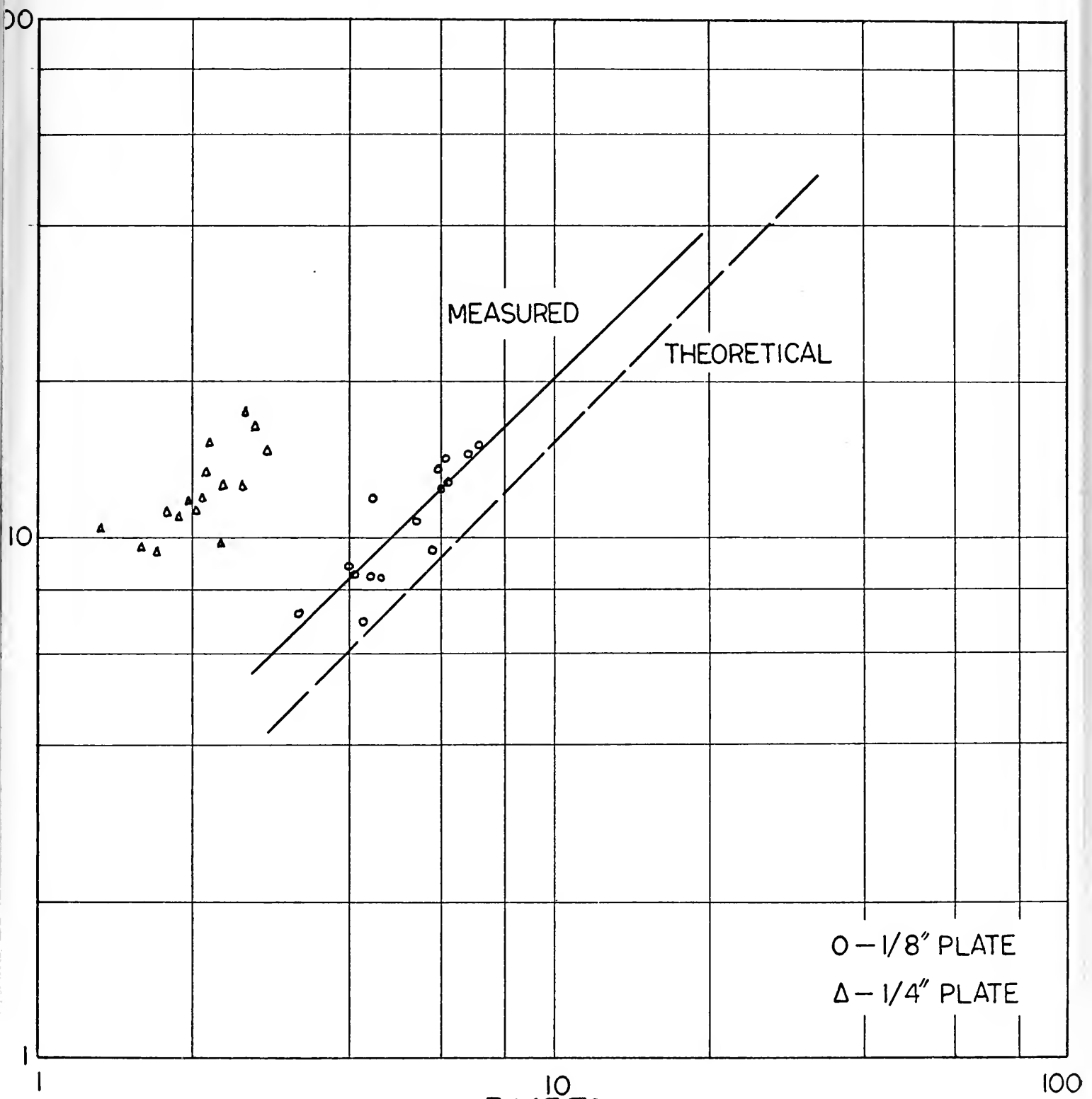


$$P = \frac{3.145EI}{2\pi\bar{a}LH_M}$$

FIGURE 2-4

that a) 2-D pools would not be obtained in water for 1/4" thick specimens and b) the width of the underwater pool should be larger than predicted while the length should be smaller.

Pools were then created under water, measurements taken and the data plotted as shown in Figures 2.5 and 2.6. The location of the data points with respect to the theoretical line was noted and compared with air welded results. Since the location was as expected it was assumed that the measurements were reasonable. Curves were fitted through the data points. These curves were not found to be parallel either to the predicted or the air welded lines, and the reason for the divergence (considered more fully in Chapter IV) could not be adequately explained due to the small size of the data sample and data scatter. Nevertheless, the correlation constants obtained from the fitted curve were used. It was consequently assumed that the length and width of an underwater pool were related to the lumped parameter, p, according to the equations:

$$x_M^* = 4.42\ p^{1.01}$$

$$W_M^* = 3.16\ p^{0.67}$$

where $x_m^*$ and $W_M^*$ are dimensionless quantities and

$$x_M = \frac{24 x_M^*}{M^{\alpha} Min} \quad , \text{ in.}$$

$$W_M = \frac{24\ W_M^*}{M \alpha Min} \quad , \text{ in.}$$

$$V$$

# MAXIMUM 2-D POOL WIDTH
# UNDERWATER WELD

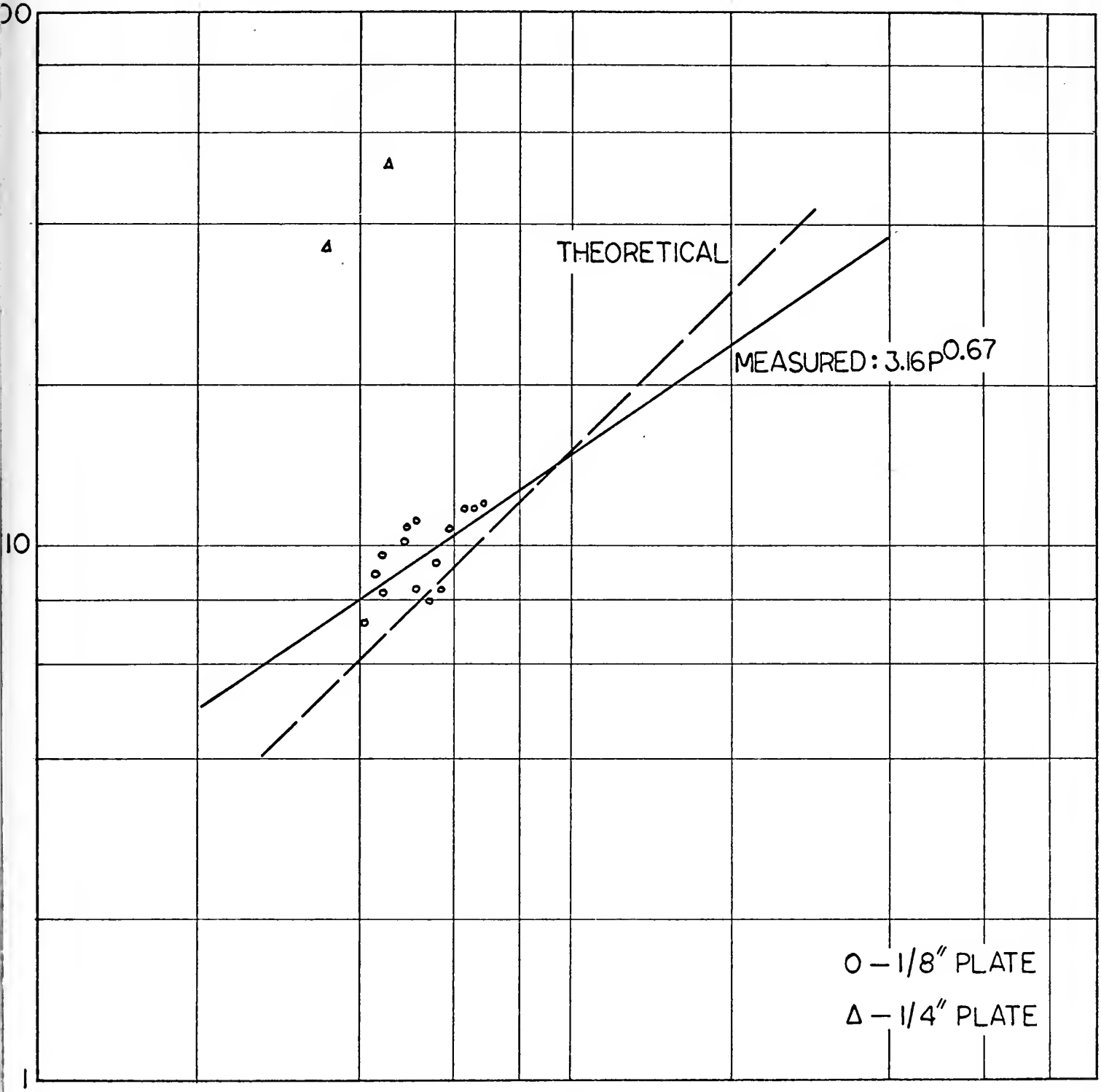


$$P = \frac{3.415EI}{2\pi \bar{a} L H_M}$$

FIGURE 2-5

# MAXIMUM 2-D POOL LENGTH
# UNDERWATER WELD

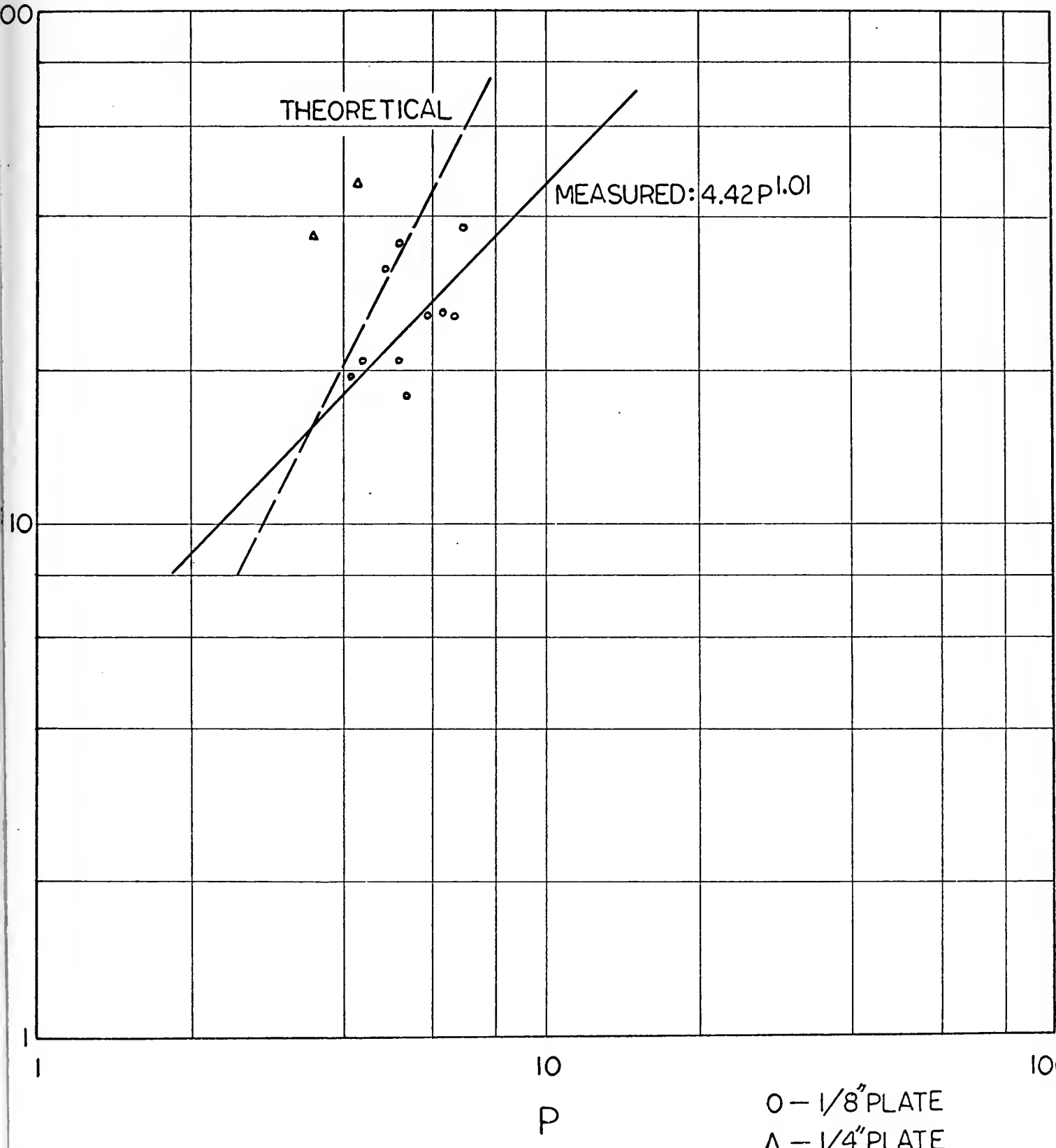


FIGURE 2-6

with the maximum pool dimension relations defined it was now possible to derive an equation that would predict the complete contour of the pool. Pavelic suggested curve fitting an equation of the form:

$$Y^2 = Bx^a(x_m - x)^b \qquad 2.8$$

to which the boundary conditions were applied,

(1) $y = o$ @ $x - x_m$

(2) $y = o$ @ $x = o$

(3) $\acute{y} = o$ @ $y = W_m/2$ , $x = x_c$

(4) $\acute{y} = \infty$ @ $y = o$ , $x = o$

where $x_c$ is the distance to the point of maximum width. After the applying of the boundary conditions, it was found that

$$B = \frac{(W_m/2)^2 \ (a+b)^{a+b}}{(ax_m)^a \ (bx_m)^b}$$

where a and b are the correlating constants. The details of the derivation have been included in Appendix 3.

Values for the constants were obtained by measuring the actual pool contours and fitting the resulting measurements with equation 2.8. A computer program, employing an M.I.T. non-linear least squares curve fitting routine, was written and has been presented in Appendix 7. It was hoped that a large number of pools would be available for measurement in order that the calculated correlating constants would be generally applicable. While a large sample size

was obtained for air welded pools, only one under water pool of acceptable quality was produced. Due to the accelerated solidification of the molten metal in water and crater walls took on a jagged appearance which made measurements difficult although the maximum dimensions were generally easily determined. Consequently, it was decided to base the calculation of the constants on data taken from the air welded pools and then compare the predicted contour with the measurements from the single under water pool. The result of this approach is presented in Figure 2.7. The predicted contour gave a wider head and narrower tail than was measured but the overall shape was considered satisfactory. Nevertheless, it was realized that the contour equation was based on a sample size of one (i.e., the single under water pool). However, it seemed reasonable to assume that the general shape of a pool would be independent of the atmosphere in which it was created since the dimensions were most strongly influenced by heat input and welding speed. With this assumption, the correlation constants

$$a = 0.83$$

$$b = 2.16$$

were used to predict the shape of the under water pool contours.

# POOL CONTOUR

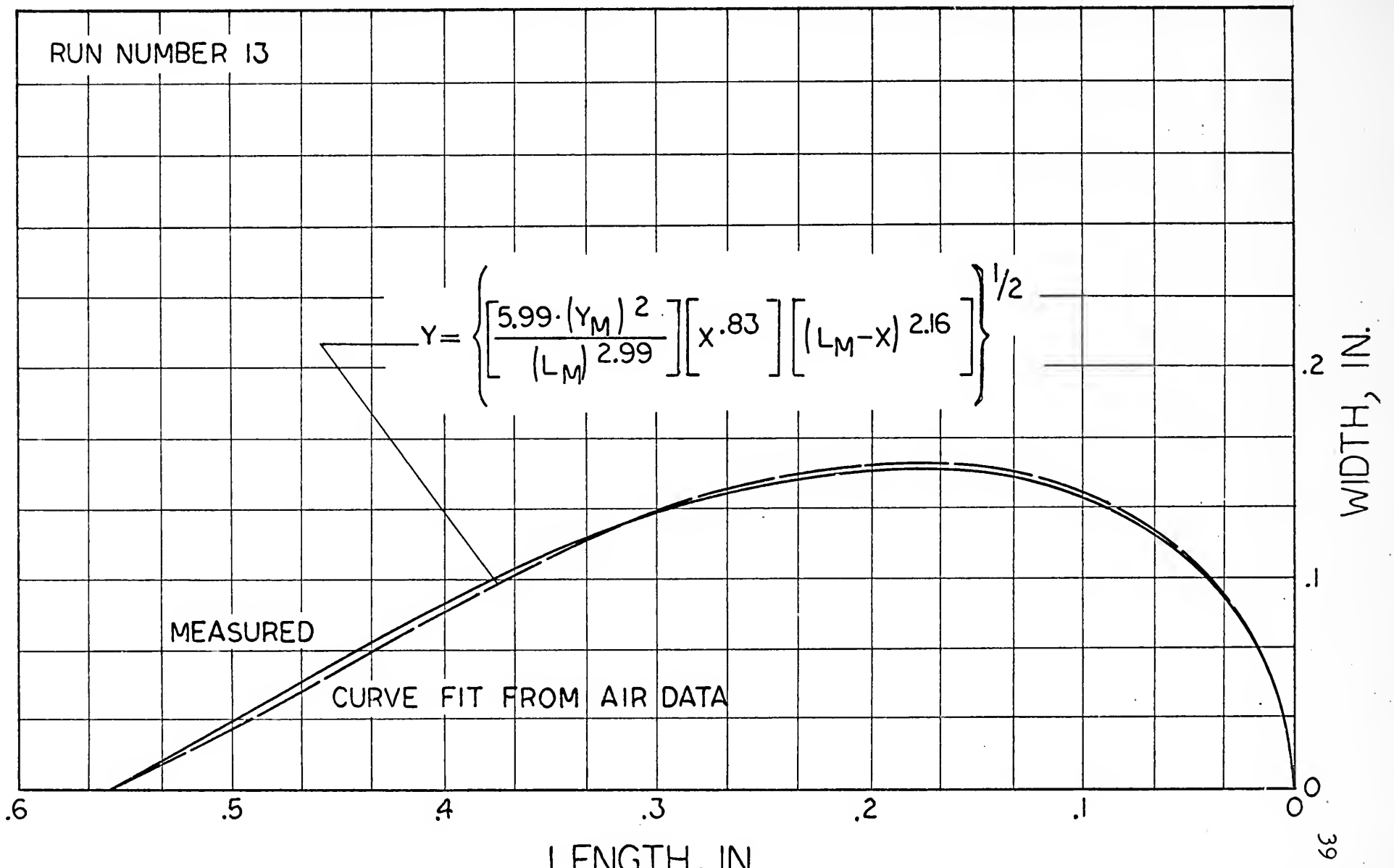


FIGURE 2-7

## D. DERIVATION OF THE HEAT LOSS TERMS, $W_i$

For this model heat losses were assumed to occur through boiling and radiation. Although convective heat flux could be considered, it was estimated that these losses would account for only 3% of the total heat input to the specimen (15,000 to 20,000 BTU/Hr) and were therefore neglected. Consequently, heat losses were considered according to three distinct regimes as depicted in Figure 2.8.

Nucleate boiling is characterized by the termination of bubbles at the heated surface which grow in size with increasing temperature. The agitation of the liquid near the surface caused by rubble activity -- formation, collapse, or ascent -- maintains a circulation of relatively cooler liquid near the surface which can result in heat fluxes on the order of $10^6$ BTU/FT$^2$-HR.

When the surface temperature reaches a value 50-90°F above saturation the number of bubbles forming has increased to the point where they begin to overlap and create a solid film of vapor. The vapor film is not immediately stable and may collapse back to the heated surface where the process repeats itself. In this transition region the cooler liquid is brought into contact with the surface only intermittently and heat flux rates are not as high as they would be during nucleation. As temperature increases the film grows more stable, insulating the surface and reducing heat transfer. Finally, the film becomes fully stable and the heat flux

# BOILING HEAT TRANSFER

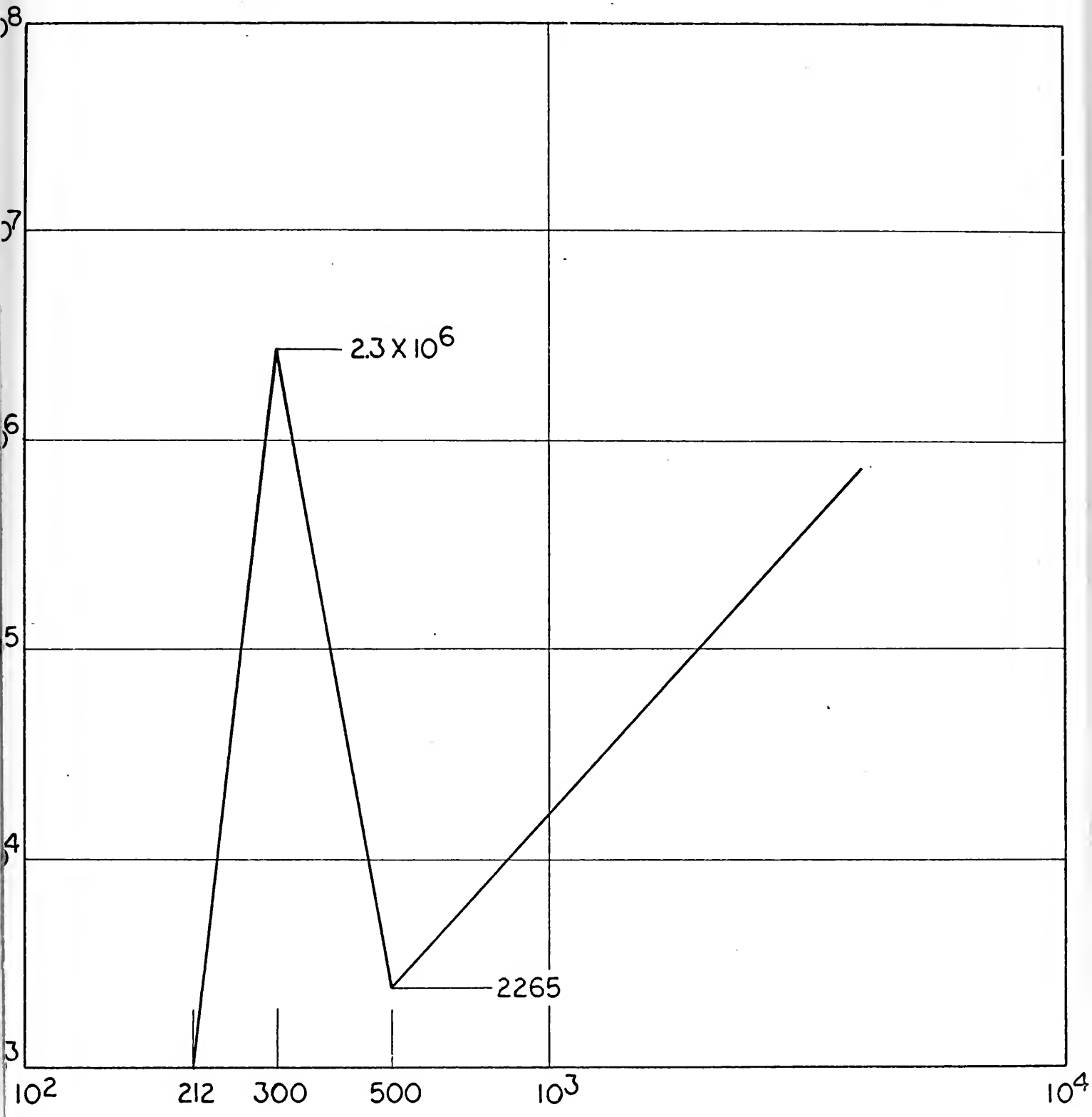


FIGURE 2-8

reaches its minimum value. At higher temperatures heat loss through radiation becomes the predominant term.

The complexity of the entire process required that each regime be treated separately in determining the appropriate relation for calculating heat flux. First, however, it was necessary to define the temperatures which bounded each regime. Since nucleation begins near saturation temperature, the lower bound was chosen to be 212°F. Burnout, or the end of nucleation, will occur at a temperature which depends upon the condition of the heated surface, the amount of dissolved gases in the liquid, and the ambient pressure. If the solubility of air at 14.7 psia is 6m ℓ/ℓ, then, from data reported by Rohsenow[15] burnout will occur neat 260°F. However, a mildly oxidized surface increases the temperature, by an unknown amount. Consequently, 300°F (as the nearest round number) was defined as the temperature at which nucleation terminates and the transition regime begins. For the minimum heat flux, the data of Borishansky and Berenson as reported by Jordan[25] indicated that transition ends near 500°F.

Once the boundary temperatures for each boiling regime were established it was necessary to determine the suitable heat flux relations. Rohsenow's[15] correlation of Addoms' data suggested that heat flux in the nucleate boiling regime varied according to the cube of the temperature difference, $T_w - T_{saT}$.

The properties of the liquid and vapor were calculated at saturation and the proper relation was found to be

$$q_N = [1.542(T_W - T_{SAT})]^3 \quad , \quad BTU/ft^2\text{-}hr.$$

The details of the calculation have been presented in Appendix 2. As indicated by Jordan[25], the data for film boiling on a horizontal surface in water is predicted withreasonable accuracy by Borishansky's relation. In this regime the heat flux was found to be

$$q_F = 32.4(T_W - T_{SAT})^{0.75} \quad , \quad BTU/hr\text{-}ft^2 \quad ,$$

where calculations have been summarized in Appendix 2.

Heat flux during transition boiling has not been well defined. However, data reported in the literature indicates that measures fluxes tend to fall along a straight line plotted with log-log coordinates. This relationship suggested the derivation of an equation with the burnout and minimum film boiling heat fluxes as boundary conditions. As summarized in Appendix 2, the results of the derivation were found to be

$$q_T = 2265.11 \left[ \frac{288}{(T_W - T_{SAT})} \right]^{5.86}$$

where

$$300° \leq T_W \leq 500°F \quad .$$

The equation for radiation heat transfer was determined by assuming the surface of specimen exchanges heat with the surrounding water. Hence,

$$q_R = 0.1317 \times 10^{-8}(T_w^4 - T_{SAT}^4) \quad , \text{BTU/hr-ft}^2 \quad .$$

## E. COMPUTATIONAL TECHNIQUE

The computer program written to calculate the temperature distribution consisted of the four main operations:

1. The shape of the pool contour is generated.
2. The grid is layed out to form a computational block.
3. The grid nodes are initialized using Rosenthal's temperature distribution equation.
4. Successive iterations are carried out over the grid until the desired accuracy is obtained.

A listing of the program is presented in Appendix 7, and instructions on its use in Appendix 6.

### Pool Contour Generation

A value for the lumped parameter, p, is calculated from the input data and the maximum dimensions of the pool are determined according to the correlation derived in Chapter II. Then, using the contour equation, which is a function of the maximum dimensions, the computer generates a series of points which define the shape of the interior boundary in the temperature field. If projected on the x-axis (i.e., the longitudinal center line) of the pool, the points would be

spaced 5/100 of an inch apart. This spacing allows from 10 (0.5 inch pool length) to 20 points in defining the shape of the boundary.

Grid Layout

Except for minor alterations, the method of arranging the grid is identical to approach developed by Tanbakuchi[20] and is sized approximately 100 lines to the inch in a rectalinear array. The grid is configured such that the specified thermocouple location appears at the intersection of a row and a column. A schematic of the grid forming a computational block is presented in Figure 2.9. Columns are arranged parallel to the center line (i.e., column number 1) of the pool; rows perpendicular. The intersection of column 1 and row 1 mark the origin of the coordinate system. In the output, rows forward, or in the direction of welding, are identified as positive quantities.

Initializing the Grid Nodes

Nodes within and on the pool boundary are given values of one ($T^* = 1$) while the exterior boundary nodes are set to zero. As suggested by Tanbakuchi,[20] the intervening nodes are initialized with Rosenthal's temperature distribution equation. Initializing the nodes considerably reduces the number of iterations required to define the temperature field.

Calculation of Temperatures

A Gauss-Seidel type iteration, which makes use of the

# COMPUTATIONAL BLOCK

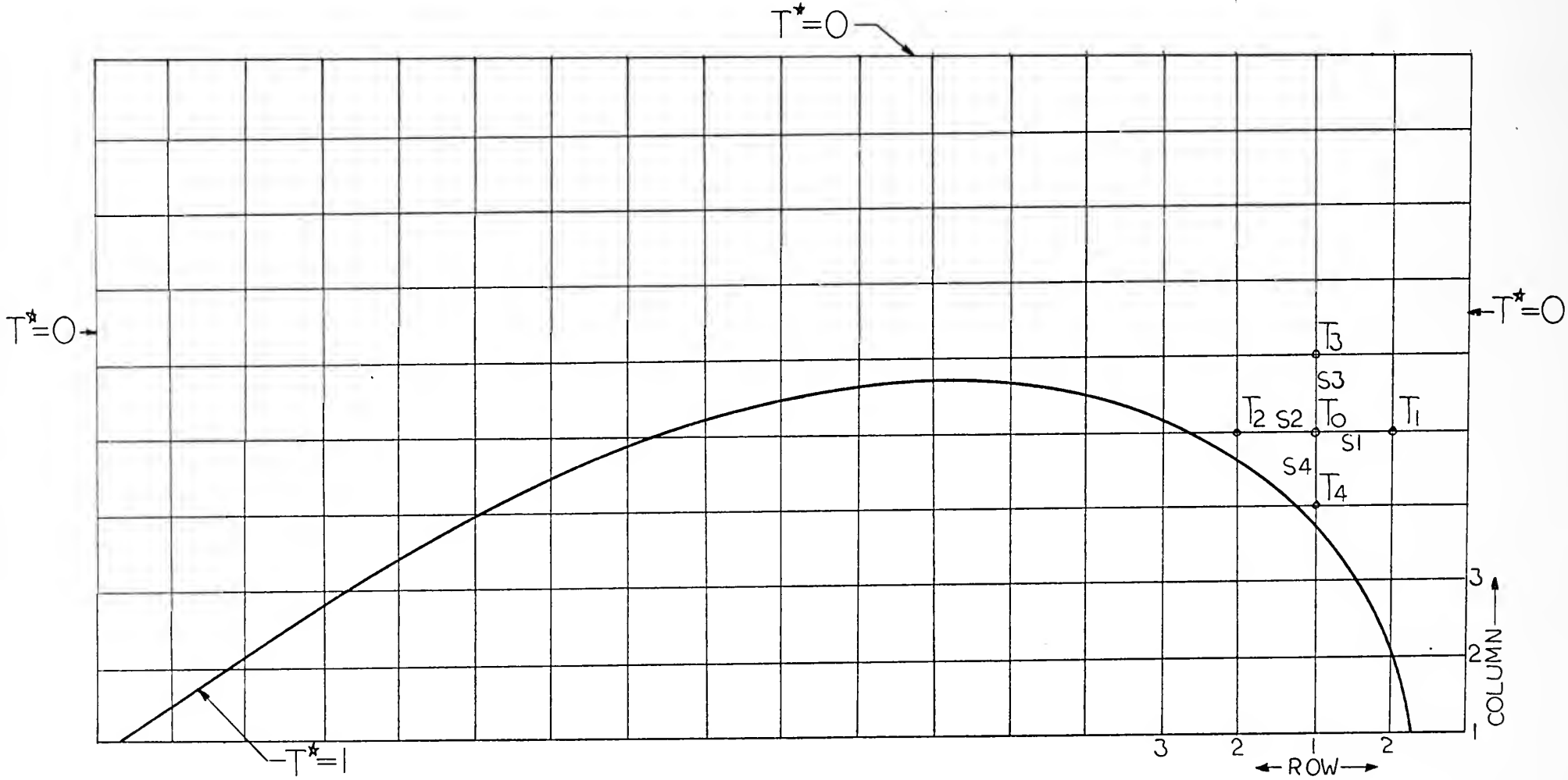


NOT TO SCALE

FIGURE 2-9

latest available temperatures, is performed until the specified accuracy is reached. The program begins each iteration cycle at the interior boundary to avoid excessive computation in that part of the field initially at zero normalized-temperature. Calculation of the value for the heat loss term is accomplished by a search routine which locates the node temperature on the boiling curve and computes the appropriate quantity.

# CHAPTER III

## UNDER WATER EXPERIMENT

The experimental verification portion of the thesis consisted of three steps: Production and measurement of molten pools made in air, production and measurement of molten pools made under water, and measurement of temperature changes in a specimen being welded under water.

### A. EQUIPMENT

The same equipment shown schematically in Fig. 3-1, was used for all three steps mentioned above and consisted of the following:

1. Water Tank
2. Gravity Welding Stand
3. Power Source
4. Blow-Out System
5. Temperature Recorders
6. Current, Voltage, and Time Recorders.

Water Tank. The welding experiments were conducted in a steel tank measuring four feet long by three feet high by two feet deep. The exterior of the tank was sheathed in wood and rubber matting to prevent electrical shocks. A platform, containing clamps for securing the specimen, was fitted to the inside of the tank. The platform was located one foot from the top of the tank so that the electrode, but not the electrode holder, would be submerged in the water. The tank was

# EQUIPMENT SCHEMATIC

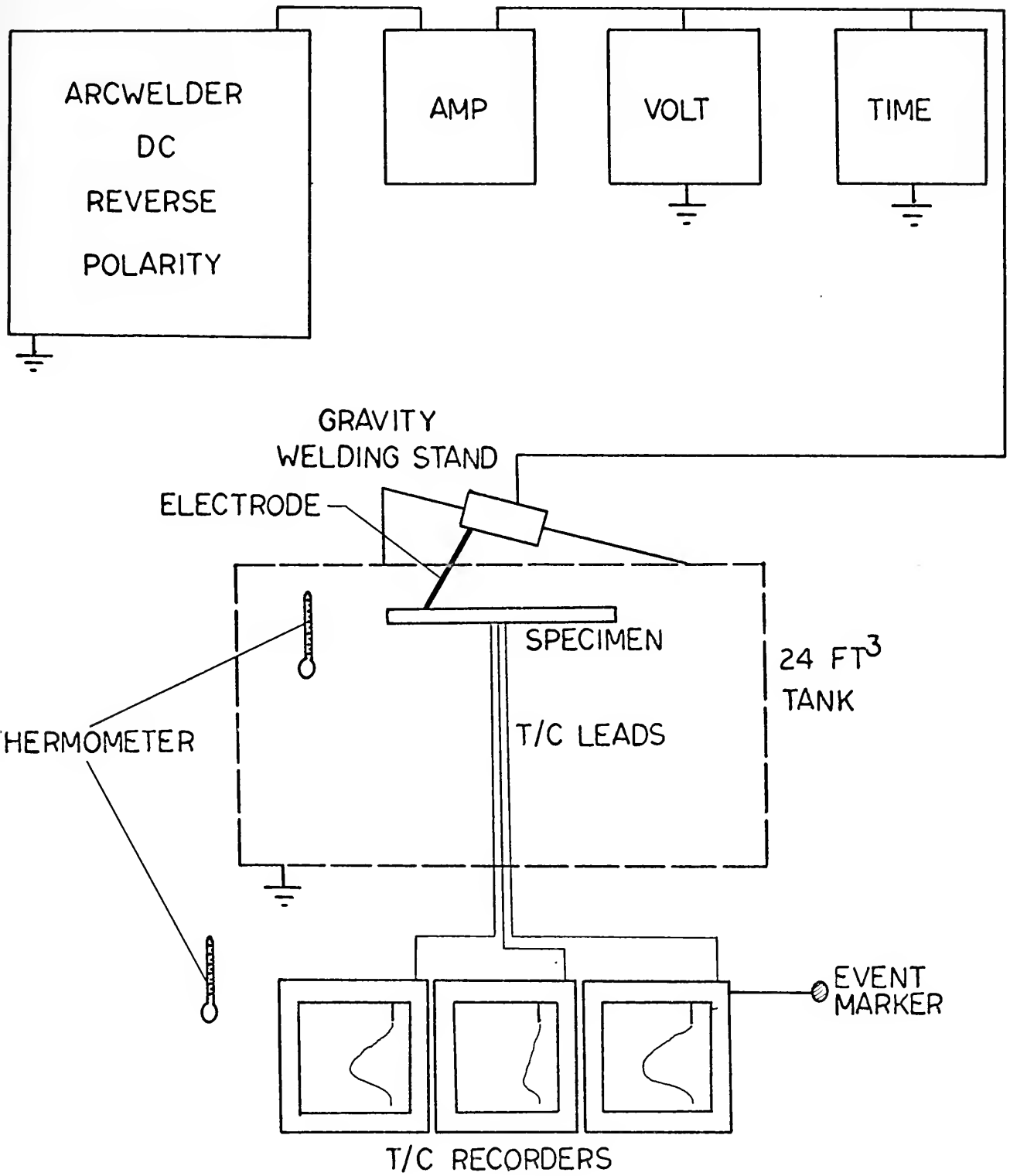


FIGURE 3-1

filled by a line supplying ordinary tap water (Boston, Mass.) and drained by gravity discharge. The tank was grounded to the power source.

Gravity Welding Stand. A Japanese gravity welder was modified and fitted to the top of the tank. The device consisted essentially of a common stick electrode holder fastened to a carriage which could be moved along an inclined rod. A guide was fitted to the rod so that the electrode would draw a straight bead on the specimen. The holder was adjusted to the carriage until the electrode maintained a constant angle of fifty-one degrees relative to the surface of the specimen in the plane of travel and ninety degrees in the plane perpendicular to direction of electrode travel. The tripping mechanism on the carriage, which rotated the electrode up and away from the specimen at the end of travel, was adjusted so that the arc would be broken after approximately six inches of weld bead was drawn.

Power Source. A Lincoln arc welder capable of supplying up to 40 volts and 350 amperes direct current was used as the power source. The device was set to operate on reverse polarity. This arrangement was selected as being similar to power sources for actual under water welding.

Pool Blowout System. A system for ejecting the molten metal from the specimen to form a weld crater was constructed and consisted of a nozzle, foot switch, and nose connected to a

400 psi air line. The nozzle was mounted on a swivel-necked holder so that adjustments could be made in directing the flow of air into the molten pool. The holder and nozzle combination were clamped to the welding platform inside the tank. Several preliminary experiments were conducted to determine the direction and angle of the jet. After considering several possible locations, it was decided that having the nozzle discharge along the axis of the bead but opposite to the direction of welding would give satisfactory results. The nozzle angle was adjusted so that the air would jet into the head of the pool, directing the molten metal back into the tank, away from the operator stationed behind the gravity welding stand. Once the proper relationships were determined, the nozzle was securely fastened in place for the duration of the experiment.

Temperature Recorders. Three clevite brush, Model 220, recording voltmeters were used to measure the output signal from the thermocouples. Each instrument contained two channels so that a total of six thermocouples could be recorded simultaneously. The event markers were connected electrically and repressing the key on any instrument would cause a simultaneous voltage signal to be recorded on all six channels. The instruments were calibrated at 200°, 700°, and 1000°F by inserting a thermocouple, of the same type and dimensions used in the experiment, into a controlled bath. The chart speed was adjusted to 25MM/sec and the gain to

1MV/Division (or, 50 MV total scale).

Common mercury-in-glass thermometers were selected to determine water and air temperatures. One thermometer was taped near the terminals of the recorders to measure the cold junction temperature; the other was suspended in the water to the depth of the specimen (approximately six inches below the surface at the far end of the tank).

Current, Voltage and Time Recorders. A General Electric D-C (0.400 amp.), Model 10H, recording ammeter was used to measure the current flowing in the welding circuit. An Esterline Angus (0.100V) recording voltmeter was selected to measure the operating voltage during welding. A timing device consisting of a General Time Co., Model 320-1, electric clock connected to a circuit breaker was used to measure the amount of time required to lay a given length of weld bead. When the arc was initiated the breaker would close and start the clock; breaking the arc would cause the clock to stop.Dividing the length of the bead by the elapsed time thus recorded served to indicate the welding speed.

All three instruments had been calibrated by the instrument lab at the Boston Naval Shipyard and were assumed to be recording properly.

## B. MATERIALS

The criteria used in selecting materials for the

experiment was based upon their being readily available at low cost and having wide usage in the industry. Three main types of materials were used: Steel plate, welding rod, and thermocouple wire.

Steel Plate. All specimens were cut from cold rolled mild steel (A.I.S.I. 1010) sheets. Three different thicknesses were selected: 1/16", 1/8", and 1/4". For the pool measurement portion of the experiments the sheets were cut into 4" by 6" sections; the specimens in which temperatures would be measured were sized 6" by 12". Both sides of all specimens were cleaned by grit blasting to provide a uniform surface.

Welding Rod. E7018-A1, 3/16" Dia., stick electrodes were found to be suitable for the experiment. This metal core of rod tended to melt faster than the flux covering disintegrated permitting the electrode to be "dragged" across the specimen during the under water operation. This feature was critical since the arc would not be observed while under water. In essence, the flux covering formed a hollow cylinder which shielded the arc from the water, and maintained the proper length necessary to sustain the arc. Since the duration of submergence in water was short (20 to 30 sec!), the electrodes were not coated with any water-proofing materials.

Thermocouples. Chromel-Alumel Type K, .020" Dia., thermocouples were selected to measure temperature changes occurring

during welding. The selection of the size required a compromise between the ability to withstand high temperatures (large diameters), and fast response (small diameters). Furthermore, the thermocouple junction should form a point (ideally) in the specimen to avoid thermal gradients. Consequently, the diameter chosen was the smallest considered practical for the experiment.

## C. EXPERIMENTAL PROCEDURE

The experiment consisted of three parts: a) production of pool craters, b) temperature measurement, and c) reduction of data.

Production of Pool Craters. Molten pools were first produced by welding in air, then under water. The essential steps for this part of the experiment were the same for both processes:

1. Specimen aligned on work table.

1a. If an under water pool was desired the tank was then flooded until the specimen was covered by six inches of water.

2. The power source was turned on and given a five minute warm up period.

3. An electrode was selected and inserted into the holder.

4. The holder and carriage on the welding stand were manipulated so that the tip of electrode was slowly brought to the point where the arc would start.

5. The carriage was drawn manually down the incline of the welding stand, laying a bead on the surface of the specimen.
6. The blow-out system was activated by depressing the foot switch at the same time the carriage reached the tripping point.
7. The voltage, current, time, ambient temperature, and bead length were recorded for the run.
8. The dimensions of the pool crater - maximum width length, and contour - were measured under a Bausch and Lomb microscope equipped with a movable, micrometer table. For the experiment, the ranges of the variables involved were:

| | |
|---|---|
| Current | 100 - 300 amps |
| Voltage | 20 - 30 volts |
| Welding Speed | 50 - 125 Ft/Hr |
| Ambient Temp | 70 - 73°F (air) |
| | 40 - 43°F (water) |

Current was varied by adjusting the rheostat on the power source in steps of 25 amps., while the voltage was allowed to seek its equilibrium value. A particular welding speed could not be chosen prior to a run since manual control was required. However, an acceptable range of speeds were produced by consciously moving the carriage along the guide rod. A mechanical system for better control of welding

speeds was attempted but the problem of starting the arc defeated the project.

The problems connected with producing two-dimensional weld pools by stick electrodes were numerous and it is estimated that only 20% of the runs resulted in acceptable data. The welding stand did not allow the freedom of movement that is normally enjoyed in "Striking" an arc. The low voltages required so small a gap that the electrode was often grounded before the arc could start. In addition, a precise relationship between the heat input and welding speed necessary to produce two-dimensional pools was observed. Since the speed could not be predetermined, there was no assurance that an acceptable pool would result from a run. In practice, a number of runs at various speeds were conducted at a given heat input until the proper pool was obtained.

Temperature Measurement. All runs were conducted under water and the essential steps involved were:

1. Preparation of the specimen.
2. Aligning the specimen with the electrode.
3. Flooding the tank until the level of water was six inches above the surface of the specimen.
4. Turning on the power source and recording equipment.
5. Welding a bead on the surface of the specimen.
6. Recording temperature, time, voltage, current and bead length for the run.

The preparation of the specimen involved drilling holes at specified locations and mounting the thermocouples. Twelve .040" Dia. holes were drilled in each plate in a manner that assured that the axis of the hole was perpendicular to the surface of the plate. (See Fig. 3.2 for relative locations.) The centers of the holes formed a locus of points five degrees from the center line of the plate. An additional hole (#12) was drilled near the edge of the specimen to record boundary temperatures. (During the experiment, however, it was observed that placing a thermocouple at this location -- about six inches from the center line -- was unnecessary since the temperature variation one-half inch from the center line was negligible!). The distance from the center line to the center of the holes varied from 0.125" for thermocouple locations #1 and #9 to 0.440" for location #8; the center-to-center spacing along the center line of the specimen was approximately one-half inch. This arrangement permitted temperature measurement within the heat affected zone but allowed sufficient spacing for mounting thermocouples.

The thermocouples required special preparation to prevent their shorting out in the water. As shown in Fig. 3-3, water-proofing required sealing all joints with expoxy cement and covering the leads with a plastic sleeve shrunk to form a tight fit. (In their commercial form, the thermocouples had already been covered with asbestos and silicon

# THERMOCOUPLE ARRANGEMENT

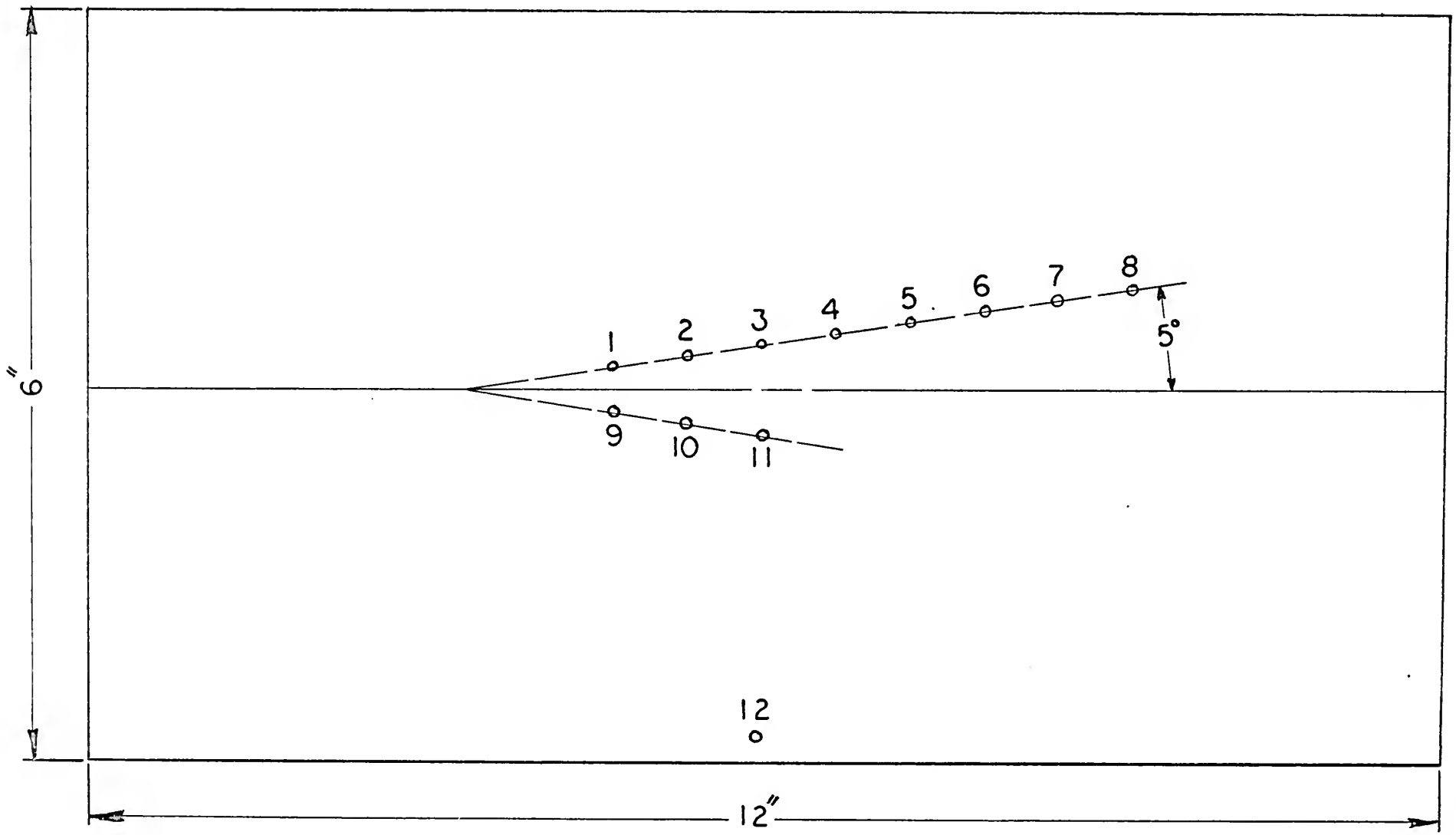


FIGURE 3-2

# THERMOCOUPLE INSTALLATION

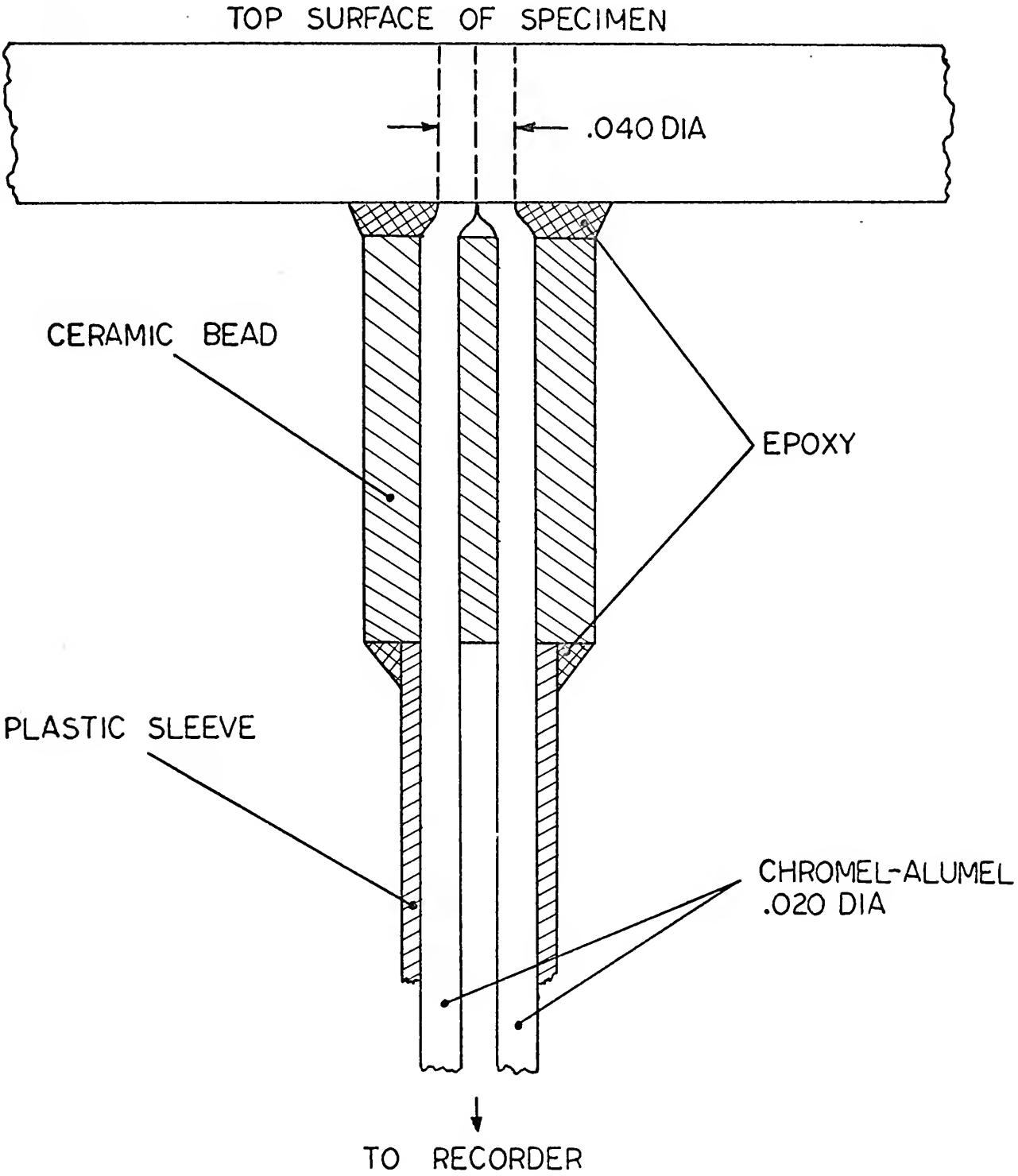


FIGURE 3-3

impregnated fiberglass.) A ceramic bead, containing separate holes for each thermocouple, was installed to prevent the leads from making a junction outside the plate. The exposed leads were cleaned with emery cloth and inserted through one of the holes in the specimen. A pair of pliers were then used to draw the leads through the hole until the ceramic bead was nearly flush with the bottom of the plate. The edges of the hole on the top surface of the specimen were given a light peening with a small prick punch, and the leads extending above the specimen were then cut off and ground flush with the surface. The purpose of the peening was to give the thermocouples a preferential junction at the surface of the specimen, and avoid, as much as possible, thermal gradients in the specimen resulting from pools that were not exactly two-dimensional. In this way, six thermocouples were installed in each specimen, leaving six open holes. Twelve specimens were prepared such that no specimen duplicated another with respect to thermocouple locations.

All specimens, with one exception, were 1/8" thick: the 1/16" plates burned through too easily and the penetration required for two-dimensional pools was not obtained with the 1/4" plates. One 1/4" specimen was prepared, however, in order to determine the response of the model to a situation where the shape of the heat source was not the ideal configuration.

A prepared specimen, containing six thermocouples,

was then placed on the table in the tank, aligned with the electrode, and clamped firmly in position. (It was first hoped that the electrode could be made to follow exactly the center line of the plate, thereby simplifying measurements taken to locate the thermocouples. Actual runs revealed, however, that although the bead would run straight it could not be made to follow any predetermined path with sufficient accuracy. Consequently, the positions of the thermocouples with respect to the longitudinal axis of the weld bead were re-calculated following the run.) The tank was filled with water until the specimens were submerged to a depth of six inches. The thermocouples were connected to the recorders and the power source turned on. The electrode was guided into position in preparation for starting the arc. At the instant of arc initiation the laboratory assistant depressed the event key on a recorder which placed marks on all six output tapes simultaneously. The carriage containing the electrode was then either allowed to move freely or was drawn by hand with a slight steady pressure down the incline of the welding stand until the tripping point was reached. The ambient temperatures (air and water), run time, current, voltage, and bead length were recorded.

## D. DATA REDUCTION

The maximum dimensions of the weld pool were correlated to the lumped parameter, p, by means of a least squares curve

fitting routine available as an option from M.I.T.'s computer library. The details of the program have been presented in Appendix 7. The correlating parameters for the equation determining the contour of the weld pool were found by a non-linear least squares curve fitting routine. (Also see Appendix 7.)

The Y-displacement of a thermocouple was measured along a line running through the center of the thermocouple hole and perpendicular to the center line of the weld bead. The X-displacement was measured along the center line from the point of arc initiation to the intersection of the perpendicular. A computer program was written to reduce the thermocouple output. The program scaled the distances on the output tape by the ratio of the chart to the welding speed, and ensured that the measured temperatures were in the same coordinate system as the model. The program, with sample input data, appears in Appendix 7.

# CHAPTER IV

# RESULTS AND CONCLUSIONS

## A. TEST RESULTS

The experimental portion of the thesis consisted of two parts: a) determining the correlation constants used to define the shape of the heat source, and b) measuring the temperature distribution in the specimen during welding. The results of the pool contour study have already been presented and described in Chapter II; it need only be added here that the results were in good agreement with theoretical predictions.

The results of comparing the temperature distribution as predicted by the model with that measured by experiment is represented in Figures 4-1 and 4-2. The coordinates have been presented in dimensionless form. The ordinates may be transformed to real temperatures by the relation

$$T = 2677T^* + 503 \quad , {}^{\circ}R$$

The abcissa for Figure 4-1 can be converted to inches with the relation

$$x = x^*/40.59 \quad , \text{in.}$$

and for Figure 4-2

$$x = x^*/41.02 \quad , \text{in.}$$

where the starred terms are the dimensionless values.

In the figures, $Y_m$ is the distance from the weld center

FIG 4-1: CALCULATED AND MEASURED TEMPERATURE CURVES

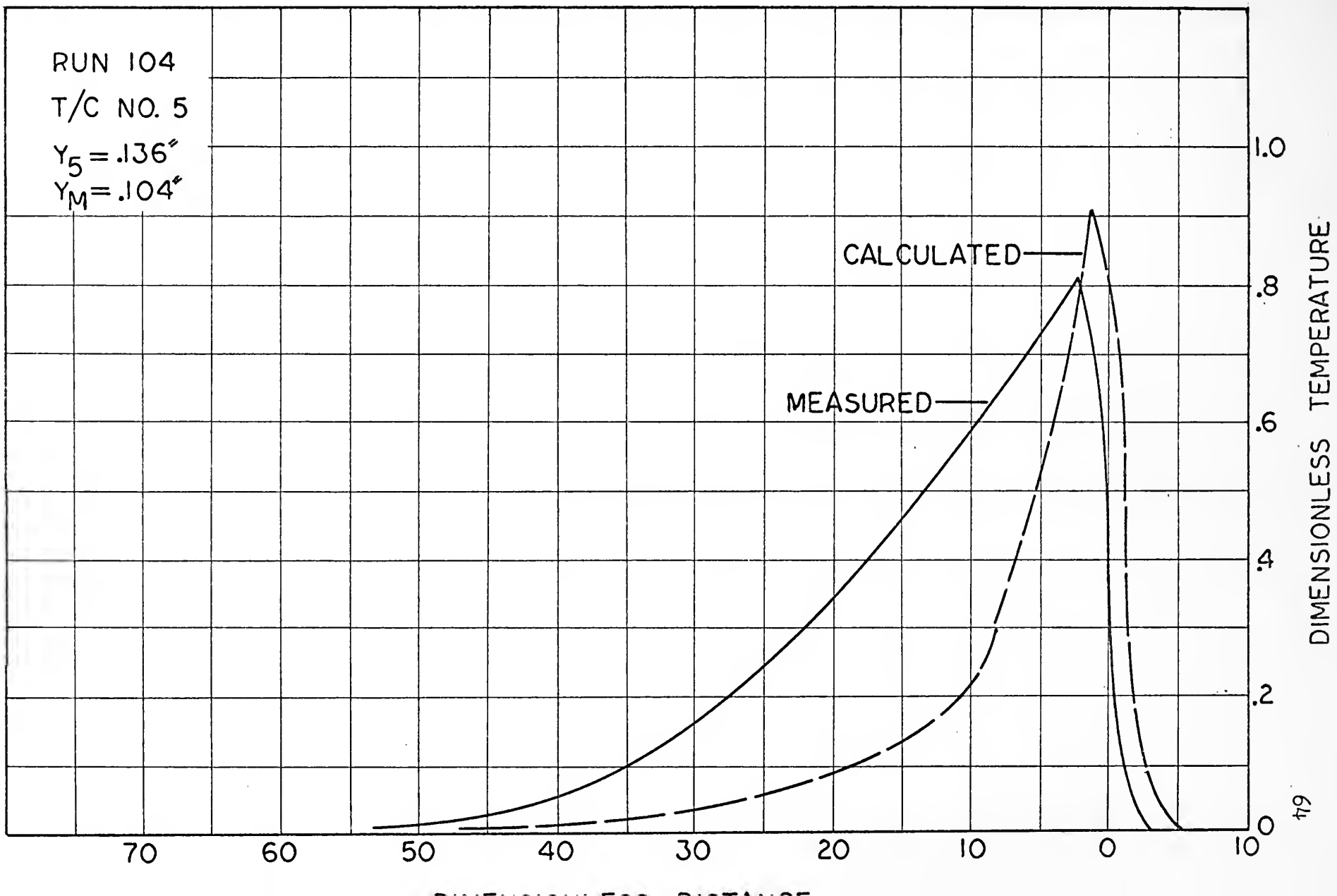

FIG 4-2: CALCULATED AND MEASURED TEMPERATURE CURVES

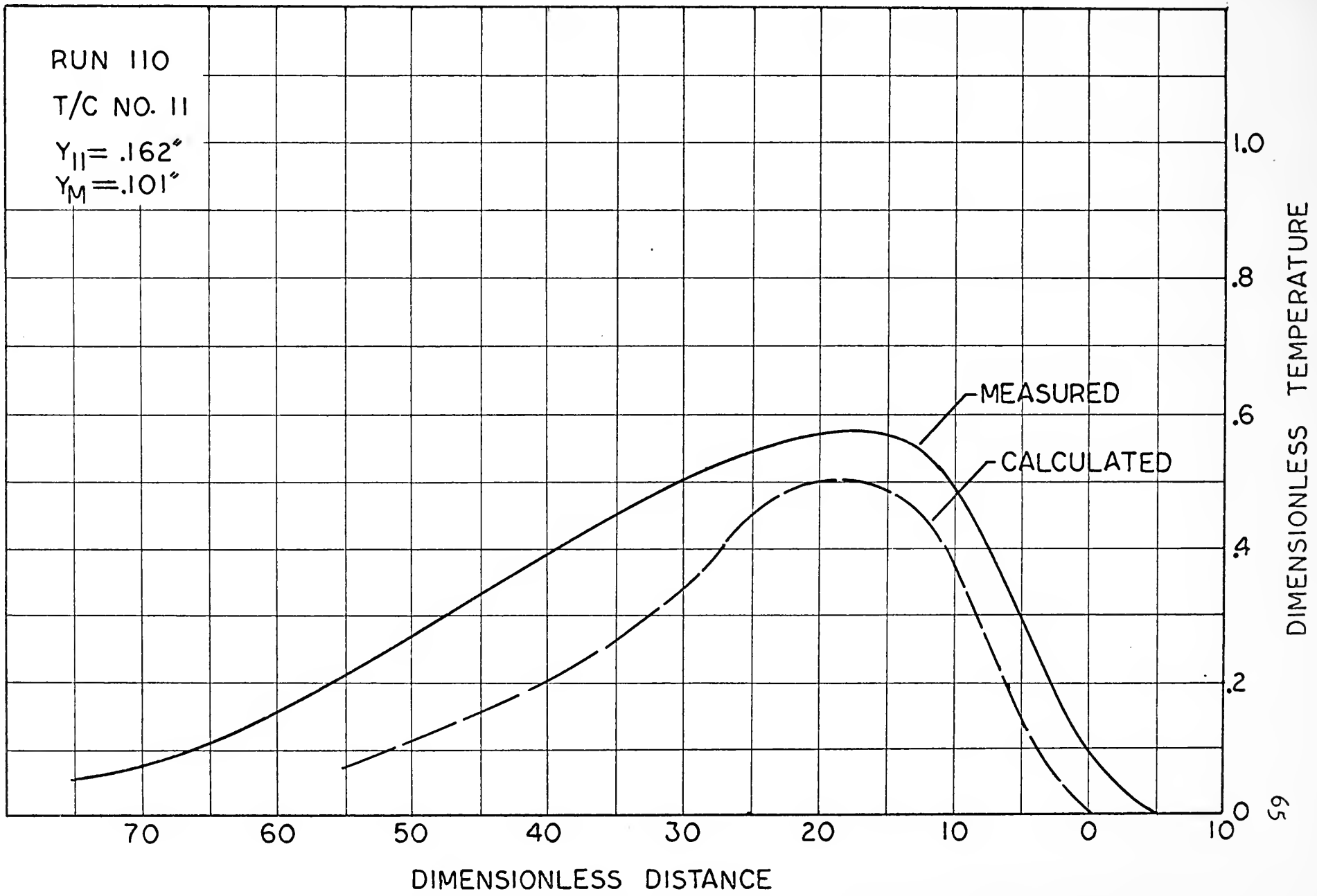

line to the point of maximum pool width; $Y_5$ (Figure 4-1) and $Y_{11}$ (Figure 4-2) are the locations in the specimen at which the temperatures were measured.

Figure 4-3 has been included so that a comparison might be made between the predicted temperature distribution for underwater and air welding: the curve labeled "without boiling" represents air welding.

Figure 4-4 presents the predicted temperature distribution at various distances from the center line.

Figure 4-5 represents a comparison between measured and calculated cooling curve slopes as a function of distance from the maximum pool width. The slope of a given curve was measured at the average temperature and was defined to be the change in dimensionless temperature with respect to the change in dimensionless distance. For example, the average measured temperature for Run 104 (Figure 4-1) was found to be 0.4 and the slope at that point was -0.025.

## B. ANALYSIS OF DATA

Prediction of peak temperatures within the haz was found to be reasonably accurate. The average error was 13% of the measured temperature with the largest variation occurring at locations nearest the molten pool.

The cooling portions of the predicted and measured curves were not found to be in good agreement. As a quantitative

# FIG 4-3: TEMPERATURE COMPARISON CURVES

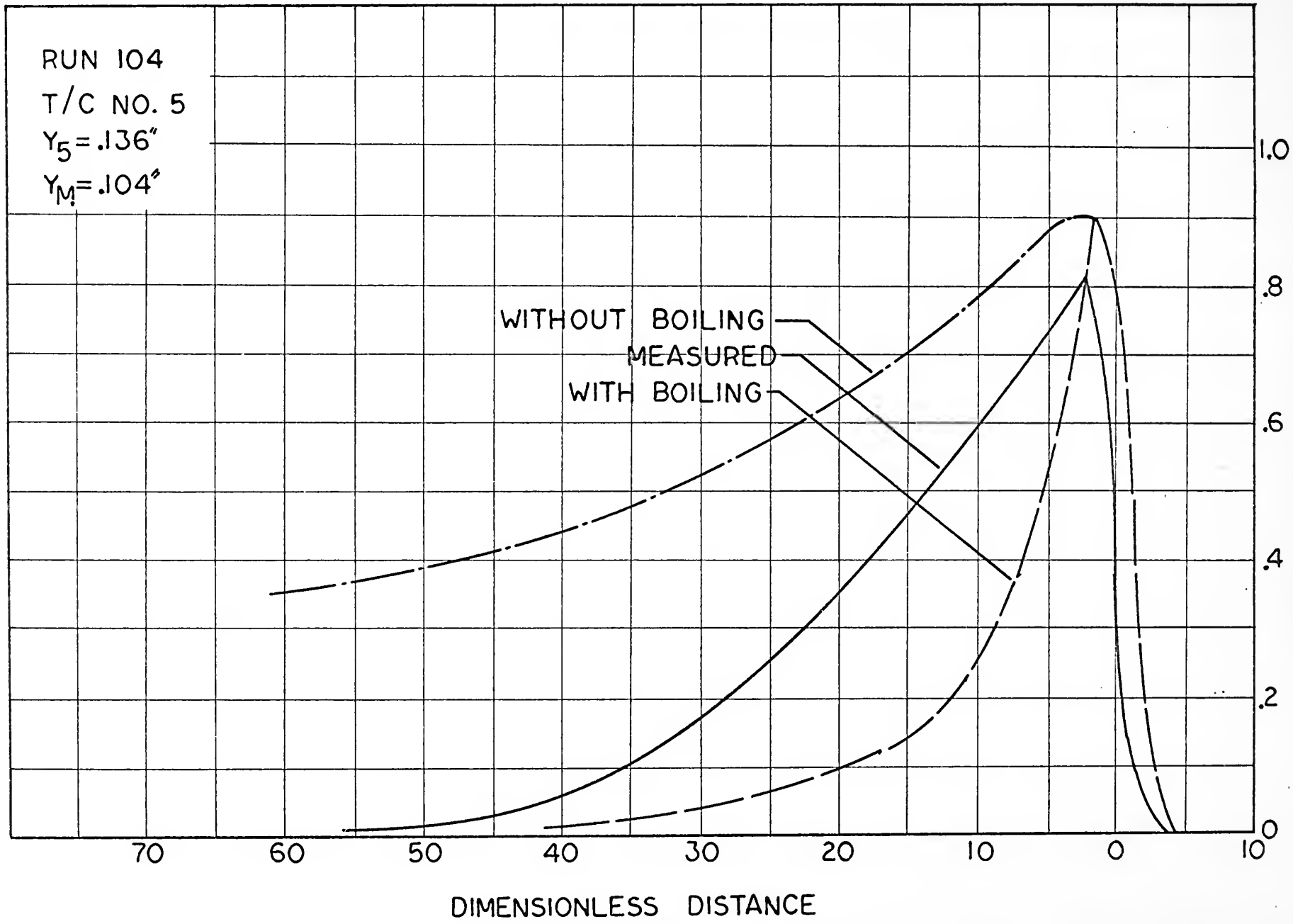

FIG 4-4: THEORETICAL TEMPERATURE DISTRIBUTION

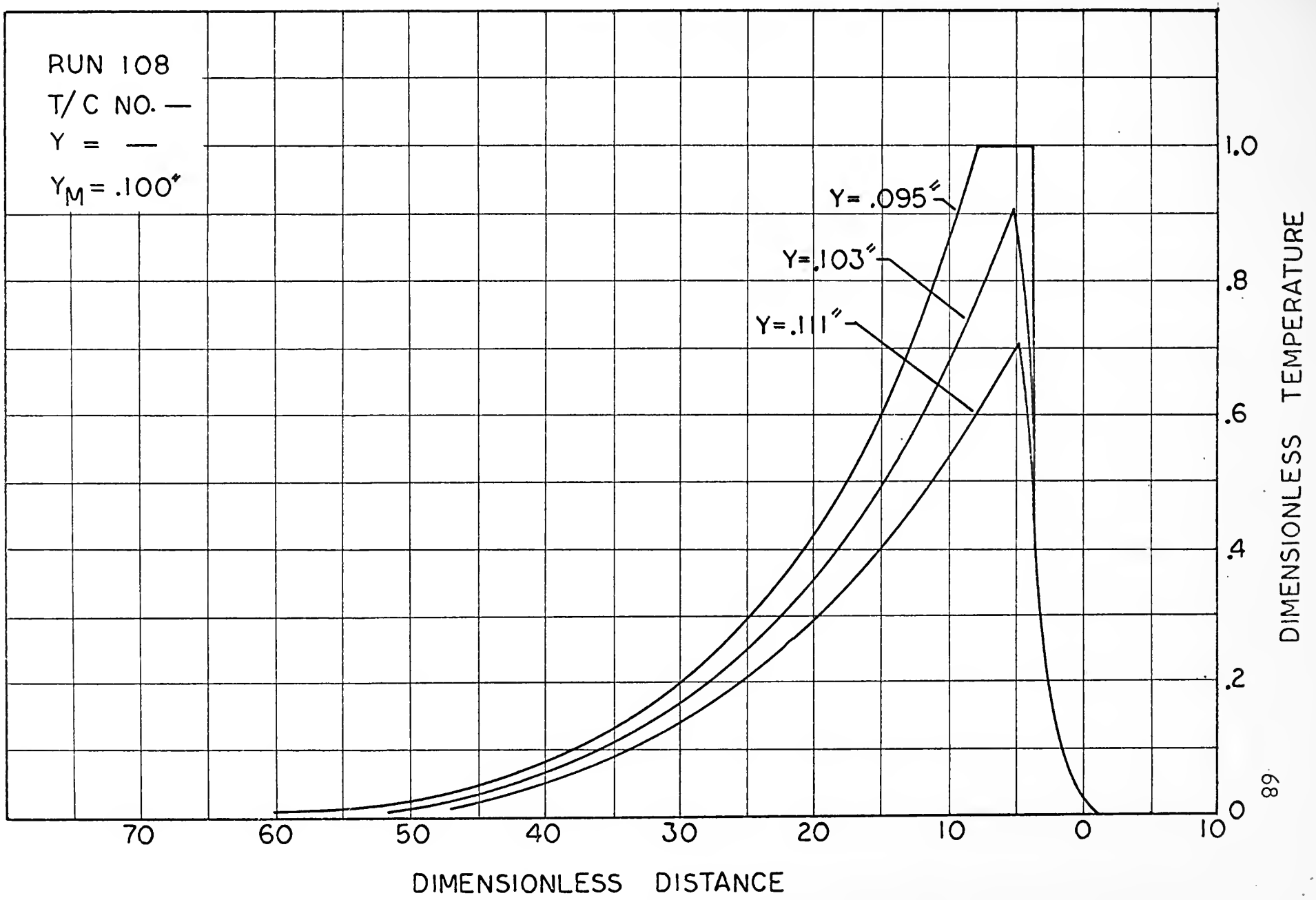

FIG 4-5: COMPARISON OF COOLING CURVE SLOPES

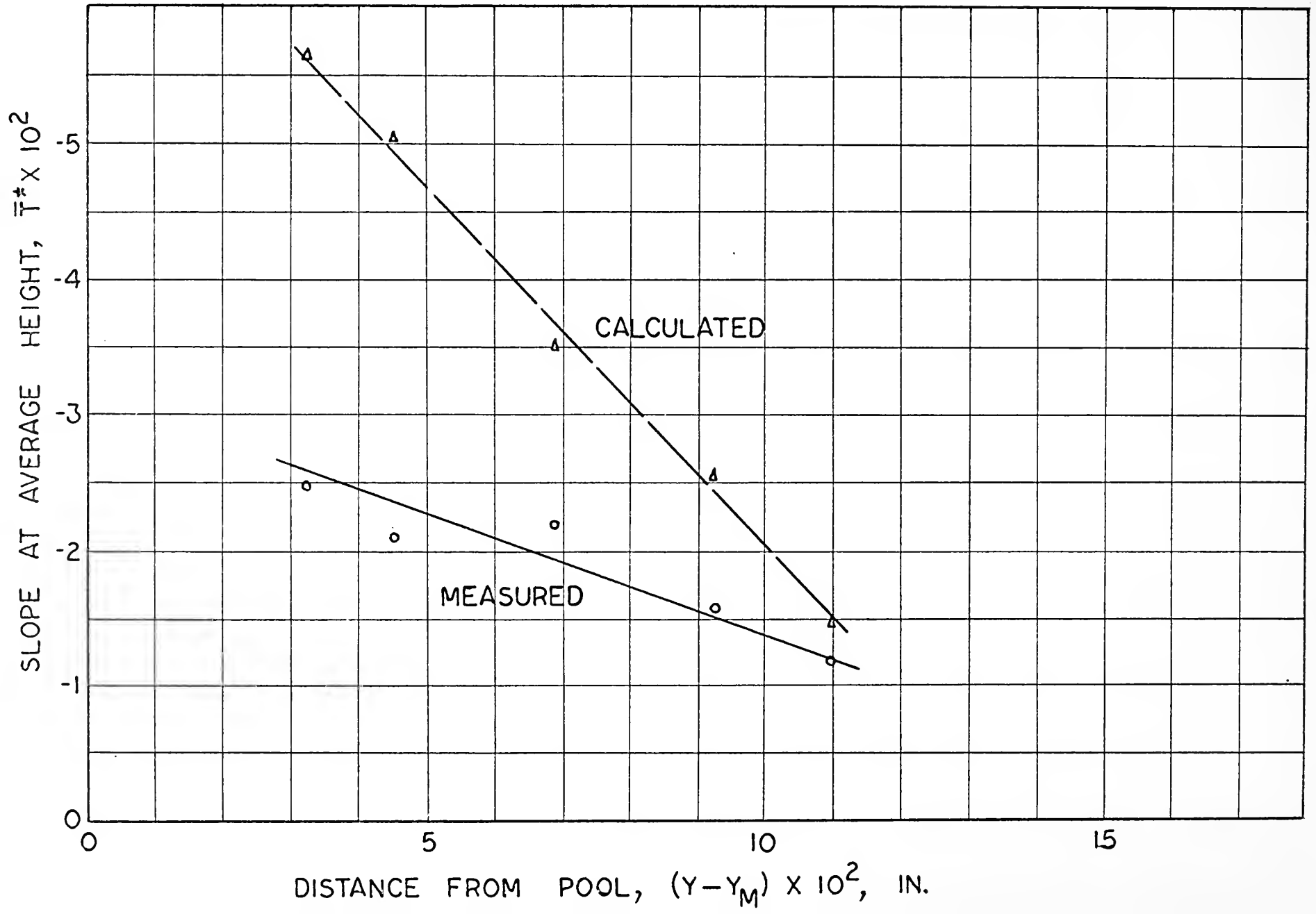

indication slopes were measured at the average temperatures of the distribution curves and plotted as in Figure 4-5. Near the molten pool the predicted slopes were in error by as much as 200% and converged with the measured values only at the edges of the haz.

Consequently, an evaluation of the effect of boiling heat transfer was made by neglecting such losses (i.e., as if the specimen were welded in air) with results presented in Figure 4-3. Such an analysis indicated that conventional boiling models were inappropriate when applied to the underwater welding process. However, nothing in the data suggested what mechanism might be controlling heat losses.

It can be speculated, nevertheless, that the gases generated from the oxidizing flux and possible dissociation of water molecules could disrupt the normal process of boiling heat transfer. These gases would collect at the tip of the electrode to form a protective envelope over a portion of the specimen's top surface. Within the envelope the predominant form of heat transfer would be radiation while exterior areas could support some boiling losses. The bottom surface (opposite to the side being welded) would not see the shielding gases and, consequently, heat losses would occur through boiling. This mixed form of heat losses would explain the slower rate of cooling observed during the experiment.

Unfortunately, the process just described has not been described in the literature and the development of the

appropriate model was beyond the scope of this research study.

## C. CONCLUSIONS

The object of this thesis was to develop a model that would predict the temperature distribution in thin plates welded underwater.

It was found that the model was reasonably accurate in predicting peak temperatures within the heat-affected-zone, but that the degree of error in predicting cooling rates was unacceptably large. The initial assumption that heat losses can occur by conventional mechanisms of boiling heat transfer was, therefore, considered invalid. Rather, the proper model for heat losses must consider the effect of the gases generated during the welding operation.

Given the above conclusions, it is recommended that

1. Heat transfer fluxes be correlated for the case involving full boiling with radiation on one surface while the opposite surface supports only radiation, and
2. The study should consist of vertical as well as horizontal surfaces.

# APPENDIX 1

## TRANSFORMATION TO QUASI-STEADY STATE

$$K\left[\frac{\partial^2 T}{\partial x^2} + \frac{\partial^2 T}{\partial y^2}\right] + \frac{\partial k}{\partial x}\frac{\partial T}{\partial x} + \frac{\partial k}{\partial y}\frac{\partial T}{\partial y} + W_i = \rho c \frac{\partial T}{\partial t} \qquad (1)$$

in the steady state system, the origin will be defined to be centered at the moving arc. Hence, the following transformation-equations apply:

$$x = \acute{x} + v_t$$

$$t = \acute{t}$$

where the primed quantities refer to the new system.

Hence,

$$\partial\acute{x} = \partial x \quad , \quad \partial\acute{x} = -v\partial t \quad , \quad \partial\acute{t} = \partial t \quad , \quad \frac{\partial\acute{t}}{\partial x} = 0$$

with these partial relationships, derivatives in the new system become,

$$\frac{\partial T}{\partial x} = \frac{\partial T}{\partial \acute{x}}\frac{\partial \acute{x}}{\partial x} + \frac{\partial T}{\partial \acute{t}}\frac{\partial \acute{t}}{\partial x} = \frac{\partial T}{\partial \acute{x}}$$

$$\frac{\partial^2 T}{\partial x^2} = \frac{\partial^2 T}{\partial \acute{x}^2}$$

$$\frac{\partial T}{\partial t} = \frac{\partial \acute{x}}{\partial t}\frac{\partial T}{\partial t} + \frac{\partial T}{\partial t}\frac{\partial \acute{t}}{\partial \acute{t}} = -v\frac{\partial T}{\partial \acute{x}} + \frac{\partial T}{\partial \acute{t}}$$

Since temperature is constant in the steady state system

$$\frac{\partial T}{\partial \acute{t}} = 0$$

and

$$\frac{\partial T}{\partial t} = -v\frac{\partial T}{\partial \acute{x}}$$

Substituting into equation (1) and dropping prime notation,

$$\frac{\partial^2 T}{\partial x2} + \frac{\partial^2 T}{\partial y2} + \frac{1}{k}\left[\frac{\partial k}{\partial x}\frac{\partial T}{\partial x} + \frac{\partial k}{\partial y}\frac{\partial T}{\partial y}\right] + \frac{W_i}{k} = \frac{-v}{\alpha}\frac{\partial T}{\partial x}$$

where

$$\alpha = k/\rho c$$

The equation is simplified by noticing that

$$\frac{1}{k}\frac{\partial k}{\partial x}\frac{\partial T}{\partial x} = \frac{1}{k}\frac{\partial k}{\partial T}\left(\frac{\partial T}{\partial x}\right)^2$$

Finally,

$$\frac{\partial^2 T}{\partial x^2} + \frac{\partial^2 T}{\partial y^2} + \frac{1}{k}\frac{\partial k}{\partial T}\left[\left(\frac{\partial T}{\partial x}\right)^2 + \left(\frac{\partial T}{\partial y}\right)^2\right] + \frac{W_i}{k} = \frac{-v}{\alpha}\frac{\partial T}{\partial x}$$

# APPENDIX 2

## DERIVATION OF HEAT LOSS TERMS

### A. Nucleate Boiling

The Rohsenow[15] correlation is

$$\frac{C_L(T_w-T_{SAT})}{h_{fg}} = C_{Sf}\left[\frac{(g/A)_N}{u_L h_{fg}}\sqrt{\frac{g_o\sigma}{g(\rho_L-\rho_v)}}\right]^{\frac{1}{3}} Pr_L \qquad 1.7$$

All quantities are taken at saturation (14.7 psia, 212°F) from the CRC HANDBOOK OF TABLES FOR APPLIED ENGINEERING SCIENCE.

$C_L$ = 1.005 BTU/lb-$^oR$

$Pr_L$ = 1.9

$u_L$ = 62.5 x $10^{-7}$ lb-sec/ft$^2$

$g_o/g$ = 1

$h_{fg}$ = 970.3 BTU/lb

$\rho_L$ = 59.8 lb/ft$^3$

$\rho_v$ = 0.0374 lb/ft$^3$

$\sigma$ = 40.4 x $10^{-4}$ lb/ft

Substitution of these values into the nucleate boiling equation yields,

$$q_N = [1.542(T_w-T_{SAT})]^3 \quad , \quad \text{BTU/hr-ft}^2 \ .$$

in normalized form,

$$q_N^* = [1.542T^* \ (T_M-T_{SAT})]^3$$

where,

$$T^* = \frac{T_w - T_{SAT}}{T_M - T_{SAT}} \quad .$$

B. Film Boiling

The Borishansky relation reported by Jordan[25] is

$$q_F = 0.425 \left[ \frac{K_v^3 g \rho_v (\rho_L - \rho_v)(h_v - h_L)}{u_v [\sigma / g(\rho_L - \rho_v)]^{\frac{1}{2}}} \right]^{\frac{1}{4}} (T_w - T_{SAT})^{0.75}$$

where,

$\rho_L$ = 59.8 lb/ft$^3$

$\rho_v$ = 0.0374 lb/ft$^3$

$\sigma$ = 40.4 x 10$^{-4}$ lb/ft

$h_{fg}$ = 970.3 BTU/lb

$u_v$ = 2.5 x 10$^{-7}$ lb-sec/ft$^2$

$K_v$ = 14.3 x 10$^{-3}$ BTU/hr-ft-$^\circ$R

Substitution of these values into the film boiling equation yields,

$$q_F = 32.4(T_w - T_{SAT})^{0.75}, \quad \text{BTU/hr-ft}^2 \quad .$$

where the normalized form becomes,

$$q_F^* = 32.4[T^*(T_M - T_{SAT})]^{0.75}$$

C. Transition Regime

The proposed relation for heat flux in this regime is

$$q_T = M(T_w - T_{SAT})^b$$

to which the boundary conditions are applied:

1) $q_T = q_N$ at $T_w$ = 300°F
2) $q_T = q_F$ at $T_w$ = 500°F

then,

$$1a) \quad M(300-212)^b = [1.542(300-212)]^3 = 2.34 \times 10^6$$

$$2a) \quad M(500-212)^b = 32.4(500-212)^{0.75} = 2265.11$$

for which

$$m = 2265.11$$

$$b = 5.86$$

Now, the transition heat flux equation becomes,

$$q_T = 2265.11 \left(\frac{288}{T_w - T_{SAT}}\right)^{5.86}$$

and the normalized relation,

$$q_T^* = 2265.11 \left[\frac{288}{T^*(T_M - T_{SAT})}\right]^{5.86}$$

D. Radiation Heat Transfer

For the heat flux during radiation,

$$q_R = \sigma F_e F_a (T_w^4 - T_{SAT}^4).$$

Since the specimen is completely enclosed by the liquid environment,

$$F_a = 1$$

and

$$F_e = 1/(1/e_1 + 1/e_2 - 1)$$

the emissivity of steel cleaned by sandblasting is approximately,

$$e_1 = 0.8$$

while the water is very nearly a black body and

$$e_2 = 0.95 \quad .$$

The heat flux equation becomes,

$$q_R = 0.1317 \times 10^{-8} (T_w^4 - T_{SAT}^4)$$

and in normalized form,

$$q_R^* = 0.1317 \times 10^{-8} \left\{ \left[ T^* (T_w - T_{SAT}) + T_{SAT} \right]^4 - T_{SAT}^4 \right\}$$

# APPENDIX 3

## Derivation of Pool Boundary Equations

Pavelic's derivation of the pool boundary equation can be summarized as follows:

1. Rosenthal's point source equation is analyzed to obtain the maximum theoretical pool dimensions.
2. A correlation of measured data is obtained based on the predicted relations.
3. A two-dimensional equation is fitted through the boundaries of experimentally obtained pools.

1. The maximum dimensions of the pool.

Rosenthal's equation for the temperature distribution from a point source,

$$T - T_\infty = \frac{Q}{2\pi L\bar{K}} K_o(\bar{\lambda}Vr) \exp[-\bar{\lambda}Vx]$$

where

$Q = 3.415\ EI$ , BTU/HR

$K_o(\bar{\lambda}Vr)$, Bessel Function

$\bar{\lambda}$, Reciprocal of the average diffusivity

V, Welding Speed (Ft/Hr)

L, Plate Thickness (Ft).

With the normalized relations,

$$\bar{\lambda}Vx = x^*$$

$$T^* = \frac{T-T_\infty}{T_m-T_\infty}$$

The temperature equation becomes

$$T^* = \frac{3.415\ EI}{2\pi\bar{\alpha}L\ H_m}\ K_o(r^*)\ \exp\ [-x^*]$$

Define the lumped welding parameter,

$$P^* = \frac{3.415\ EI}{2\pi\bar{\alpha}\ L\ H_m}$$

where,

$$H_m = \bar{\bar{\rho}}\bar{e}\ (T_M - T_\infty).$$

so that (with star notation dropped),

$$T = pK_o(r)\ \exp\ [-x]$$

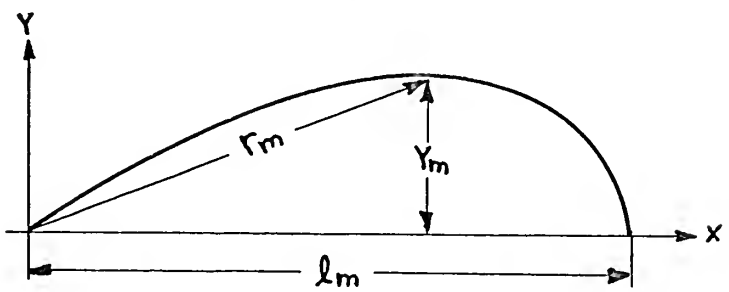


The maximum dimensions are found since,

$$\frac{\partial T}{\partial x} = 0 \quad \text{at maximum width} \qquad 1.$$

$$r = x \text{ and } y = 0 \text{ at maximum length.} \qquad 2.$$

From condition 1., the value for the maximum width is

$$Y_m = r_m \left[ 1 - \left[ \frac{K_o(r_m)}{K_1(r_m)} \right]^2 \right]^{\frac{1}{2}}$$

and from condition 2.,

$$\ell_m = 2r_m \frac{K_o(r_m)}{K_1(r_m)}$$

where $r_m$ is defined at T = 1 and

$$P = \frac{\text{Exp}[-r_m K_o(r_m)/K_1(r_m)]}{K_o(r_m)}$$

2. Pool Contour Equation:

An equation is arbitrarily selected to match the boundary conditions for the pool,

$$\acute{y} = \infty \quad , \text{at} \quad x = 0, \ell_m$$

$$\acute{y} = 0 \quad , \text{at} \quad y = y_m$$

$$y = 0 \quad , \text{at} \quad x = 0, \ell_m$$

A candidate is then,

$$y^2 = BX^m (\ell_m - x)^n$$

From the boundary condition, $\acute{y} = 0$ at $y = y_m$,

$$B = \frac{y_m^2}{\left(\frac{m\ \ell_m}{n+m}\right)^m \left(\frac{n\ \ell_m}{n+m}\right)^n}$$

where "m" and "n" are parameters to be determined experimentally.

## APPENDIX 4

## NORMALIZING THE HEAT FLOW EQUATION

The objective is to nondimensionalize all quantities. Consequently, the dimensionless temperature is defined to be,

$$T^* = \frac{T - T_o}{T_m - T_o}$$

where,

$T_o$ = Ambient temperature

$T_m$ = Melting temperature of the metal

and,

$T^* = 1$ , at the weld pool

$T^* = 0$ , at the specimen edge

the coordinate dimensions are transformed by a length scale, H, so that

$$x^* = x/H$$

$$y^* = y/H$$

By making the appropriate substitutions, we convert the equation of heat flow

$$\frac{\partial^2 T}{\partial x^2} + \frac{\partial^2 T}{\partial y^2} + \frac{1}{k}\frac{\partial k}{\partial T}\left[\left(\frac{\partial T}{\partial x}\right)^2 + \left(\frac{\partial T}{\partial y}\right)^2\right] + \frac{1}{KL}\left(-\dot{q}_R - \dot{q}_B\right) = \frac{-v}{\alpha}\frac{\partial T}{\partial x}$$

to non-dimensional form,

$$\frac{\partial^2 T}{x} + \frac{\partial^2 T}{y} + \frac{1}{k}\frac{dK}{dT}\left[\left(\frac{\partial T}{x}\right)^2 + \left(\frac{\partial T}{y}\right)^2\right] + \frac{H^2}{LK}\left[-q_R - q_B\right] = \frac{-VH}{\alpha}\frac{\partial T}{\partial x}$$

with the star notation dropped.

A value for H can be obtained by examining the

convergence criterion* for the related linear equation*,

$$\frac{\partial^2 T}{\partial x^2} + \frac{\partial^2 T}{\partial y^2} + \frac{H^2}{K}\left(-\dot{q}_R - \dot{q}_B\right) + \frac{VH}{\alpha}\frac{\partial T}{\partial x} = 0$$

Ames[2] suggests that the solution will converge when

$$0 < S < 2\alpha/VH$$

where the value, S, is the grid spacing for the numerical solution. We arbitrarily establish the upper bound on S to be one so that

$$H = 2\alpha/v$$

Since a small grid spacing is desirable for accuracy, we allow the diffusivity, $\alpha$, to assume its least value. Hence,

$$H = 2\alpha_{Min}/v$$

Finally, the complete non-dimensional equation of heat flow becomes:

$$\frac{\partial^2 T}{\partial x^2} + \frac{\partial^2 T}{\partial y^2} + \frac{1}{k}\frac{dK}{dT}\left[\left(\frac{\partial T}{\partial x}\right)^2 + \left(\frac{\partial T}{\partial y}\right)^2\right] + \frac{4\alpha_{Min}^2}{LV^2K}\left(-\dot{q}_R - \dot{q}_B\right) = \frac{-2\alpha_{Min}}{\alpha}\frac{\partial T}{\partial x}$$

## APPENDIX 5

## FINITE DIFFERENCE EQUATION OF HEAT FLOW

Consider the following grid node:

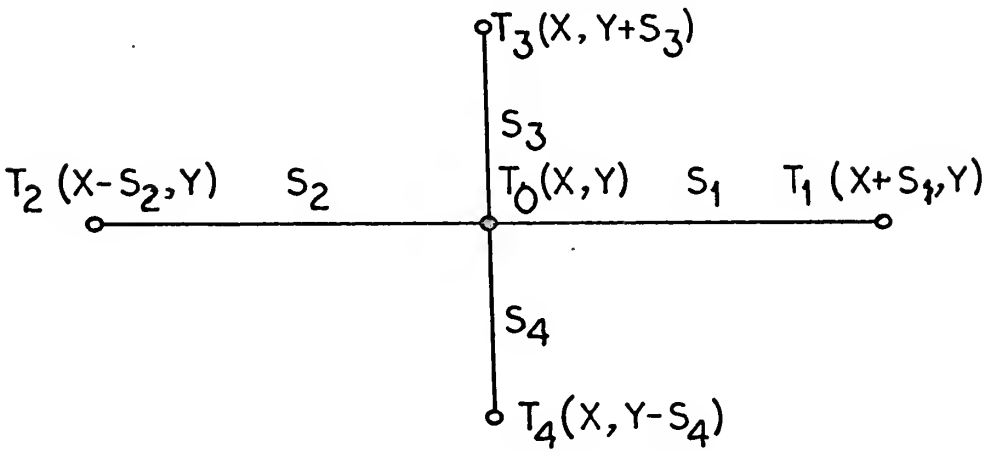


The $S_i$ represent grid spacings between nodes and $T_o$ will be a weighted "average" of the values at the four surrounding nodes. The following treatment is a summary of the approach employed by Tanbachuchi[20] and presented in detail by Greenspan.[6]

First, Taylor's expansion of the bounding temperatures about $T_o$ is taken:

$$T_1 = T_0+S_1 \frac{\partial T}{\partial x} + \frac{S_1^2}{2} \frac{\partial^2 T}{\partial X^2} + \cdots \quad (1)$$

$$T_2 = T_0-S_2 \frac{\partial T}{\partial x} + \frac{S_2^2}{2} \frac{\partial^2 T}{\partial x^2} + \cdots \quad (2)$$

$$T_3 = T_0+S_3 \frac{\partial T}{\partial y} + \frac{S_3^2}{2} \frac{\partial^2 T}{\partial y^2} + \cdots \quad (3)$$

$$T_4 = T_0-S_4 \frac{\partial T}{\partial y} + \frac{S_4^2}{2} \frac{\partial^2 T}{\partial y^2} + \cdots \quad (4)$$

where,

$$a_i = f\ (S\ )$$

by comparing equation (5) with equation (1) and (2) and collecting like terms, we find

$$a_o = \frac{S_1 - S_2}{S_1\ S_2} \quad , \quad a_1 = \frac{S_2}{S_1(S_1+S_2)} \quad , \quad a_2 = \frac{-S_1}{S_2(S_1+S_2)}$$

Similarly, for the second derivative at $T_o$

$$\frac{\partial^2 T}{\partial x^2} = a_o t_o + a_1 T_1 + a_2 T_2 \qquad (6)$$

where comparison with equation (1) and (2) yields

$$a_o = \frac{-2}{s_1 s_2} \quad , \quad a_1 = \frac{2}{S_1(S_1+S_2)} \quad , \quad a_2 = \frac{2}{S_2(S_1+S_2)}$$

changes in the y-direction are treated in like manner.

Substituting the different forms for $\partial T/\partial x$, $\partial T/\partial y$, $\partial^2 T/\partial x^2$, and $\partial^2 T/\partial y^2$ in the equation of heat flow, we find the value of $T_o$ as a function of $T_1$, $T_2$, $T_3$, $T_4$, and the grid spacing.

# APPENDIX 6

Notes on the use of the computer model

## A. Cost and Size

The computer program is Fortran coded and consists of approximately 1300 input cards. Runs were done on an IBM 360 using the G compiler. The program requires between 400 K and 450 K bytes of core and generally took six minutes to execute. With low priority specified, then, costs averaged around thirty dollars per run.

## B. Stability

The model is data sensitive and will diverge rapidly with the slightest provocation. Stability can be controlled by input of the proper grid multipliers: Y MULT 1, Y MULT 2, GX 12, and GX 34 . The model will not converge if these multipliers are greater than one. The particular values required for convergence depend on the magnitude of the welding speed: higher speeds require smaller multipliers. As a reference, it was found that a speed of 50 ft/hr and a multiplier of 0.75 will assure convergence. Unfortunately, as the multipliers are decreased the core requirements increase to the point where the program exceeds capability.

## C. Output

The output is presented in terms of node point temperatures.

Columns run parallel to the welding direction with column one identifying the long axis of the weld pool. Rows run perpendicular to the welding direction. The intersection of row one and column one mark the location of the origin of the system. Rows with positive incremental distances are read forward of row one in the direction of welding; these with negative distances in the opposite direction.

The output may be plotted in two ways. Each node temperature may be transferred to a grid, thereby identifying the isothermal contours surrounding the molten pool, or, the temperatures along a particular column may be so plotted to indicate how the temperature varies at some desired point from the center line of the pool (column one being at zero distance).

D. Description of Input Cards

1. First sixty cards are Bessel functions: argument, $I_0$, $I_1$, $K_0$, $K_1$. Format (5F 10.5)
2. NOPRP. Format (I3). Number of temperatures for the thermal properties of the specimen.
3. TRED, TKRD, TDRD. Format (3F10.5). Temperature, Conductivity, and Diffusivity of the specimen.
4. VOLT, AMP. Format (2F10.5). Voltage and amps for particular welding run.

5. TM, THIKRD, DISTV, TIME. Format (4F10.5). Melting Temp. ($^{o}$R), Specimen Thickness (IN), arc travel distance (In), Time (Min).
6. TA. Format (F10.5). Ambient Temp. ($^{o}$R).
7. CRAD. Format (E12.4). Radiation Heat Transfer Coefficient = $\sigma$ ($E_t+E_b$), BTU/ft$^2$-hr-R$^4$.
8. AVCON. Format (F10.5). Average Conductivity of Specimen, BTU/ft-hr-R.
9. XLONG, YLONG, XLONF. Format (3F10.5). Length (In) and Width (In) of Computational Block. XLONF is the distance in inches from front of pool to forward edge of block.
10. 6X12, 6X34, YMULT1, YMULT2. Format (4F10.5). Grid multipliers which control the fineness of the grid: forward of the arc, behind the arc, from the base line to the thermocouple, and from the thermocouple to the edge of block.
11. NWANT. Format (I3). Specifies the number of grid lines between each two points on the molten pool boundary. (2 works well.)
12. ITCHK. Format (I3). Number of iterations. (100-150).
13. ITCHK. Format (I3). Number of iterations at which output is printed to check convergence.
14. ICONV. Format (I3). Number of convergence checks.

15. ITFRNT. Format (I3). Number of iterations forward of the pool.
16. NDONT. Format (I3). Number of rows that need not be printed since convergence was not attained.
17. IFPRT. Format (I3). "1" if printed output is desired; "0" if not.
18. NEVIS1. Format (I3). First column to be printed.
19. NEVIS2. Format (I3). Last column to be printed.
20. NEVISI. Format (I3). Steps between first and last column.
21. EPSI. Format (F10.5). Tolerance for calculated Temperatures. (.001)
22. AKHAR. Format (F10.5). Coefficient in Rosenthal's equation for initializing grid.
23. JWAN. Format (I3). Number of curves to be plotted. (2 maximum)
24. NTC. Format (I3). Number of thermocouples or points, required (max of 2).
25. YTC(I). Format (F10.5). Distance in inches for each thermocouple from base line.
26. ITCN(I). Format (I5). Thermocouple number, or any dummy identification.

# APPENDIX 7

## COMPUTER MODEL FOR

## TEMPERATURE DISTRIBUTION

```
      DIMENSION X(50),Y(50),XN(50),YN(50),XNO(50),TCPL(2)
      DIMENSION CONTF(40),RFOF(40),WHATF(40),XNF(25),YND(99),YNF(25)
      DIMENSION XFF(75),YFF(75)
      DIMENSION XNEWB(80),YNEWB(80),CKOBF(40),AFF(35),SLOPF(40),XND(99)
      DIMENSION XFB(80),YFB(80),AXF(50, 70),AYF(50, 70),AXB(300, 70)
      DIMENSION AYB(300, 70),TNF(50, 70),TNB(300, 70),NPRT(6),XPB(300)
      DIMENSION XGRPL(50),YGRPL(50),XTGR(300),TGRP(300),JGRP(15),XPF(75)
      DIMENSION YTC(2)
      DIMENSION MAJBOR(50)
      DIMENSION BIORD(60),BKORD(60),BK1RD(60),RRED(60)
      DIMENSION BI1RD(60)
      DIMENSION TRED(50),TKRD(50),TDRD(50)
      DIMENSION ITCN(2)
      COMMON BIORD,BI1RD,BKORD,BK1RD,RRED
      COMMON TRED,TKRD,TDRD
      COMMON QBOIL
      COMMON TM,TA,AMIN,TDEL,CN,CCONV,CRAD,SPD,THICK
      COMMON TKXTD,TDXTD,TKMTD,TDMTD,NOPRP
      WRITE(6,99)
 99   FORMAT(2X,6H CHECK)
      READ 4000,(RRED(I),BIORD(I),BI1RD(I),BKORD(I),BK1RD(I),I=1,60)
 4000 FORMAT(5F12.5)
      READ 4001,NOPRP
 4001 FORMAT(I3)
      READ 4002,(TRED(I),TKRD(I),TDRD(I),I=1,NOPRP)
 4002 FORMAT(3F10.5)
      READ 4003,VOLT,AMP
      READ 4004,TM,THIKRD,DISTV,TIME
      PRINT 4004,TM,THIKRD,DISTV,TIME
C
C
      READ 4006,TA
      READ 4005,CRAD
      READ 4006,AVCON
      READ 4002,XLONG,YLONG,XLONF
      PRINT 4002,XLONG,YLONG,XLONF
```

```
C
C
      READ 4004,GX12,GX34,YMULT1,YMULT2
      READ 4001,NWANT
      READ 4001,ITCHK
      READ 4001,ITPCK
      READ 4001,ICONV
      WRITE(6,99)
      READ 4001,ITERNT
      READ 4001,NDONT
      READ 4001,IFPRT
      READ 4001,NEVIS1
      READ 4001,NEVIS2
C
C
      READ 4001,NEVISI
      READ 4006,EPSI
      READ 4006,AKHAR
      PRINT 4006,AKHAR
C
C
      READ 4001,JWAN
 4006 FORMAT(F10.5)
 4008 FORMAT(F20.5)
 4003 FORMAT(2F10.5)
 6000 FORMAT(2F10.5)
 4004 FORMAT(4F10.5)
 4005 FORMAT(E12.4)
      AMIN=TORD(1)
      DO 2001 I=2,NOPRP
      IF(AMIN-TORD(I))2001,2001,2002
 2002 AMIN=TORD(I)
 2001 CONTINUE
      THICK=THIKRD/12.
      SPD=DISTV*5./TIME
      CN=SPD/(24.*AMIN)
```

```
      TDEL=TM-TA
      WRITE(6,99)
      IF(JWAN-2)1000,1000,1001
 1001 JWAN=JWAN-2
      READ 4001,(JGRP(I+2),I=1,JWAN)
      JWAN=JWAN+2
C
C            CALCULATE POINTS ON POOL CONTOUR
C
 1000 T=3.415*VOLT*AMP/(2.*3.1416*AVCON*THICK*TDEL)
      YMN=3.16*T**.67/2.
      XMN=4.42*T**1.01
      YM=YMN/CN
      XM=XMN/CN
      N1=XM/.03
      PRINT 4001,N1
      X(1)=0.
      Y(1)=0.
      DO 1002 I=2,N1
      X(I)=X(I-1)+.03
      Y(I)=((1./XM**2.99)*5.86*YM**2*X(I)**.83*(XM-X(I))**2.16)**.5
      XN(I)=X(I)*CN
 1002 YN(I)=Y(I)*CN
      WRITE(6,99)
      XN(1)=0.
      YN(1)=0.
      XN(N1+1)=XMN
      YN(N1+1)=0.
      X(N1+1)=XMN/CN
      Y(N1+1)=0.
      N=N1+1
      YMAX=0.
      J=0
      DO 1003 I=1,N1
      IF(Y(I)-YMAX)1003,1004,1004
 1004 YMAX=Y(I)
```

```
      J=I
 1003 CONTINUE
      XWN=X(J)*CN
      YWN=Y(J)*CN
      WRITE(6,99)
      PRINT 6000,(XN(I),YN(I),I=1,N)
C
C     NORMALIZE THE INPUTS
C
      TKXTD=(TKRD(NOPRP)-TKRD(NOPRP-1))/(TRED(NOPRP)-TRED(NOPRP-1))
      TDXTD=(TDRD(NOPRP)-TDRD(NOPRP-1))/(TRED(NOPRP)-TRED(NOPRP-1))
      TKMTD=(TKRD(1)-TKRD(2))/(TRED(1)-TRED(2))
      TDMTD=(TDRD(1)-TDRD(2))/(TRED(1)-TRED(2))
      IF(N-2)2998,2998,2999
 2999 CONTINUE
      CALL  ORBLW(RF,AO,XN(N),XWN,YWN,XWN/2. ,SCF)
      PRINT 1,RF,AO,XN(N),XMN,YMN,SCF
 1    FORMAT(6F10.5)
      GO TO 2997
 2998 SCF=1.
      CALL ORIGIN(RF,AMIN/AMIN,XN(N),XN(N)/2.,1.,SCF)
C
C           FIND THE ORIGIN FOR THE EXP POINTS
C
 2997 DO 2004 I=1,N
 2004 XNO(I)=RF-XN(I)
      PRINT 2,(XNO(I), I=1,N)
 2    FORMAT(3F10.5)
      READ 4001,NTC
      IF(NTC-1)2996,2995,2995
 2996 GY13=YMULT1
      GY24=YMULT2
      YLG13=YLONG/2.
      GO TO 2994
 2995 READ 7000,(YTC(I),I=1,NTC)
 7000 FORMAT(F10.5)
```

```
      IF(NTC-1)2996,2993,2992
 2993 GY24=YMULT2
      GO TO 2991
 2992 GY24=AUTSCL(YTC(2)-YTC(1),YMULT2/CN)*CN
 2991 GY13=AUTSCL(YTC(1),YMULT1/CN)*CN
      YLG13=YTC(1)
 2994 XFP=XLONF
      XL=XLONG
      YL=YLONG
C
C             SET UP GRID
C
C
C             FIND LNUMBER OF NODES
C
      NF=(XFP*CN+RF)/GX12+1.
      NB=((XL-XFP)*CN-RF)/GX34+1.
      NP1=YLG13*CN/GY13+1.
      NP2=(YL-YLG13)*CN/GY24
      NPT=NP1+NP2
      NP1T=NP1-1
      NVF=NF-1
      NVT=NPT-1
C
      WRITE(6,99)
      IF(NTC-1)2889,2889,2888
 2889 NPRT(3)=NVT
      GO TO 2887
 2888 NPRT(3)=(YTC(2)-YTC(1))/(GY24/CN)+YTC(1)/(GY13/CN)+1.
 2887 NPRT(2)=NP1
      NPRT(1)=1
      DO 2885 J=1,NP1T
      DO 2885 I=1,NVF
      AXF(I,J)=GX12
      AYF(I,J)=GY13
      TNF(I,J)=0.
```

```
 2005 CONTINUE
      DO 2006 J=NP1,NVT
      DO 2006 I=1,NVF
      AXF(I,J)=GX12
      AYF(I,J)=GY24
      TNF(I,J)=0.
 2006 CONTINUE
C
C             LAYOUT GRID IN BACK OF POOL
C
      NVB=NB-1
      DO 2007 J=1,NP1T
      DO 2007 I=1,NVB
      AXB(I,J)=GX34
      AYB(I,J)=GY13
      TNB(I,J)=0.
 2007 CONTINUE
      DO 2800 J=NP1,NVT
      DO 2800 I=1,NVB
      AXB(I,J)=GX34
      AYB(I,J)=GY24
      TNB(I,J)=0.
 2800 CONTINUE
C
C             FIT EXP POINTS TO GRID
C
      CK=0.
      DO 2009 I=1,N
      IF(XNO(I))2008,2008,2009
 2008 IF(CK-1.)2010,2009,2009
 2010 CK=CK+1.
      NPF=I-1
 2009 CONTINUE
C
      WRITE(6,99)
C
```

```
C            FIND INTERSECTIIN OF POOL WITH Y-AXIS
C
      CALL POLFN(XNJ(NPF),YN(NPF),XNJ(NPF+1),YN(NPF+1),1.,ACENT,CSKOC,
     1SLOPC,CONSC,RCEN,WHATC,REGIN,R1,R2,SCF)
      IF(WHATC-1.)2011,2012,2011
 2011 IF(WHATC-2.)2013,2014,2013
 2012 CALL COLUMN(YPS,0.,ACENT,CSKOC,1.,1.,SCF)
      IF (N-2)2015,2015,2700
 2700 IF(ABS(YPS)-YN(NPF+1))2015,2015,2013
 2014 YPS=RCEN
      GO TO 2015
 2013 YPS=CONSC
 2015 JATOF=YPS/GY13+1.
      ZARUF=JATOF
      AYF(1,JATOF)=ZARUF*GY13-YPS
      AYB(1,JATOF)=AYF(1,JATOF)
      XGRPL(1)=0.
      YGRPL(1)=YPS
      DO 2016 J=1,JATOF
      TNF(1,J)=1.
 2016 TNB(1,J)=1.
      IF(JATOF-1)2017,2017,2018
 2018 AYF(1,JATOF-1)=2.*GY13-AYF(1,JATOF)
      AYB(1,JATOF-1)=AYF(1,JATOF-1)
 2017 NCF=NPF+1
C
      WRITE(6,99)
C
C            NUMBER THE EXP POINTS FROM THE ORIGIN
C
      DO 2019 I=1,NCF
      IF(I-1)2020,2020,2021
 2020 XFF(I)=0.
      YFF(I)=YPS
      GO TO 2019
 2021 NTF=NCF-I+1
```

```
      XFF(I)=XNO(NTF)
      YFF(I)=YN(NTF)
 2019 CONTINUE
C
C     FIT CURVE THRU POINTS IN FRONT OF THE POOL
C
      NF1=NPF
      NF2=NF1
 2022 NXM=0
      DO 2029 I=1,NF1
      IF(NXM-1)2023,2024,2024
 2023 CALL PNTFND(XFF(I),YFF(I),XFF(I+1),YFF(I+1),GX12,GY13/20,10,NWANT,
     1NEXSF,XBT,YBT,SCF)
      IF(NEXSF-1)2029,2026,2026
 2026 NXM=NEXSF
      I2=I+1
      NF2=NF1+NEXSF
      XND(I)=XFF(I)
      YND(I)=YFF(I)
      XND(I2)=XBT
      YND(I2)=YBT
      DO 2027 I3=I2,NF2
      XND(I3+1)=XFF(I3)
 2027 YND(I3+1)=YFF(I3)
      NF3=NF2+1
      DO 2028 I4=I,NF3
      XFF(I4)=XND(I4)
 2028 YFF(I4)=YND(I4)
 2029 CONTINUE
 2024 IF(NF2-NF1)2030,2030,2499
 2499 NF1=NF2
      GO TO 2022
 2030 NCF=NF1+1
C
      PRINT 4001,NCF
C
```

```
      WRITE(6,99)
      NPF=NF1
      ZARCL=0.
      DO 2031 I=1,NCF
      IF(NPF-I)2031,2032,2032
2032 CALL POLFN(XFF(I),YFF(I),XFF(I+1),YFF(I+1),1.,AFF(I),CKOBF(I),
     1SLOPF(I),CONTF(I),RFOF(I),WHATF(I),REGF,R1,R2,SCF)
      NL1=XFF(I)/GX12
      NL2=XFF(I+1)/GX12
      FDLCN=NL1-NL2
      NCLDF=ABS(FDLCN)
      NCNEW=NCLDF+1
      DO 2033 K=1,NCNEW
      IF(NCLDF-K)2033,2034,2034
2034 ZARCL=ZARCL+1.
      IGRPL=2
      IF(ABS(XFF(I+1)-ZARCL*GX12)-GX12/20.)2035,2035,2036
2036 IF(WHATF(I)-1.)2037,2038,2037
2037 IF(WHATF(I)-2.)2039,2040,2039
2038 CALL COLUMN(YCALF,ZARCL*GX12,AFF(I),CKOBF(I),(YFF(I+1)+YFF(I))/2.,
     11.,SCF)
      IF(YCALF-(YFF(I)+GY13))2041,2041,2039
2040 YCALF=SQRT(RFOF(I)**2-(ZARCL*GX12)**2)
      GO TO 2041
2039 YCALF=SLOPF(I)*ZARCL*GX12+CONTF(I)
      GO TO 2041
2035 YCALF=YFF(I+1)
2041 JCALF=YCALF/GY13+1.
      ICALF=ZARCL+1.
      ZARIF=JCALF
      AYF(ICALF,JCALF)=ZARIF*GY13-YCALF
      XGRPL(IGRPL)=ZARCL*GX12
      YGRPL(IGRPL)=YCALF
      DO 2042 J=1,JCALF
2042 TNF(ICALF,J)=1.
      IF(JCALF-1)2033,2033,2043
```

```
 2043 AYF(ICALF,JCALF-1)=2.*GY13-AYF(ICALF,JCALF)
 2033 CONTINUE
 2031 CONTINUE
C
      WRITE(6,99)
      ICENF=XFF(NCF)/GX12+1.
      ZARCF=ICENF
      AXF(ICENF,1)=ZARCF*GX12-XFF(NCF)
      TNF(ICENF,1)=1.
      IF(ICENF-1)2044,2044,2045
 2045 AXF(ICENF-1,1)=2.*GX12-AXF(ICENF,1)
 2044 ZARRW=0.
      DO 2046 I=1,NCF
      IF(NPF-I)2046,2047,2047
 2047 NK=NCF-I+1
      NROW1=YFF(NK)/GY13
      NROW2=YFF(NK-1)/GY13
      FDJRN=NROW1-NROW2
      NRODF=ABS(FDJRN)
      NRNEW=NRODF+1
      DO 2048 KROWF=1,NRNEW
      IF(NRODF-KROWF)2048,2049,2049
 2049 ZARRW=ZARRW+1.
      IGRPL=3
      IF(ABS(YFF(NK-1)-ZARRW*GY13)-GY13/2.)2050,2050,2051
 2051 IF(WHATF(NK-1)-1.)2052,2053,2052
 2052 IF(WHATF(NK-1)-2.)2054,2055,2054
 2053 CALL ROWPS(XCALF,ZARRW*GY13,AFF(NK-1),CKOBF(NK-1),(XFF(NK)+XFF(NK-
     11))/2.,1.,SCF)
      IF(XCALF-(XFF(NK)+GX12))2056,2056,2054
 2055 XCALF=SQRT(RFOF(NK-1)**2-(ZARRW*GY13)**2)
      GO TO 2056
 2054 XCALF=(1./SLOPF(NK-1))*(ZARRW*GY13)+(-1./SLOPF(NK-1))*CONTF(NK-1)
      GO TO 2056
 2050 XCALF=XFF(NK-1)
 2056 ICALR=XCALF/GX12+1.
```

```
      JCALR=ZARRW+1.
      ZARIR=ICALR
      AXF(ICALR,JCALR)=ZARIR*GX12-XCALF
      XGRPL(IGRPL)=XCALF
      YGRPL(IGRPL)=ZARRW*GY13
      IF(ICALR-1)2048,2048,2057
 2057 AXF(ICALR-1,JCALR)=2.*GX12-AXF(ICALR,JCALR)
 2048 CONTINUE
 2046 CONTINUE
C
      WRITE(6,99)
C
C            FIT CURVE BEHIND ARC
C
      XFB(1)=0.
      YFB(1)=YPS
      NPB=N-NPF
      NCB=NPB+1
      NMR=0
      DO 2058 I=2,NCB
      NMR=NMR+1
      NTB=NPF+NMR
      XFB(I)=XND(NTB)
 2058 YFB(I)=YN(NTB)
      NB1=NPB
      NB2=NB1
 2067 NEXTM=0
      DO 2059 I=1,NB1
      IF(NEXTM-1)2060,2061,2061
 2060 CALL PNTFND(XFB(I),YFB(I),XFB(I+1),YFB(I+1),GX34,GY13/2.,1.,NWANT,
     1NEXB,XBTB,YBTB,SCF)
      IF(NEXB-1)2059,2062,2062
 2062 NEXTM=1
      I2=I+1
      NB2=NB1+1
      XND(I)=XFB(I)
```

```
      YND(I)=YFB(I)
      XND(I2)=XBTB
      YND(I2)=YBTB
      DO 2063 I3=I2,NB2
      XND(I3+1)=XFB(I3)
 2063 YND(I3+1)=YFB(I3)
      NB3=NB2+1
      DO 2064 I4=I,NB3
      XFB(I4)=XND(I4)
 2064 YFB(I4)=YND(I4)
 2059 CONTINUE
 2061 IF(NB2-NB1)2065,2065,2066
 2066 NB1=NB2
      GO TO 2067
 2065 NCB=NB1+1
C
      WRITE(6,99)
      NPB=NB1
      ZARCB=0.
      JMAX=1
C
      PRINT 4001,NCB
      DO 2068 I=1,NCB
      IF(NPB-I)2068,2069,2069
 2069 CALL POLFN(XFB(I),YFB(I),XFB(I+1),YFB(I+1),1.,AFOB,CKOBB,SLOPB,
     1CONTB,RFOB,WHATB,REGB,R1,R2,SCF)
      NCL1=XFB(I)/GX34
      NCL2=XFB(I+1)/GX34
      FDLCN=NCL1-NCL2
      NCLDF=ABS(FDLCN)
      NBNEW=NCLDF+1
      DO 2070 K=1,NBNEW
      IF(NCLDF-K)2070,2071,2071
 2071 ZARCB=ZARCB-1.
      IGRPL=4
      IF(ABS(XFB(I+1)-ZARCB*GX34)-GX34/20.)2072,2072,2073
```

```
 2073 IF(WHATB-1.)2074,2075,2074
 2074 IF(WHATB-2.)2076,2077,2076
 2075 CALL COLUMN(YCALB,ZARCB*GX34,AFOB,CKOBB,(YFB(I+1)+YFB(I))/2.,1.,SC
     1F)
      IF(YCALB-(YFB(I)+2.*GY13))2078,2078,2076
 2077 YCALB=SQRT(RFOB**2-(ZARCB*GX34)**2)
      GO TO 2078
 2076 YCALB=SLOPB*ZARCB*GX34+CCNTB
      GO TO 2078
 2072 YCALB=YFB(I+1)
 2078 JCALB=YCALB/GY13+1.
      IF(JMAX-JCALB)2079,2080,2080
 2079 JMAX=JCALB
      IMAX=-ZARCB+1.
 2080 ICALB=-ZARCB+1.
      ZARIB=JCALB
      AYB(ICALB,JCALB)=ZARIB*GY13-YCALB
      XGRPL(IGRPL)=ZARCB*GX34
      YGRPL(IGRPL)=YCALB
      DO 2081 J=1,JCALB
 2081 TNB(ICALB,J)=1.
      XNEWB(ICALB)=ZARCB*GX34
      YNEWB(ICALB)=YCALB
      IF(JCALB-1)2070,2070,2083
 2083 AYB(ICALB,JCALB-1)=2.*GY13-AYB(ICALB,JCALB)
 2070 CONTINUE
 2068 CONTINUE
C
      WRITE(6,99)
      ICENB=ABS(XFB(NCB))/GX34+1.
      ZARCB=ICENB
      AXB(ICENB,1)=ZARCB*GX34-ABS(XFB(NCB))
      TNB(ICENB,1)=1.
      IF(ICENB-1)2084,2084,2085
 2085 AXB(ICENB-1,1)=2.*GX34-AXB(ICENB,1)
 2084 ZARWB=0.
```

```
      IF(AXB(ICENB,1)-GX34)2086,2087,2086
2087  ICNEW=ICENB
      GO TO 2088
2086  ICNEW=ICENB+1
2088  XNEWB(ICNEW)=XFB(NCB)
      YNEWB(ICNEW)=0.
      XNEWB(1)=0.
      YNEWB(1)=YPS
      ARW=1.
      OVER=0.
      DO 2089 I=2,ICNEW
2090  NKB=ICNEW-I+2
      NRWB1=YNEWB(NKB)/GY13
      NRWB2=YNEWB(NKB-1)/GY13
      BOORN=NRWB1-NRWB2
      NROOB=ABS(BOORN)
      IF(NROOB-1)2089,2091,2091
2091  CALL POLFN(XNEWB(NKB),YNEWB(NKB),XNEWB(NKB-1),YNEWB(NKB-1),1.,AFOB
     1,CKOBB,SLOPB,CONTB,RFOB,WHATB,REGB,R1,R2,SCF)
      DO 2092 KROWB=1,NROOB
      ZARWB=ZARWB+ARW
      IGRPL=5
2312  IF(WHATB-1.)2093,2094,2093
2093  IF(WHATB-2.)2095,2096,2095
2094  CALL ROWPS(XCALB,ZARWB*GY13,AFOB,CKOBB,(XNEWB(NKB)+XNEWB(NKB-1))/
     12.,1.,SCF)
      IF(ABS(XCALB)-ABS(XNEWB(NKB)-GX34))2097,2097,2095
2096  XCALB=SQRT(RFOB**2-(ZARWB*GY13)**2)
      GO TO 2097
2095  XCALB=((1./SLOPB)*(ZARWB*GY13)+(-1./SLOPB)*CONTB)
      GO TO 2097
2311  XCALB=XNEWB(NKB-1)
2097  ICALB=ABS(XCALB/GX34)+1.
      ZARIB=ICALB
      JCALB=ZARWB+1.
      IF(JCALB-JMAX)2098,2099,2100
```

```
 2099 IF(OVER-1.)2101,2102,2102
 2101 ARW=1.
      OVER=1.
      GO TO 2103
 2098 IF(OVER-1.)2104,2102,2102
 2103 OVER=1.
 2102 ARW=-1.
      GO TO 2103
 2104 ARW=1.
 2103 AXB(ICALB,JCALB)=ZARIB*GX34-ABS(XCALB)
      XGRPL(IGRPL)=XCALB
      YGRPL(IGRPL)=ZARWB*GY13
      IF(ICALB-1)2092,2092,2106
 2106 AXB(ICALB-1,JCALB)=2.*GX34-AXB(ICALB,JCALB)
 2092 CONTINUE
 2089 CONTINUE
 2107 IMAX1=IMAX-1
      DO 2108 J=1,JMAX
      DO 2109 I=1,IMAX
      IF(TNB(I,J)-1.)2110,2108,2110
 2110 IF(AXB(I,J)-GX34)2111,2109,2112
 2111 AXB(I,J)=GX34-AXB(I,J)
      GO TO 2109
 2112 AXB(I,J)=GX34
 2109 CONTINUE
 2108 CONTINUE
C
      WRITE(6,99)
C
C           GRID LAYOUT FINISHED
C
      DO 2113 I2=1,NF
      ZRGR=NF-I2
 2113 XTGR(I2)=GX12*ZRGR
      DO 2114 I2=1,NVB
      ZRGR=I2
```

```
      ID=NF+I2
 2114 XTGR(ID)=-GX34*ZRGR
      IGT=NB+NVF
      MFG=IGT-NDONT
C
C           INITIALIZE NODES IN FRONT OF ARC
C
      CALL BESSEL(-XNO(N),BIOJ,BI1J,BKOJ,BK1J)
      ATMP=1.
      CTMP=EXP(ATMP*XNO(N))/(AKHAR*BKOJ)
      DO 2115 J=1,NVT
      AXB(NVB,J)=GX34*.1
      TNF(NF,J)=.
 2115 TNB(NB,J)=.
      DO 2116 I=1,NF
      AYF(I,NVT)=GY24*.1
 2116 TNF(I,NPT)=.
      DO 2117 I=1,NB
      AYB(I,NVT)=GY24*.1
 2117 TNB(I,NPT)=.
      DO 2118 J=1,NP1
      DO 2118 I=1,NF
      IF (TNF(I,J)-1.)2119,2118,2120
 2119 ZARX=I-1
      ZARY=J-1
      TNF(I,J)=DRAJH(CTMP,ATMP,ZARX*GX12,ZARY*GY13)
      IF(TNF(I,J)-1.)2118,2120,2120
 2120 TNF(I,J)=.9
 2118 CONTINUE
      ZANP1=NP1-1
      NODP2=NP2+1
      DO 2121 K=2,NODP2
      DO 2121 I=1,NF
      J=K+NP1-1
      IF(TNF(I,J)-1.)2122,2121,2123
 2122 ZARX=I-1
```

```
      ZARY=K-1
      TNF(I,J)=DRAJH(CTMP,ATMP,ZARX*GX12,ZANP1*GY13+ZARY*GY24)
      IF(TNF(I,J)-1.)2121,2123,2123
 2123 TNF(I,J)=.9
 2121 CONTINUE
C
      WRITE(6,99)
C
C           INITIALIZE NODES BEHIND ARC
C
      DO 2124 J=1,NP1
      DO 2124 I=1,NVB
      IF(TNB(I,J)-1.)2125,2124,2127
 2125 ZARX=1-I
      ZARY=J-1
      TNB(I,J)=DRAJH(CTMP,ATMP,ZARX*GX34,ZARY*GY13)
      IF(TNB(I,J)-1.)2124,2127,2127
 2127 TNB(I,J)=.9
 2124 CONTINUE
      DO 95 J=1,NP1
      CK=0.
      DO 95 I=1,NVB
      IF(TNB(I+1,J)-TNB(I,J))96,95,95
 96   IF(CK-1.)97,98,98
 97   CK=CK+1.
      ZARX=I
      XNUM=ZARX*GX34
 98   ZARX=I
      DEN=ZARX*GX34
      TNB(I,J)=TNB(I,J)*(XNUM/DEN)**2
 95   CONTINUE
      DO 2128 K=2,NODP2
      DO 2128 I=1,NVB
      J=K+NP1-1
      IF(TNB(I,J)-1.)2129,2128,2131
 2129 ZARX=1-I
```

```
      ZARY=K-1
      TNB(I,J)=DRAJH(CTMP,ATMP,ZARX*GX34,ZANP1*GY13+ZARY*GY24)
      IF(TNB(I,J)-1.)2128,2131,2131
 2131 TNB(I,J)=.9
 2128 CONTINUE
      DO 90 K=2,NODP2
      CK=0.
      DO 90 I=1,NVB
      J=K+NP1-1
      IF(TNB(I+1,J)-TNB(I,J))91,90,90
 91   IF(CK-1.)92,93,93
 92   CK=CK+1.
      ZARX=I
      XNUM=ZARX*GX34
 93   ZARX=I
      DEN=ZARX*GX34
      TNB(I,J)=TNB(I,J)*(XNUM/DEN)**2
 90   CONTINUE
C
C            S<ART CALCULATING TEMP PROFILES
C
      ITER=-1
      NGRAPH=0
      ITPRT=ITPCK
      DO 2132 J=1,NVT
 2132 MAJBOR(J)=IMAX
 2133 IF(ITER-ITCHK)2134,2135,2136
 2134 ITER=ITER+1
      ITPRT=ITPRT+1
      IF(ITPRT-ITPCK)2137,2138,2138
 2138 DO 2139 IPRT=1,ICONV
      NPRTD=NPRT(IPRT)
      PRINT 9999
 9999 FORMAT(1H1)
      PRINT 25.,(ITER,NPRTD,I,AXF(I,NPRTD),AYF(I,NPRTD),TNF(I,NPRTD),
     1I=1,NF)
```

```
2500 FORMAT(15X,18HNO. OF ITERATIONS=I3,3X,9HCOLUMN=  ,I3,3X,6HROW=  ,
    1I3,3X,9HX-INCR.= ,F10.5,3X,9HY-INCR.= F10.5,3X,7HTEMP=  ,F10.5)
      PRINT 9999
2139  PRINT 2500,(ITER,NPRTD,I,AXB(I,NPRTD),AYB(I,NPRTD),TNB(I,NPRTD),
    1I=1,NB)
      PRINT 9999
      DO 2140 I2=1,NF
      ID=NF-I2+1
2140  TGRP(I2)=TNF(ID,NP1)
      DO 2141 I2=1,NVB
      ID=NF+I2
2141  TGRP(ID)=TNB(I2+1,NP1)
      ITPRT=0
      NGRAPH=NGRAPH+1
2137  DO 2146 J=1,NVT
      IJDID=MAJBOR(J)
9222  DO 2147 I=IMAX,IJDID
      IF(TNB(I,J)-1.)2148,2147,2148
2148  IF(J-1)2147,2149,2150
2149  BBMN=AYB(I,J)
      T4MN=TNB(I,J+1)
      GO TO 2151
2150  BBMN=AYB(I,J-1)
      T4MN=TNB(I,J-1)
2151  CALL DIFEQ(TNB(I,J),TNB(I,J),TNB(I-1,J),TNB(I+1,J),TNB(I,J+1),T4MN
    1,AXB(I-1,J),AXB(I,J),AYB(I,J),BBMN,1.)
2147  CONTINUE
      DO 2152 I=IJDID,NVB
      IF(TNB(I,J)-1.)2153,2152,2153
2153  IF(J-1)2152,2154,2155
2154  BBMN=AYB(I,J)
      T4MN=TNB(I,J+1)
      GO TO 2156
2155  BBMN=AYB(I,J-1)
      T4MN=TNB(I,J-1)
2156  CALL DIFEQ(TNBDI,TNB(I,J),TNB(I-1,J),TNB(I+1,J),TNB(I,J+1),T4MN,AX
```

```
     1B(I-1,J),AXB(I,J),AYB(I,J),BBMN,1.)
      IF(ABS(TNBDI-TNB(I,J))-EPSI)2157,2157,2158
2158 TNB(I,J)=TNBDI
2152 CONTINUE
2157 IF(I-NVB)2159,2160,2160
2160 MAJBOR(J)=I
     TNB(NB,J)=1.1*TNB(NVB,J)-.1*TNB(NVB-1,J)
     GO TO 2161
2159 MAJBOR(J)=I+1
2161 IF(IMAX-2)2162,2162,2163
2163 DO 2164 II=2,IMAXI
     I=IMAX-II+1
     IF(TNB(I,J)-1.)2165,2164,2165
2165 CALL DIFEQ(TNB(I,J),TNB(I,J),TNB(I-1,J),TNB(I+1,J),TNB(I,J+1),TNB(
    1I,J-1),AXB(I-1,J),AXB(I,J),AYB(I,J),AYB(I,J-1),1.)
2164 CONTINUE
2162 IF(TNF(1,J)-1.)2166,2167,2166
2166 CALL DIFEQ(TNF(1,J),TNF(1,J),TNF(2,J),TNB(2,J),TNF(1,J+1),TNF(1,J-
    11),AXF(1,J),AXB(1,J),AYF(1,J),AYF(1,J-1),1.)
     TNB(1,J)=TNF(1,J)
2167 IF(ITER-ITERNT)2168,2168,2146
2168 DO 2169 I=2,NVF
     IF(TNF(I,J)-1.)2170,2169,2170
2170 IF(J-1)2169,2171,2172
2171 BBMN=AYF(I,J)
     T4MN=TNF(I,J+1)
     GO TO 2173
2172 BBMN=AYF(I,J-1)
     T4MN=TNF(I,J-1)
2173 CALL DIFEQ(TNF(I,J),TNF(I,J),TNF(I+1,J),TNF(I-1,J),TNF(I,J+1),T4MN
    1,AXF(I,J),AXF(I-1,J),AYF(I,J),BBMN,1.)
2169 CONTINUE
2146 CONTINUE
     DO 2174 KD=1,NB
2174 TNB(KD,NPT)=1.1*TNB(KD,NVT)-.1*TNB(KD,NVT-1)
     DO 2175 KD=2,NF
```

```
 2175 TNF(KD,NPT)=1.1*TNF(KD,NVT)-.1*TNF(KD,NVT-1)
      GO TO 2133
C
C            OUTPUT FORMS
C
 2135 PRINT 3000
 3000 FORMAT(44X,29H******** MATERIAL DATA ********,//)
      PRINT 3001
 3001 FORMAT(20X,31HMATERIAL .......... MILD STEEL,/)
      PRINT 3002,TM
 3002 FORMAT(51X,34HMELTING TEMPERATURE,(DEG.R) ..... F12.5,/)
      PRINT 3003,THIKRD
 3003 FORMAT(64X,24HTHICKNESS,(IN.) ....... F12.5,///)
      PRINT 3004
 3004 FORMAT(45X,29H ******** WELDING DATA ********,//)
      PRINT 3005,SPD
 3005 FORMAT(56X,35H SPEED OF TRAVEL, (IN/MIN) ....... F12.5,/)
      PRINT 3006,VOLT
 3006 FORMAT(64X,26H VOLTAGE, (VOLTS) ....... F12.5,/)
      PRINT 3007,AMP
 3007 FORMAT(65X,25H CURRENT, (AMPS) ....... F12.5,///)
      PRINT 3008
 3008 FORMAT (45X,33H ******** MOLTEN POOL DATA ********,//)
      XWARD=XWN/CN
      YWARD=YWN/CN
      PRINT 3009,X(N)
 3009 FORMAT(67X,22H LENGTH, (IN) ....... F12.5,/)
      PRINT 3010,XWARD,IMAX
 3010 FORMAT(5X,65H DISTANCE FROM THE FROMT OF THE POOL TO MAX. WIDTH, (
     1IN) ....... F12.5,5X,27H CORRESPONDING ROW ....... I3)
      PRINT 3011,YWARD, JMAX
 3011 FORMAT(41X,29H MAXIMUM WIDTH, (IN) ....... F12.5,2X,30H CORRESPOND
     1ING COLUMN ....... I3,///)
      PRINT 3012
 3012 FORMAT(28X,65H ******** DATA SUPPLIED FOR CURVE FITTING OF THE WELD
     1 POOL ********,//)
```

```
      PRINT 3013
3013 FORMAT(23X,20H DISTANCE FROM FRONT,2X,26H NORMALIZED VALUE MESSURE
     1D,2X,18H DISTANCE FROM THE,8X,11H NORMALIZED)
      PRINT 3014
3014 FORMAT(15X,3HNO.,6X,18HOF THE POOL, (IN.),2X,16H FROM THE ORIGIN,1
     111X,17H LINE OF SYMMETRY,9X,6H VALUE)
      DO 3015 I=1,N
3015 PRINT 3016,I,X(I),XNO(I),Y(I),YN(I)
3016 FORMAT(15X,I3,10X,F10.5,13X,F10.5,13X,F10.5,13X,F10.5)
      PRINT 3017
3017 FORMAT(///)
      PRINT 3018
3018 FORMAT(43X,33H ******* MEASUREMENT DATA *******,//)
      DO 3019 I=1,NTC
      READ 10,ITCN(I)
10    FORMAT(I5)
      PRINT 3020,ITCN(I)
3020 FORMAT(64X,23H THERCOUPLE NO. .......,5X,I5)
      PRINT 3021,YTC(I)
3021 FORMAT(39X,46H DISTANCE FROM LINE OF SYMMETRY, (IN) ....... F12.5)
      JTHRM=NPRT(I+1)
      PRINT 3022,JTHRM
3022 FORMAT(38X,51H COLUMN CORRESPONDING TO THE ABOVE DISTANCE .....,
     15X,I3,///)
3019 CONTINUE
      PRINT 3023
3023 FORMAT(35X,49H ******* COMPUTATION DATA AND ASSUMPTIONS *******,//
     1)
      PRINT 3024,CRAD
3024 FORMAT(29X,61H RADIANT HEAT TRANSFER COEF.,(BTU/FT**2-HR-DEG.R**4)
     1 ....... E12.4,/)
      PRINT 3026,TA
3026 FORMAT(52X,36H AMBIENT WATER TEMP.,(DEG.R) ....... F12.5,/)
      PRINT 3027,AMIN
3027 FORMAT(32X,56H MINIMUN VALUE OF THERMAL DIFFUSIVITY,(FT**2/HR) ...
     1.... F12.5,/)
```

```
      PRINT 3028,CN
3028 FORMAT(53X,34H NORMALIZING DISTANCE,(IN) ooooooo F12o5,/)
      PRINT 3029,TDEL
3029 FORMAT(48X,40H NORMALIZING TEMPERATURE,(DEGoR) ooooooo F12o5,/)
      PRINT 3030,SCF
3030 FORMAT(68X,21H SCALE FACTOR ooooooo F12o5,/)
      ITER=ITER+1
      PRINT 3031,ITER
3031 FORMAT(68X,29H NUMBER OF ITERATIONS ooooooo,5X,I3,/)
      JGRP(1)=NPRT(2)
      JGRP(2)=NPRT(3)
      NGRAPH=-1
      PRINT 3032
3032 FORMAT(///)
      PRINT 3033
3033 FORMAT(42X,36H ******* CURVE PLOTTING DATA *******,///)
      DO 3034 J=1,JWAN
      JD=JGRP(J)
      IF(JD-NP1)3035,3035,3036
3035 ZJD=JD-1
      DJD=ZJD*GY13
      GO TO 3037
3036 ZJD1=NP1-1
      ZJD2=JD-NP1
      DJD=ZJD1*GY13+ZJD2*GY24
3037 PRINT 3038,J,DJD,JD
3038 FORMAT(6X,52H DIMENSIONSESS DISTANCE FOR CURVE WITH SYMBOL CODE,(I
     13,9H) ooooooo,F10o5,2X,29H CORRESPONDING CLUUMN ooooooo,I3,//)
      DO 3039 I2=1,NF
      ID=NF-I2+1
3039 TGRP(I2)=TNF(ID,JD)
      DO 3040 I2=1,NVB
      ID=NF+I2
3040 TGRP(ID)=TNB(I2+1,JD)
      NGRAPH=NGRAPH+1
3034 CONTINUE
```

```
      IF(IFPRT-1)2136,3042,3042
3042  DO 3043 I=1,NB
      ZARIB=I-1
3043  XPB(I)=-ZARIB*GX34
      DO 3044 I=1,NF
      ZARIB=I-1
3044  XPF(I)=ZARIB*GX12
      DO 3045 J=NEVIS1,NEVIS2,NEVIS1
      IF(J-NP1)3046,3046,3047
3046  ZARIB=J-1
      YPRNT=ZARIB*GY13
      GO TO 3048
3047  ZARIB=NP1-1
      ZARB2=J-NP1
      YPRNT=ZARIB*GY13+ZARB2*GY24
3048  PRINT 3049
3049  FORMAT(10X,71H ********** CALCULATED TEMP. IN FLAT PLATE BEING WELDED
     1 UNDERWATER **********,///)
      PRINT 3050,(J,YPRNT,I,XPF(I),AXF(I,J),AYF(I,J),TNF(I,J),I=1,NVF)
3050  FORMAT(5X,8HCOLUMN =I3,17H COR. D-L DIS. = F8.3,2X,5HROW =I3,17H,
     1COR. D-L DIS. = F8.3,2X,7HX-IN, = F6.3,2X,7HY-IN. = F6.3,2X,10HD-L
     2 TEMP =,F8.5)
      PRINT 3051
3051  FORMAT(///)
      PRINT 3050,(J,YPRNT,I,XPB(I),AXB(I,J),AYB(I,J),TNB(I,J),I=1,NVB)
3045  CONTINUE
2136  CONTINUE
      CALL EXIT
      END
      SUBROUTINE BESSEL (Z,BI0T,BI1T,BK0T,BK1T)
      DIMENSION BI0RD(60),BI1RD(60),BK0RD(60),BK1RD(60),RRED(60)
      DIMENSION TRED(50),TKRD(50),T0RD(50)
      COMMON BI0RD,BI1RD,BK0RD,BK1RD,RRED
      COMMON QBOIL
      COMMON TRED,TKRD,T0RD
      COMMON TM,TA,AMIN,TDEL,CN,CCONV,CRAD,SPD,THICK
```

```
      COMMON TKXTD,TDXTD,TKMTD,TDMTD,NOPRP
      VALF(A,B,C,D,E)=A+(B-A)/(C-D)*(E-D)
      IF(Z-.05)8,9,9
9     IF(Z-2.95)1,1,2
1     Z2=20.*Z
      I=Z2
      BIOT=VALF(BIORD(I),BIORD(I+1),RRED(I+1),RRED(I),Z)
      BI1T=VALF(BI1RD(I),BI1RD(I+1),RRED(I+1),RRED(I),Z)
      BK0T=VALF(BK0RD(I),BK0RD(I+1),RRED(I+1),RRED(I),Z)
      BK1T=VALF(BK1RD(I),BK1RD(I+1),RRED(I+1),RRED(I),Z)
      GO TO 7
2     IF(Z-3[illegible].)3,3,4
3     Z1=Z
      GO TO 5
4     Z1=3[illegible].
5     BIOT=EXP(Z1)/SQRT(6.28318*Z1)*(1.+1./(8.*Z1))
      BI1T=BIOT*(1.-3./(8.*Z))/(1.+1./(8.*Z))
      BK0T=SQRT(1.57/Z)*EXP(-Z)*(1.-1./(8.*Z))
      BK1T=BK0T*(1.+3./(8.*Z))/(1.-1./(8.*Z))
      GO TO 7
8     BIOT=1.+Z**2/4.
      BI1T=Z/2.*(1.+Z**2/8.)
      BK0T=ALOG(2./Z)-.5772
      BK1T=1./Z
7     RETURN
      END
      SUBROUTINE ORIGIN(RF,A,BIN,RINTL,TN,S)
      DIMENSION BIORD(60),BI1RD(60),BK0RD(60),BK1RD(60),RRED(60)
      DIMENSION TRED(50),TKRD(50),TDRD(50)
      COMMON BIORD,BI1RD,BK0RD,BK1RD,RRED
      COMMON TRED,TKRD,TDRD
      COMMON TM,TA,AMIN,TDEL,CN,CCONV,CRAD,SPD,THICK
      COMMON QBOIL
      COMMON TKXTD,TDXTD,TKMTD,TDMTD,NOPRP
      R1=RINTL/S
      B=BIN/S
```

```
  102  CALL BESSEL(A*R1,BIO1,BI11,BKO1,BK11)
       CALL BESSEL(A*(B-R1),BIO2,BI12,BKO2,BK12)
       TABE=TN*EXP(A*B)*BKO2-BKO1
       DRIV=A*(TN*EXP(A*B)*BK12+BK11)
       RF=R1-TABE/DRIV
       IF(ABS(R1-RF)-.001)100,100,101
  101  R1=RF
       GO TO 102
  100  RF=RF*S
       RETURN
       END
       SUBROUTINE PROP(TK,TKDRV,TD,TND,TRDD,TMIN,TMAX,TKMNT,TDMNT,TKMXT,
      1TDMXT,TKXDR,TDXDR,TKMDR,TDMDR)
       DIMENSION BIORD(60),BI1RD(60),BKORD(60),BK1RD(60),RRED(60)
       DIMENSION TRED(50),TKRD(50),TDRD(50)
       COMMON BIORD,BI1RD,BKORD,BK1RD,RRED
       COMMON TRED,TKRD,TDRD
       COMMON QBOIL
       COMMON TM,TA,AMIN,TDEL,CN,CCONV,CRAD,SPD,THICK
       COMMON TKXTD,TDXTD,TKMTD,TDMTD,NOPRP
       VINTF(A,B,C,D,E)=A+(B-A)/(C-D)*(E-D)
       VINTD(A,B,C,D)=(A-B)/(C-D)
       T=TND*TDEL+TA
       IF(T-TMIN)208,208,209
  209  IF(T-TMAX)201,202,202
  201  T2=T/TRDD
       I=T2
       IF(TRED(I)/TRDD-T2)203,204,205
  203  IB=I
       GO TO 206
  205  IB=I-1
  206  TK=VINTF(TKRD(IB),TKRD(IB+1),TRED(IB+1),TRED(IB),T)
       TD=VINTF(TDRD(IB),TDRD(IB+1),TRED(IB+1),TRED(IB),T)
       TKDRV=VINTD(TKRD(IB),TKRD(IB+1),TRED(IB),TRED(IB+1))
       IF(TD-AMIN)210,207,207
  204  TK=TKRD(I)
```

```
      TD=TDRD(I)
      TKDRV=VINTD(TKRD(I+1),TKRD(I-1),TRED(I+1),TRED(I-1))
      IF(TD-AMIN)210,207,207
  208 TK=TKMNT+TKMDR*(T-TMIN)
      TD=TDMNT+TDMDR*(T-TMIN)
      TKDRV=TKMDR
      IF(TD-AMIN)210,207,207
  202 TK=TKMXT+TKXDR*(T-TMAX)
      TD=TDMXT+TDXDR*(T-TMAX)
      TKDRV=TKXDR
      IF(TD-AMIN)210,207,207
  210 TD=AMIN
  207 RETURN
      END
      SUBROUTINE ROWPS(X,YIN,A,C,XINTL,TN,S)
      DIMENSION BIORD(60),BI1RD(60),BKORD(60),BK1RD(60),RRED(60)
      DIMENSION TRED(50),TKRD(50),TDRD(50)
      COMMON BIORD,BI1RD,BKORD,BK1RD,RRED
      COMMON TRED,TKRD,TDRD
      COMMON QBOIL
      COMMON TM,TA,AMIN,TDEL,CN,CCONV,CRAD,SPD,THICK
      COMMON TKXTD,TDXTD,TKMTD,TDMTD,NOPRP
      TABEF(XDIS,BFUTO)=C*EXP(-A*XDIS)*BFUTO-TN
      DRIVF(XDIS,RDIS,BFUTO,BFUT1)=-C*A*EXP(-A*XDIS)*(BFUTO+XDIS/RDIS*
     1BFUT1)
      X1=XINTL
      Y=YIN/S
  302 R1=SQRT(X1**2+Y**2)
      CALL BESSEL(A*R1,BIORW,BI1RW,BKORW,BK1RW)
      X=X1-TABEF(X1,BKORW)/DRIVF(X1,R1,BKORW,BK1RW)
      IF(ABS(X-X1)-.001)300,300,301
  301 X1=X
      GO TO 302
  300 RETURN
      END
      SUBROUTINE COLUMN(Y,X,A,C,YINTL,TN,S)
```

```
      DIMENSION BIORD(60),BI1RD(60),BKORD(60),BK1RD(60),RRED(60)
      DIMENSION TRED(50),TKRD(50),TDRD(50)
      COMMON BIORD,BI1RD,BKORD,BK1RD,RRED
      COMMON TRED,TKRD,TDRD
      COMMON QBOIL
      COMMON TM,TA,AMIN,TDEL,CN,CCONV,CRAD,SPD,THICK
      COMMON TKXTD,TDXTD,TKMTD,TDMTD,NOPRP
      Y1=YINTL/S
402   R1=SQRT(X**2+Y1**2)
      CALL BESSEL(A*R1,BIOCL,BI1CL,BKOCL,BK1CL)
      TAUDR=R1*(TN*EXP(A*X)/C-BKOCL)/(Y1*A*BK1CL)
      Y=Y1-TAUDR
      IF(ABS(Y-Y1)-.0001)400,400,401
401   Y1=Y
      GO TO 402
400   Y=Y*S
      RETURN
      END
      SUBROUTINE POLFN(X1,Y1IN,X2,Y2IN,TN,A,CPSKO,SLOPE,CONST,R,WHAT,REG
     1IN,R1,R2,S)
      DIMENSION BIORD(60),BI1RD(60),BKORD(60),BK1RD(60),RRED(60)
      DIMENSION TRED(50),TKRD(50),TDRD(50)
      COMMON BIORD,BI1RD,BKORD,BK1RD,RRED
      COMMON TRED,TKRD,TDRD
      COMMON QBOIL
      COMMON TM,TA,AMIN,TDEL,CN,CCONV,CRAD,SPD,THICK
      COMMON TKXTD,TDXTD,TKMTD,TDMTD,NOPRP
      Y1=Y1IN/S
      Y2=Y2IN/S
      R1=SQRT(X1**2+Y1**2)
      R2=SQRT(X2**2+Y2**2)
      Z1=R1+X1
      Z2=R2+X2
      IF(R2-R1)500,501,502
500   IF(Z2-Z1)504,504,503
502   IF(Z2-Z1)503,504,504
```

```
503   A=ALOG(R1/R2)/(2.*(Z2-Z1))
      CALL BESSEL(A*R1,BI0,BI1,BK0,BK1)
      CPSK0=EXP(A*X1)*TN/BK0
      WHAT=1.
      GO TO 505
501   R=R1
      WHAT=2.
      GO TO 505
504   WHAT=3.
505   IF(X1+X2)506,507,507
506   REGIN=-1.
      GO TO 508
507   REGIN=1.
508   SLOPE=(Y2-Y1)*S/(X2-X1)
      CONST=Y1IN-SLOPE*X1
      RETURN
      END
      SUBROUTINE PNTFND(X1,Y1,X2,Y2,GRDX,GRDY,TN,NW,NEXT,XBTWN,YBTWN,S)
      DIMENSION BI0RD(60),BI1RD(60),BK0RD(60),BK1RD(60),RRED(60)
      DIMENSION TRED(50),TKRD(50),TDRD(50)
      COMMON BI0RD,BI1RD,BK0RD,BK1RD,RRED
      COMMON TRED,TKRD,TDRD
      COMMON QBOIL
      COMMON TM,TA,AMIN,TDEL,CN,CCONV,CRAD,SPD,THICK
      COMMON TKXTD,TDXTD,TKMTD,TDMTD,NOPRP
      SLINF(SLA,SLARG,SLB,SLC)=SLA*SLARG+SLB*SLC
      CIRCLF(RCIR,ARCIR)=SQRT(RCIR**2-ARCIR**2)
      NPT1=X1/GRDX
      NPT2=X2/GRDX
      FNPT=NPT2-NPT1
      NPT=ABS(FNPT)
      IF(NPT-NW)601,602,602
602   NEXT=1
      XBTWN=(X1+X2)/2.
      CALL POLFN(X1,Y1,X2,Y2,TN,AF,CK,SLOP,CONT,R,WHAT,REG,R1,R2,S)
      IF(WHAT-1.)635,636,635
```

```
635   IF(WHAT-2.)637,638,637
636   CALL COLUMN(YBTWN,XBTWN,AF,CK,(Y1+Y2)/2.,TN,S)
      IF(YBTWN-((Y1+Y2)/2.+GRDY))639,639,637
633   YBTWN=CIRCLF(R,XBTWN)*S
      GO TO 639
637   YBTWN=SLINF(SLOP,XBTWN,1.,CONT)
      GO TO 639
611   NEXT=0
639   RETURN
      END
      SUBROUTINE ORBLW(RFS,A,XL,XL1,W,RGS,S)
      DIMENSION BIORD(60),BI1RD(60),BKORD(60),BK1RD(60),RRED(60)
      DIMENSION TRED(50),TKRD(50),TDRD(50)
      COMMON BIORD,BI1RD,BKORD,BK1RD,RRED
      COMMON TRED,TKRD,TDRD
      COMMON QBOIL
      COMMON TM,TA,AMIN,TDEL,CN,CCONV,CRAD,SPD,THICK
      COMMON TKXTD,TDXTD,TKMTD,TDMTD,NCPRP
      RF=RGS
      CRITE1=1.E-6
802   XW=RF-XL1
      RW1=SQRT(XW**2+XL1**2/4.)
805   FUNT=(RW1+RF-XL1)*ALOG(RF/(XL-RF))-2.*RF*ALOG(RW1/(XL-RF))
      FDRV=ALOG(RF/(XL-RF))-2.*RF/RW1
      RW=RW1-FUNT/FDRV
      IF(ABS(RW-RW1)-.001)803,803,804
804   RW1=RW
      GO TO 805
813   G=ALOG(RF/RW)
      H=XW+RW-2.*RF
      A=.5*G/H
      CALL BESSEL(A*RW,BIO,BI1,BKO,BK1)
      BKOD=-BK1
      BK1D=-BKO-BK1/(A*RW)
      RWD=XW/RW
      GO=(RW-RWD*RF)/(RW*RF)
```

```
      HD=RWD-1.
      AD=.5*(GD*H-HD*G)/H**2
      TABE=BK0+XW*BK1/RW
      DRIV=(AD*RW+A*RWD)*(BK0D+XW*BK1D/RW)+(RW-RWD*XW)*BK1/RW**2
      RFS=RF-TABE/DRIV
      CRITE2=(DRIV*BK0+BK1*TABE)/BK0**2
      IF(CRITE1-CRITE2)800,800,801
  801 CRITE1=CRITE2
      RF=RFS
      GO TO 802
  800 S=W/SQRT(RW**2-XW**2)
      RETURN
      END
      SUBROUTINE COEF(A,A1,A2,HLOSS,TKDEP,DIFFR,T,AF,AB,BF,BB,TK,TD,
     1TKDRV)
      DIMENSION BIORD(60),BI1RD(60),BK0RD(60),BK1RD(60),RRED(60)
      DIMENSION TRED(50),TKRD(50),TDRD(50)
      COMMON BIORD,BI1RD,BK0RD,BK1RD,RRED
      COMMON TRED,TKRD,TDRD
      COMMON QBOIL
      COMMON TM,TA,AMIN,TDEL,CN,CCONV,CRAD,SPD,THICK
      COMMON TKXTD,TDXTD,TKMTD,TDMTD,NOPRP
      A=1./(AF*AB)+1./(BF*BB)
      A1=1./(AF+AB)
      A2=1./(BF+BB)
      IF(T)9,10,10
    9 T=0.
   10 CONTINUE
      IF(T-.635)1,1,2
    2 IF(T-.96)3,3,4
    4 IF(T-.1707)5,5,6
    3 QBOIL=(1.542*T*(TM-672.))**3
      GO TO 8
    5 QBOIL=2265.11*(288./(T*(TM-672.)))**5.86
      GO TO 8
    6 QBOIL=32.4*(T*(TM-672.))**.75
```

```
      GO TO 8
1     QBOIL=0.
8     CONTINUE
      CCONV=0.
      HLOSS=(1./(12.*CN))**2/(TK*THICK)*(CCONV*T+QBOIL/TDEL+CRAD/TDEL*((
     1T*TDEL+TA)**4-TA**4))
      TKDEP=TDEL*TKDRV/(2.*TK)
      DIFFR=AMIN/TD
      RETURN
      END
      SUBROUTINE DIFEQ(TNEW,TMP,T1D,T2D,T3D,T4D,AFD,ABD,BFD,BBD,TN)
      DIMENSION BIORD(60),BI1RD(60),BKORD(60),BK1RD(60),RRED(60)
      DIMENSION TRED(50),TKRD(50),TDRD(50)
      COMMON BIORD,BI1RD,BKORD,BK1RD,RRED
      COMMON QBOIL
      COMMON TM,TA,AMIN,TDEL,CN,CCONV,CRAD,SPD,THICK
      COMMON TRED,TKRD,TDRD
      COMMON TKXTD,TDXTD,TKMTD,TDMTD,NOPRP
      T(A,A1,A2,AF,AB,BF,BB,HLOSS,TKDEP,DIFFR,T1,T2,T3,T4)=(A1*(T1*(1./
     1AF+DIFFR)+T2*(1./AB-DIFFR))+A2*(T3/BF+T4/BB)+TKDEP*(A1**2*(T1-T2)
     2**2+A2**2*(T3-T4)**2)-HLOSS)/A
      CALL PROP(TK,TKDRV,TD,TMP,TRED(1),TRED(1),TRED(NOPRP),TKRD(1),
     1TDRD(1),TKRD(NOPRP),TDRD(NOPRP),TKXTD,TDXTD,TKMTD,TDMTD)
      CALL COEF(AD,A1D,A2D,HLOSD,TKDPD,DIFRD,TMP,AFD,ABD,BFD,BBD,TK,TD,
     1TKDRV)
      TNEW=T(AD,A1D,A2D,AFD,ABD,BFD,BBD,HLOSD,TKDPD,DIFRD,T1D,T2D,T3D,
     1T4D)
      IF(TNEW-1.)1,2,2
2     TNEW=.9999
1     CONTINUE
      RETURN
      END
      FUNCTION AUTSCL(YD,DN)
      DIMENSION BIORD(60),BI1RD(60),BKORD(60),BK1RD(60),RRED(60)
      DIMENSION TRED(50),TKRD(50),TDRD(50)
      COMMON BIORD,BI1RD,BKORD,BK1RD,RRED
```

```
      COMMON TRED,TKRD,TDRD
      COMMON TM,TA,AMIN,TDEL,CN,CCONV,CRAD,SPD,THICK
      COMMON TKXTD,TDXTD,TKMTD,TDMTD,NOPRP
      J=YD/DN
      ZARB1=J
      IF(YD-ZARB1*DN)701,700,701
  701 ZARB2=J+1
      AUTSCL=YD/ZARB2
      GO TO 702
  700 AUTSCL=DN
  702 RETURN
      END
      FUNCTION DRAJH(C,A,X,Y)
      DIMENSION BIORD(60),BI1RD(60),BKORD(60),BK1RD(60),RRED(60)
      DIMENSION TRED(50),TKRD(50),TDRD(50)
      COMMON BIORD,BI1RD,BKORD,BK1RD,RRED
      COMMON TRED,TKRD,TDRD
      COMMON TM,TA,AMIN,TDEL,CN,CCONV,CRAD,SPD,THICK
      COMMON TKXTD,TDXTD,TKMTD,TDMTD,NOPRP
      R=SQRT(X**2+Y**2)
      CALL BESSEL(A*R,BIO,BI1,BKO,BK1)
      DRAJH=C*EXP(-A*X)*BKO
      RETURN
      END
```

| | | | | |
|---|---|---|---|---|
| .05 | 1.0006 | .025 | 3.1142 | 19.91 |
| .1 | 1.0025 | .05006 | 2.4271 | 9.8538 |
| .15 | 1.0056 | .07521 | 2.03 | 6.4775 |
| .2 | 1.01 | .1005 | 1.7527 | 4.776 |
| .25 | 1.0156 | .12598 | 1.5415 | 3.747 |
| .3 | 1.0226 | .15169 | 1.3725 | 3.056 |
| .35 | 1.0309 | .17769 | 1.2327 | 2.5591 |
| .4 | 1.0404 | .20403 | 1.1145 | 2.1844 |
| .45 | 1.0513 | .23074 | 1.0129 | 1.8915 |
| .5 | 1.0635 | .25789 | .92442 | 1.6564 |
| .55 | 1.0771 | .28553 | .84659 | 1.4637 |
| .6 | 1.092 | .3137 | .77754 | 1.3028 |

| | | | | |
|---|---|---|---|---|
| .65 | 1.1084 | .34247 | .71589 | 1.1668 |
| .7 | 1.1263 | .37188 | .66054 | 1.0503 |
| .75 | 1.1456 | .40199 | .6106 | .94957 |
| .8 | 1.1665 | .43286 | .56536 | .86178 |
| .85 | 1.1889 | .46456 | .52424 | .78467 |
| .9 | 1.213 | .49713 | .48674 | .71653 |
| .95 | 1.2387 | .53064 | .45246 | .65597 |
| 1. | 1.2661 | .56516 | .42103 | .6019 |
| 1.05 | 1.2952 | .60075 | .39218 | .55341 |
| 1.1 | 1.3261 | .63749 | .36562 | .50975 |
| 1.15 | 1.359 | .67544 | .34114 | .47031 |
| 1.2 | 1.3937 | .71467 | .31853 | .43458 |
| 1.25 | 1.4304 | .75528 | .29762 | .40211 |
| 1.3 | 1.4692 | .79732 | .27827 | .37254 |
| 1.35 | 1.5102 | .84089 | .26033 | .34553 |
| 1.4 | 1.5534 | .88609 | .24368 | .32082 |
| 1.45 | 1.5989 | .93298 | .22821 | .29817 |
| 1.5 | 1.6467 | .98167 | .21382 | .27737 |
| 1.55 | 1.6971 | 1.0322 | .20044 | .25824 |
| 1.6 | 1.75 | 1.0848 | .18797 | .24062 |
| 1.65 | 1.8056 | 1.1395 | .17636 | .22436 |
| 1.7 | 1.8604 | 1.1963 | .16553 | .20934 |
| 1.75 | 1.9252 | 1.2555 | .15541 | .19546 |
| 1.8 | 1.9895 | 1.3172 | .14597 | .1826 |
| 1.85 | 2.0557 | 1.3814 | .13713 | .17069 |
| 1.9 | 2.1277 | 1.4482 | .12888 | .15964 |
| 1.95 | 2.2018 | 1.5179 | .12115 | .14938 |
| 2. | 2.2795 | 1.5906 | .11393 | .13984 |
| 2.05 | 2.3609 | 1.6664 | .10716 | .13097 |
| 2.1 | 2.4463 | 1.7455 | .10082 | .12272 |
| 2.15 | 2.5356 | 1.828 | .09487 | .11503 |
| 2.2 | 2.6291 | 1.9141 | .0893 | .10787 |
| 2.25 | 2.7271 | 2.0044 | .08407 | .10118 |
| 2.3 | 2.8296 | 2.0978 | .07918 | .09495 |
| 2.35 | 2.9369 | 2.1958 | .07458 | .08913 |
| 2.4 | 3.0492 | 2.2981 | .07026 | .08369 |

| | | | | |
|---|---|---|---|---|
| 2.45 | 3.1668 | 2.405 | .06621 | .07861 |
| 2.5 | 3.2898 | 2.5167 | .0624 | .07385 |
| 2.55 | 3.4185 | 2.6334 | .05882 | .06941 |
| 2.6 | 3.5532 | 2.7554 | .05545 | .06524 |
| 2.65 | 3.6941 | 2.8829 | .05229 | .06134 |
| 2.7 | 3.8416 | 3.0161 | .04931 | .05769 |
| 2.75 | 3.9958 | 3.1554 | .04651 | .05427 |
| 2.8 | 4.1573 | 3.3011 | .04388 | .05106 |
| 2.85 | 4.3261 | 3.4533 | .0414 | .04805 |
| 2.9 | 4.5027 | 3.6120 | .03917 | .04523 |
| 2.95 | 4.6875 | 3.7792 | .03687 | .04258 |
| 3. | 4.8818 | 3.9534 | .03482 | .04009 |

| | | |
|---|---|---|
| 50 | | |
| 50. | 45.5 | 2.31225 |
| 100. | 44.5 | 2.05584 |
| 150. | 43.5 | 1.57996 |
| 200. | 42.5 | 1.39509 |
| 250. | 41.8 | 1.12693 |
| 300. | 41. | 1.04429 |
| 350. | 40. | .99457 |
| 400. | 39.2 | .89311 |
| 450. | 38.5 | .82750 |
| 500. | 37.6 | .76845 |
| 550. | 36.8 | .7378 |
| 600. | 36.1 | .70351 |
| 650. | 35.2 | .65597 |
| 700. | 34.5 | .60482 |
| 750. | 33.8 | .58294 |
| 800. | 32.8 | .56199 |
| 850. | 32. | .54489 |
| 900. | 31.2 | .52739 |
| 950. | 30.5 | .50348 |
| 1000. | 29.7 | .47212 |
| 1050. | 29. | .44432 |
| 1100. | 28.2 | .41701 |
| 1150. | 27.5 | .39462 |

```
12100.          26.8          .39177
12500.          25.9          .35928
13000.          25.           .33571
13500.          24.5          .31919
14000.          23.8          .29566
14500.          23.1          .27598
15000.          22.2          .24465
15500.          21.8          .22843
16000.          21.1          .20136
16500.          20.6          .14922
17000.          20.           .14046
17500.          19.5          .12877
18000.          19.           .13384
18500.          18.8          .1528
19000.          18.1          .18214
19500.          17.8          .2351
20000.          17.2          .22717
21000.          17.           .22453
21500.          16.5          .21793
21500.          16.1          .21264
22000.          15.9          .21
22500.          15.5          .20533
23000.          15.2          .20165
23500.          15.           .19935
24000.          14.9          .19855
24500.          14.5          .19379
25000.          14.1          .18895
29.          135.
31800.          .116          4.98          .19
5000.
   .1317E-08
18.8
3.              .5            1.
1.              .35           .35           .5
  2
 30
```

15
3
1
1
1
1
2
1
11
1
2
1
15
31

# APPENDIX 8

## UTILITY PROGRAMS

```
C
C             THIS PROGRAM DETERMINES THE CORRELATION PARAMETERS
C             NECESSARY FOR COMPUTING THE MAXIMUM DIMENSIONS
C             OF THE WELD POOL.
C
      DIMENSION VOLT(1[illegible]),AMP(1[illegible]),THICK(1[illegible]),RN(1[illegible]),DIST(1[illegible])
      DIMENSION TIME(1[illegible]),HW(1[illegible]),X(1[illegible]),WI(1[illegible]),XI(1[illegible]),SPD(1[illegible])
      DIMENSION WN(1[illegible]),XN(1[illegible]),B(2),XL(1[illegible]),WL(1[illegible]),P(1[illegible])
      DIMENSION PL(1[illegible]),PW(1[illegible]),RW(1[illegible]),RL(1[illegible]),P1(1[illegible]),P2(1[illegible])
      READ 1[illegible],N
      READ 2[illegible],TM,TA,AMIN,AVCON
      READ 3[illegible],(RN(I),VOLT(I),AMP(I),DIST(I),TIME(I),THICK(I),X(I),
     1HW(I),I=1,N)
 1[illegible] FORMAT(I3)
 2[illegible] FORMAT(4F1[illegible].5)
 3[illegible] FORMAT(8F1[illegible].5)
      PC=3.415/(2.*3.1416*AVCON*(TM-TA))
      DISTV=1./(2.*AMIN)
      NW=0
      NL=0
      PRINT 11
 11   FORMAT(4X,4HRUN#,6X,4HVOLT,6X,3HAMP,3X,12HVEL(FT/HR),1X,10HLENGTH(
     1IN),2X,9HWIDTH(IN),1X,6HLUMPAR,1X,9HTHICK(IN),/)
      DO 1 I=1,N
      SPD(I)=5.*DIST(I)/TIME(I)
      DISTN=SPD(I)*DISTV
      WN(I)=2.*HW(I)/(25.4*12.)*DISTN
      XN(I)=X(I)/(25.4*12.)*DISTN
      WI(I)=2.*HW(I)/25.4
      XI(I)=X(I)/25.4
      P(I)=PC*VOLT(I)*AMP(I)*12./THICK(I)
      PRINT 12,RN(I),VOLT(I),AMP(I),SPD(I),XI(I),WI(I),P(I),THICK(I)
 12   FORMAT(8F1[illegible].5)
      IF(XN(I))3[illegible],32,3[illegible]
 3[illegible] NL=NL+1
      XN(NL)=XN(I)
```

```
      RL(NL)=RN(I)
      P1(NL)=P(I)
32    IF(WN(I))33,1,33
33    NW=NW+1
      WN(NW)=WN(I)
      RW(NW)=RN(I)
      P2(NW)=P(I)
1     CONTINUE
      DO 4 I=1,NL
      XL(I)=ALOG(XN(I))
      PL(I)=ALOG(P1(I))
4     CONTINUE
      DO 5 I=1,NW
      WL(I)=ALOG(WN(I))
      PW(I)=ALOG(P2(I))
5     CONTINUE
      CALL LSFIT(NW,2,PW,WL,B)
      A=EXP(B(1))
      PRINT 13
13    FORMAT(///)
      PRINT 14
14    FORMAT(20X,51H ********** PLOTTING INFO MAX LENGTH AND WIDTH **********,
     1///)
      PRINT 15
15    FORMAT(4X,4HRUN#,5X,4HLOGP,8X,1HP,5X,9HLOGLENGTH,1X,9HNORLENGTH,/)
      PRINT 16,(RL(I),PL(I),P1(I),XL(I),XN(I),I=1,NL)
16    FORMAT(5F10.5)
      PRINT 13
      PRINT 2
2     FORMAT(4X,4HRUN#,5X,4HLOGP,8X,1HP,6X,8HLOGWIDTH,2X,8HNORWIDTH,/)
      PRINT 21,(RW(I),PW(I),P2(I),WL(I),WN(I),I=1,NW)
21    FORMAT(5F10.5)
      PRINT 13
      PRINT 17,A,B(2)
17    FORMAT(17H COEFF FOR WIDTH=F10.5,/,15H EXP FOR WIDTH=F10.5)
      RN(1)=1.
```

```
      DO 10  I=2,20
 10   RN(I)=RN(I-1)+1.
      DO 6  I=1,2
 60   WI(I)=A*RN(I)**B(2)
      PRINT 13
      CALL LSFIT(NL,2,PL,XL,B)
      C=EXP(B(1))
      PRINT 18,C,B(2)
 18   FORMAT(18H COEFF FOR LENGTH=F10.5,/,16H EXP FOR LENGTH=F10.5)
      DO 7  I=1,2
 7    XI(I)=C*RN(I)**B(2)
      PRINT 13
      PRINT 19
 19   FORMAT(6X,23HVALUES FOR FITTED CURVE,//)
      PRINT 8
 8    FORMAT(2X,6HLUMPAR,2X,8HNORWIDTH,2X,9HNORLENGTH,/)
      PRINT 81,(RN(I),WI(I),XI(I),I=1,20)
 81   FORMAT(3F1 .5)
 15
```

| | | | | | | | |
|---|---|---|---|---|---|---|---|
| 31 | 513. | .12877 | 18.8 | | | | |
| 41. | 25. | 19 . | 3.87 | .164 | .126 | 0. | 3.56 |
| 42. | 31. | 175. | 1.66 | .1 3 | .125 | 0. | 4. 6 |
| 43. | 31. | 169. | 2.18 | .15 | .128 | 19.65 | 4.3 |
| 44. | 31. | 14 . | 2.44 | .13 | .127 | 16. | 3.45 |
| 45. | 27. | 16 . | 4.18 | .18 | .126 | 0. | 3.3 |
| 46. | 26. | 19 . | 3.67 | .17 | .125 | 14.99 | 3.25 |
| 47. | 27. | 2 5. | 3.59 | .16 | .128 | 0. | 3.25 |
| 48. | 32. | 2 0. | 2.52 | .11 | .131 | 18. 3 | 4. |
| 49. | 31. | 215. | 3.9 | .17 | .131 | 18.8 | 3.95 |
| 5 . | 32. | 125. | 2.4 | .14 | .126 | 15.75 | 3.3 |
| 51. | 23. | 155. | 4.29 | .19 | .131 | 0. | 3. .5 |
| 52. | 29. | 17 . | 1.74 | . 8 | .132 | 2 .83 | 3.65 |
| 53. | 3 . | 165. | 4. | .16 | .125 | 2 .83 | 3.56 |
| 54. | 33. | 18 . | 1.82 | . 8 | .131 | 17.53 | 3.7 |
| 55. | 35. | 19 . | 4.36 | .15 | .126 | 2 .97 | 3.25 |

```
C
C
C
C
C
C               THIS PROGRAM DETERMINES THE CORRELATION PARAMETERS NECESSARY
C               FOR THE POOL CONTOUR EQUATION.
C
      XL=.827
      HW=.11
      D1=(P(1)*XL/(P(1)+P(2)))**P(1)
      D2=(XL-P(1)*XL/(P(1)+P(2)))**P(2)
      XK=HW**2/(D1*D2)
      E=((XK*X(1)**P(1)*(XL-X(1))**P(2))**.5)
      D(1)=E/2.*(ALOG(P(1)+P(2))-ALOG(P(1)*XL)+ALOG(X(1)))
      D(2)=E/2.*(ALOG(P(1)+P(2))-ALOG(P(2)*XL)+ALOG(XL-X(1)))
      RETURN
      END
PROBL1RUN#53    2    2     17    2 .0   .1 .0001 100    1
(2F10.5)
.092          .031
.159          .079
.198          .098
.138          .106
.177          .11
.216          .098
.256          .098
.295          .087
.335          .079
.374          .075
.413          .067
.453          .063
.492          .059
.531          .059
.571          .055
.689          .043
```

| | | |
|---|---|---|
| .768 | .12 | |
| MAXMUM | 100. | 100. |
| MINMUM | .1 | .1 |
| PARAM | 3. | .75 |

```
C
C
C
C
C
C           THIS PROGRAM REDUCES THE DATA AND PUTS THE RESULTS IN
C           SAME COORDINATE SYSTEM AS THE MODEL.
C
      DIMENSION EMECA(6  ),TCA(6  )
      DIMENSION XCHRT(1  ), YTEMP(1  ),XCCHRT(1  ),XCFOR(1  ),XNFOR(1  )
      DIMENSION TMPN(1  ),X(5  ),Y(5  ),T(1  ),XTGR(1  ),TGRP(1  )
      DIMENSION XEME(1  )
      DIMENSION YNDIT(1  )
      COMMON EMECA,TCA
      READ 3  ,NOCA
      READ 1  ,(EMECA(I),TCA(I),I=1,NOCA)
      READ 3  ,NRUN
      DO 1  IRUN=1,NRUN
      READ 3  ,NRUNN
      READ 2  ,ALMIN,TMELT,THIKRD,TAMB
      READ 2  ,DISTV,TIME,VOLT,AMP
      READ 7  ,TAMBCA
      READ 3  ,NOGRAP
      VEL=DISTV*5./TIME
      DISIN=24.*ALMIN/VEL
      TDIFF=TMELT-TAMB
 1  FORMAT(6F1 .5)
 2  FORMAT(4F1 .5)
 3  FORMAT(I3)
 5  FORMAT(2F1 .5)
 7  FORMAT(F1 .5)
 8999 FORMAT(///)
      PRINT 16
 1600 FORMAT(43X,34H ******* EXPERIMENTAL DATA *******,///)
      PRINT 15
 1500 FORMAT(44X,32H ******* SPECIMEN DATA *******,//)
```

```
      PRINT 4040
4040  FORMAT (20X,39H MATERIAL ..............AISI 1010 STEEL,/)
      PRINT 4500,TMELT
4500  FORMAT(51X,37H MELTING TEMPERATURE, (DEG.R) .......,F12.5,/)
      PRINT 5500,THIKRD
5500  FORMAT(64X,25H THICKNESS, (IN.) .......,F12.5,///)
      PRINT 6500
6500  FORMAT (45X,29H ********** WELDING DATA **********,//)
      PRINT 7500,VEL
7500  FORMAT(56X,33H SPEED OF TRAVEL, (FT/HR) .......,F12.5,/)
      PRINT 8000,VOLT
8000  FORMAT (64X,25H VOLTAGE, (VOLTS) .......F12.5,/)
      PRINT 8500,AMP
8500  FORMAT(65X,24H CURRENT, (AMPS) .......,F12.5,/)
      READ 8501,EDIA,EANG
8501  FORMAT(2F10.5)
      PRINT 8502
8502  FORMAT(20X,39H TYPE ELECTRODE ..............7018-A1,/)
      PRINT 8503,EDIA
8503  FORMAT(51X,37H ELECTRODE DIA., (IN.) .............,F12.5,/)
      PRINT 8504,EANG
8504  FORMAT(51X,37H ELECTRODE ANGLE, (DEG.) .............,F12.5,///)
      PRINT 9000
9000  FORMAT(35X,49H ********** COMPUTATION DATA AND ASSUMPTIONS **********,/)
      PRINT 9300,TAMB
9300  FORMAT(52X,37H AMBIENT TEMPERATURE, (DEG.R) .......,F12.5,/)
      PRINT 9400,ALMIN
9400  FORMAT(32X,55H MINIMUNVLLUE OF THERMAL DIFFUSIVITY, (FT2/HR) .....
     1..,F12.5,/)
      PRINT 9500,DISIN
9500  FORMAT(53X,35H NORMALIZING DISTANCE, (IN.) ......,F12.5,/)
      PRINT 9600,TDIFF
9600  FORMAT(48X,41H NORMALIZING TEMPERATURE, (DEG.R) .......,F12.5,/)
      DO 1004 ID=1,NOGRAP
      READ 3000,ITCN
      READ 7000,XTCPL
```

```
      READ 7[illegible],VELR
      READ 30[illegible],NOOP
      READ 50[illegible],(XCHRT(I),XEMF(I),I=1,NOOP)
      XCCHRT(1)=[illegible]
      DO 1[illegible]1 I=2,NOOP
      XCHRT(I)=XCHRT(I)/2.54
1[illegible]01 XCCHRT(I)=XCCHRT(I-1)+XCHRT(I)
      XCONV=11.81*VELR/VEL
      XFORC=XCONV*XTCPL
      DO 1[illegible]2 I=1,NOOP
1[illegible]02 XCFOR(I)=XFORC-XCCHRT(I)
      DO 1[illegible]3 I=1,NOOP
      XNFOR(I)=XCFOR(I)/(XCONV*DISIN)
      TMPN(I)=(TMPF(XEMF(I))-TAMB+459.69)/TDIFF
1[illegible]3 T(I)=TMPN(I)*TDIFF+TAMB
      READ 7[illegible],YDIST
      DO 8681 I=1,NOOP
8681  YNDIT(I)=YDIST/DISIN
      PRINT 8999
      PRINT 868[illegible]
8680 FORMAT(43X,33H ********** MEASUREMENT DATA **********,//)
      PRINT 13,NRUNN
13    FORMAT(7[illegible]X,19H RUN NUMBER ........,I3,//)
      PRINT 1[illegible]11,ITCN
1[illegible]11 FORMAT(63X,28H THERMOCOUPLE NUMBER .......,I3,//)
      PRINT 1[illegible]1[illegible]
1[illegible]1[illegible] FORMAT(37X,52H TYPE OF THERMOCOUPLE USED IS ....... CHROMEL-ALUMEL
     1,//)
      PRINT 1[illegible]4[illegible],YDIST
1[illegible]49 FORMAT(28X,56H THERCOUPLE DISTANCE FROM LLINE OF SYMMETRY,(IN.) ..
     1.....,F12.5,/)
      VELR=VELR*2.36
      PRINT 1[illegible]3[illegible],VELR
1[illegible]3[illegible] FORMAT(6[illegible]X,29H CHART SPEED,(IN/MIN) .......,F12.5,///)
      PRINT 28[illegible]
28[illegible] FORMAT(33X,5[illegible]H ********** MEASURED TEMPERATURE DISTRIBUTION **********,/
```

```
     1//)
      PRINT 1250
 1250 FORMAT(2X,32HDIM-LESS SIST. FROM LINE OF SYM.,5X,25HDIM-LESS DIST.
     1FROM ORIGIN,5X,2?HDIM-LESS TEMPERATURE,5X,19HTEMPERATURE,(DEG.R))
      PRINT 18[ ,(YNDIT(I),XNFOR(I),TMPN(I),T(I),I=1,NOOP)
 18[ FORMAT(12X,F12.5,22X,F12.5,16X,F12.5,13X,F12.5)
 1[ 4 CONTINUE
 1    CONTINUE
      END
      FUNCTION TMPF(EMFD)
      DIMENSION EMFCA(6[ ),TCA(6[0)
      COMMON EAMBCA
      COMMON EMFCA,TCA
      VALF(A,B,C,D,E)=A+(B-A)/(D-C)*(E-C)
      EMULT=1./(EMFCA(2)-EMFCA(1))
      EMFD1=EMFD+EAMBCA
      E=EMFD1*EMULT
      I=E+1.
      TMPF=VALF(TCA(I),TCA(I+1),EMFCA(I),EMFCA(I+1),EMFD1)
      RETURN
      END
      END
537
C
C             THE FOLLOWING IS A LISTING OF MILLIVOLTS VS.DEGREES F
          FOR CHROMEL-ALUMEL THERMOCOUPLES.
C
.0          32.          .1          36.4444     .2          40.9629
.3          45.4815        .4        5[.         .5          54.5454
.6          59.[9[9        .7        63.6363       .8        68.1818
.9          72.7272      1.          77.2727     1.1         81.6614
1.2         86.[5[2        1.3       9[.4[95       1.4       94.7688
1.5         99.1281        1.6       103.6581    1.7         1[8.188
1.8         112.5628     1.9         116.9376       2.       121.2917
2.1         125.6459     2.2         13[.        2.3         134.3478
2.4         138.6956       2.5       143.0435       2.6      147.3913
```

| | | | | | |
|---|---|---|---|---|---|
| 2.7 | 151.7391 | 2.8 | 156.0869 | 2.9 | 160.4348 |
| 3. | 164.7826 | 3.1 | 169.1304 | 3.2 | 173.311 |
| 3.3 | 177.4916 | 3.4 | 181.8049 | 3.5 | 186.1181 |
| 3.6 | 190.4562 | 3.7 | 194.7943 | 3.8 | 199.1324 |
| 3.9 | 203.4794 | 4. | 207.8265 | 4.1 | 212.1742 |
| 4.2 | 216.5218 | 4.3 | 220.8696 | 4.4 | 225.2174 |
| 4.5 | 229.5652 | 4.6 | 233.913 | 4.7 | 238.2609 |
| 4.8 | 242.6087 | 4.9 | 246.9565 | 5. | 251.3043 |
| 5.1 | 255.9522 | 5.2 | 260. | 5.3 | 264.5454 |
| 5.4 | 269.[illegible]99 | 5.5 | 273.4545 | 5.6 | 277.8182 |
| 5.7 | 282.33 | 5.8 | 286.8417 | 5.9 | 291.3791 |
| 6. | 295.9164 | 6.1 | 300.4595 | 6.2 | 305.1026 |
| 6.3 | 309.5457 | 6.4 | 314.091 | 6.5 | 318.6364 |
| 6.6 | 323.[illegible]7 | 6.7 | 327.3776 | 6.8 | 331.8856 |
| 6.9 | 336.3936 | 7. | 340.9291 | 7.1 | 345.4645 |
| 7.2 | 350. | 7.3 | 354.5454 | 7.4 | 359.[illegible]9 |
| 7.5 | 363.6364 | 7.6 | 368.1818 | 7.7 | 372.5589 |
| 7.8 | 376.9367 | 7.9 | 381.4499 | 8. | 385.9457 |
| 8.1 | 390.4793 | 8.2 | 395.013 | 8.3 | 399.5466 |
| 8.4 | 404.0922 | 8.5 | 408.2578 | 8.6 | 412.774 |
| 8.7 | 417.2903 | 8.8 | 421.8294 | 8.9 | 426.3686 |
| 9. | 430.7658 | 9.1 | 435.1631 | 9.2 | 439.5603 |
| 9.3 | 444.[illegible]993 | 9.4 | 448.6383 | 9.5 | 453.[illegible]82 |
| 9.6 | 457.3781 | 9.7 | 461.8859 | 9.8 | 466.3937 |
| 9.9 | 470.7828 | 10. | 475.172 | 10.1 | 479.5611 |
| 10.2 | 483.9516 | 10.3 | 488.2602 | 10.4 | 492.6083 |
| 10.5 | 496.9563 | 10.6 | 501.4542 | 10.7 | 505.952 |
| 10.8 | 510.342 | 10.9 | 514.732 | 11. | 519.122 |
| 11.1 | 523.4732 | 11.2 | 527.8244 | 11.3 | 532.1728 |
| 11.4 | 536.5212 | 11.5 | 540.8692 | 11.6 | 545.2172 |
| 11.7 | 549.5652 | 11.8 | 553.913 | 11.9 | 558.2609 |
| 12. | 562.6087 | 12.1 | 566.9565 | 12.2 | 571.3043 |
| 12.3 | 575.6522 | 12.4 | 580. | 12.5 | 584.3478 |
| 12.6 | 588.6956 | 12.7 | 593.0435 | 12.8 | 597.3913 |
| 12.9 | 601.7391 | 13. | 606.1869 | 13.1 | 610.4348 |
| 13.2 | 614.7826 | 13.3 | 619.1304 | 13.4 | 623.4783 |

| | | | | | |
|---|---|---|---|---|---|
| 13.5 | 627.8261 | 13.6 | 632.1739 | 13.7 | 636.5217 |
| 13.8 | 64[illegible].733 | 13.9 | 644.9456 | 14. | 649.1576 |
| 14.1 | 653.4946 | 14.2 | 657.8315 | 14.3 | 662.1774 |
| 14.4 | 666.5233 | 14.5 | 667.6448 | 14.6 | 668.7663 |
| 14.7 | 669.8878 | 14.8 | 677.9327 | 14.9 | 685.9776 |
| 15. | 69[illegible].9856 | 15.1 | 695.9936 | 15.2 | 70[illegible].5118 |
| 15.3 | 7[illegible].[illegible]3 | 15.4 | 7[illegible].5482 | 15.5 | 713.7289 |
| 15.6 | 717.9[illegible]96 | 15.7 | 722.2276 | 15.8 | 726.5456 |
| 15.9 | 73[illegible].75 | 16. | 734.9546 | 16.1 | 739.1591 |
| 16.2 | 743.4955 | 16.3 | 747.8312 | 16.4 | 752.[illegible]277 |
| 16.5 | 756.2237 | 16.6 | 76[illegible].5288 | 16.7 | 764.6339 |
| 16.8 | 769.139 | 16.9 | 773.3163 | 17. | 777.4936 |
| 17.1 | 781.8[illegible]62 | 17.2 | 786.1187 | 17.3 | 79[illegible].3252 |
| 17.4 | 794.5316 | 17.5 | 798.7381 | 17.6 | 8[illegible].[illegible]696 |
| 17.7 | 8[illegible].4[illegible]11 | 17.8 | 811.6[illegible]7 | 17.9 | 815.8[illegible]4 |
| 18. | 82[illegible]. | 18.1 | 824.3478 | 18.2 | 828.6956 |
| 18.6 | 845.6897 | 18.7 | 85[illegible]. | 18.8 | 854.1667 |
| 18.9 | 858.3333 | 19. | 862.5 | 19.1 | 866.6667 |
| 19.2 | 87[illegible].9677 | 19.3 | 875.2688 | 19.4 | 879.5699 |
| 19.5 | 883.7419 | 19.6 | 887.914 | 19.7 | 892.[illegible]816 |
| 19.8 | 896.2492 | 19.9 | 9[illegible].4161 | 2[illegible]. | 9[illegible]4.583 |
| 2[illegible].1 | 9[illegible]8.7499 | 2[illegible].2 | 913.[illegible]769 | 2[illegible].3 | 917.4038 |
| 2[illegible].4 | 921.6[illegible]25 | 2[illegible].5 | 925.8[illegible]13 | 2[illegible].6 | 93[illegible]. |
| 2[illegible].7 | 934.1667 | 2[illegible].8 | 938.3333 | 2[illegible].9 | 942.6543 |
| 21. | 946.9753 | 21.1 | 951.1768 | 21.2 | 955.3783 |
| 21.3 | 959.5798 | 21.4 | 963.9216 | 21.5 | 968.2633 |
| 21.6 | 972.455 | 21.7 | 976.6466 | 21.8 | 98[illegible].8196 |
| 21.9 | 984.9925 | 22. | 989.1654 | 22.1 | 993.3326 |
| 22.2 | 997.4997 | 22.3 | 1[illegible].81[illegible]2 | 22.4 | 1[illegible]6.12[illegible]6 |
| 22.5 | 1[illegible]10.3264 | 22.6 | 1[illegible]14.5323 | 22.7 | 1018.7382 |
| 22.8 | 1022.9[illegible]92 | 22.9 | 1[illegible]27.[illegible]892 | 23. | 1031.3868 |
| 23.1 | 1[illegible]35.6934 | 23.2 | 1[illegible]4[illegible]. | 23.3 | 1044.1666 |
| 23.4 | 1[illegible]48.3333 | 23.5 | 1052.49999 | 23.6 | 1056.6666 |
| 23.7 | 1[illegible]6[illegible].9676 | 23.8 | 1[illegible]65.2687 | 23.9 | 1[illegible]69.5698 |
| 24. | 1[illegible]73.7418 | 24.1 | 1[illegible]77.9139 | 24.2 | 1[illegible]81.7367 |
| 24.3 | 1[illegible]85.5595 | 24.4 | 1[illegible]88.996 | 24.5 | 1[illegible]92.4325 |

| | | | | | |
|---|---|---|---|---|---|
| 24.6 | 1096.869 | 24.7 | 1101.9193 | 24.8 | 1106.9697 |
| 24.9 | 1111.3131 | 25. | 1115.6565 | 25.1 | 1120. |
| 25.2 | 1124.1666 | 25.3 | 1128.3333 | 25.4 | 1132.6543 |
| 25.5 | 1136.9753 | 25.6 | 1141.1768 | 25.7 | 1145.3783 |
| 25.8 | 1149.5798 | 25.9 | 1153.7478 | 26. | 1157.9159 |
| 26.1 | 1162.2316 | 26.2 | 1166.5474 | 26.3 | 1170.7513 |
| 26.4 | 1174.9552 | 26.5 | 1179.1592 | 26.6 | 1183.4955 |
| 26.7 | 1187.8318 | 26.8 | 1192.1775 | 26.9 | 1196.5233 |
| 27. | 1200.7347 | 27.1 | 1204.946 | 27.2 | 1209.1577 |
| 27.3 | 1213.4946 | 27.4 | 1217.8315 | 27.5 | 1222. 275 |
| 27.6 | 1226.2235 | 27.7 | 1230.5286 | 27.8 | 1234.8228 |
| 27.9 | 1239.1389 | 28. | 1243.4833 | 28.1 | 1247.8277 |
| 28.2 | 1252.1725 | 28.3 | 1256.2223 | 28.4 | 1260.5278 |
| 28.5 | 1264.8333 | 28.6 | 1269.1388 | 28.7 | 1273.3161 |
| 28.8 | 1277.4935 | 28.9 | 1281.8016 | 29. | 1286.1186 |
| 29.1 | 1290.4565 | 29.2 | 1294.7944 | 29.3 | 1299.1324 |
| 29.4 | 1303.3122 | 29.5 | 1307.492 | 29.6 | 1311.8 51 |
| 29.7 | 1316.1182 | 29.8 | 1320.4562 | 29.9 | 1324.7943 |
| 30. | 1329.1323 | 30.1 | 1333.4793 | 30.2 | 1337.8264 |
| 30.3 | 1342.0241 | 30.4 | 1346.2219 | 30.5 | 1350.5275 |
| 30.6 | 1354.8332 | 30.7 | 1359.1388 | 30.8 | 1363.4832 |
| 30.9 | 1367.8277 | 31. | 1372.1749 | 31.1 | 1376.5222 |
| 31.2 | 1380.734 | 31.3 | 1384.9458 | 31.4 | 1389.1576 |
| 31.5 | 1393.4945 | 31.6 | 1397.8315 | 31.7 | 1402.1773 |
| 31.8 | 1406.5232 | 31.9 | 1410.8715 | 32. | 1415.2179 |
| 32.1 | 1419.5652 | 32.2 | 1423.913 | 32.3 | 1428.2608 |
| 32.4 | 1432.6036 | 32.5 | 1436.9565 | 32.6 | 1441.3043 |
| 32.7 | 1445.6521 | 32.8 | 1450. | 32.9 | 1454.5454 |
| 33. | 1459.0909 | 33.1 | 1463.4545 | 33.2 | 1467.8181 |
| 33.3 | 1472.1687 | 33.4 | 1476.5189 | 33.5 | 1480.8679 |
| 33.6 | 1485.2165 | 33.7 | 1489.5651 | 33.8 | 1494.102 |
| 33.9 | 1498.639 | 34. | 1503.0085 | 34.1 | 1507.3782 |
| 34.2 | 1511.7305 | 34.3 | 1516.0828 | 34.4 | 1520.4319 |
| 34.5 | 1524.781 | 34.6 | 1529.1301 | 34.7 | 1533.6592 |
| 34.8 | 1538.1883 | 34.9 | 1542.563 | 35. | 1546.9377 |
| 35.1 | 1551.4419 | 35.2 | 1555.9461 | 35.3 | 1560.3379 |

| | | | | | |
|---|---|---|---|---|---|
| 35.4 | 1564.7297 | 35.5 | 1569.1216 | 35.6 | 1573.4729 |
| 35.7 | 1577.8243 | 35.8 | 1582.3338 | 35.9 | 1586.8432 |
| 36. | 1591.38 | 36.1 | 1595.9168 | 36.2 | 16[illegible].3178 |
| 36.3 | 16[illegible].7198 | 36.4 | 16[illegible].1198 | 36.5 | 1613.6532 |
| 36.6 | 1618.1866 | 36.7 | 1622.5619 | 36.8 | 1626.9372 |
| 36.9 | 1631.4416 | 37. | 1635.946 | 37.1 | 164[illegible].4795 |
| 37.2 | 1645.[illegible]13 | 37.3 | 1649.5466 | 37.4 | 1653.9[illegible]21 |
| 37.5 | 1658.2577 | 37.6 | 1662.7739 | 37.7 | 1667.29[illegible]2 |
| 37.8 | 1671.8294 | 37.9 | 1676.3686 | 38. | 168[illegible].9124 |
| 38.1 | 1685.4562 | 38.2 | 169[illegible] | 38.3 | 1694.3478 |
| 38.4 | 1698.6956 | 38.5 | 17[illegible]3.2173 | 38.6 | 17[illegible]7.7391 |
| 38.7 | 1712.2891 | 38.8 | 1716.8212 | 38.9 | 1721.3656 |
| 39. | 1725.91 | 39.1 | 173[illegible].4551 | 39.2 | 1735.[illegible].3 |
| 39.3 | 1739.5454 | 39.4 | 1744.[illegible]9.8 | 39.5 | 1748.6363 |
| 39.6 | 1753.1817 | 39.7 | 1757.7272 | 39.8 | 1762.4485 |
| 39.9 | 1767.1678 | 4[illegible]. | 1771.75[illegible]7 | 4[illegible].1 | 1776.3336 |
| 4[illegible].2 | 178[illegible].889 | 4[illegible].3 | 1785.4445 | 4[illegible].4 | 179[illegible]. |
| 4[illegible].5 | 1794.5454 | 4[illegible].6 | 1799.[illegible]9.9 | 4[illegible].7 | 18[illegible]3.6363 |
| 4[illegible].8 | 18[illegible]8.1818 | 4[illegible].9 | 1812.9[illegible]9 | 41. | 1817.6363 |
| 41.1 | 1822.2154 | 41.2 | 1826.7945 | 41.3 | 1831.3481 |
| 41.4 | 1835.9[illegible]17 | 41.5 | 184[illegible].6[illegible]11 | 41.6 | 1845.3[illegible]5 |
| 41.7 | 185[illegible]. | 41.8 | 1854.5454 | 41.9 | 1859.[illegible] |
| 42. | 1863.6363 | 42.1 | 1868.182 | 42.2 | 1872.9[illegible]9 |
| 42.3 | 1877.6363 | 42.4 | 1882.2154 | 42.5 | 1886.7945 |
| 42.6 | 1891.51[illegible]7 | 42.7 | 1896.227 | 42.8 | 19[illegible].9763 |
| 42.9 | 19[illegible]5.7256 | 43. | 191[illegible].33[illegible]2 | 43.1 | 1914.9348 |
| 43.2 | 1919.529 | 43.3 | 1924.2942 | 43.4 | 1929.[illegible]49 |
| 43.5 | 1933.81[illegible]3 | 43.6 | 1938.5716 | 43.7 | 1943.1429 |
| 43.8 | 1947.7143 | 43.9 | 1952.4395 | 44. | 1957.1648 |
| 44.1 | 1961.9185 | 44.2 | 1966.6723 | 44.3 | 1971.208 |
| 44.4 | 1975.864 | 44.5 | 198[illegible].5758 | 44.6 | 1985.2879 |
| 44.7 | 199[illegible]. | 44.8 | 1994.7619 | 44.9 | 1999.5238 |
| 45. | 2[illegible]04.2857 | 45.1 | 2[illegible]9[illegible].476 | 45.2 | 2[illegible]13.8[illegible]95 |
| 45.3 | 2[illegible]18.5714 | 45.4 | 2[illegible]31.6666 | 45.5 | 2[illegible]44.7619 |
| 45.9 | 2047.912 | 46. | 2[illegible]52.389 | 46.1 | 2[illegible]56.866 |
| 46.2 | 2[illegible]61.5567 | 46.3 | 2[illegible]66.2474 | 46.4 | 2[illegible]71.159 |

```
46.5        2076.6716  46.6        2[illegible]8738  46.7        2085.677
46.8        2[illegible]4513  46.9        2095.2256  47.         2100.
47.1        21[illegible]4.7619  47.2        21[illegible]9.5238  47.3        2114.5124
47.4        2119.5[illegible]11  47.5        2124.2733  47.6        2129.[illegible]455
47.7        2134.[illegible]248  47.8        2139.[illegible]41  47.9        2143.7849
48.         2148.5657  48.1        2153.5371  48.2        2158.5[illegible]85
48.3        2163.2966  48.4        2168.[illegible]847  48.5        2173.[illegible]494
48.6        2178.[illegible]141  48.7        2182.8[illegible]84  48.8        2187.6[illegible]28
48.9        2192.5616  49.         2197.52[illegible]5  49.1        22[illegible]2.5123
49.2        22[illegible]7.5[illegible]41  49.3        2212.5[illegible]24  49.4        2217.5[illegible]8
49.5        2222.5[illegible]4  49.6        2227.5[illegible]1  49.7        2232.3[illegible]77
49.8        2237.1154  49.9        2242.[illegible]71  5[illegible].         2247.[illegible]266
5[illegible].1        2252.[illegible]163  5[illegible].2        2257.[illegible]61  5[illegible].3        2262.[illegible]037
5[illegible].4        2267.2[illegible]8  5[illegible].5        2272.2[illegible]8  5[illegible].6        2277.4[illegible]2
5[illegible].7        2282.44[illegible]1  5[illegible].8        2287.48[illegible]  5[illegible].9        22[illegible]2.488
51.         2297.496  51.1        23[illegible]2.4976  541.2       23[illegible]7.4992
51.3        2312.4995  51.4        2317.4998  51.5        2322.7[illegible]82
51.6        2327.9166  51.7        2332.9513  51.8        2337.9861
51.9        23[illegible]3.2[illegible]95  52.         2348.4329  52.1        2353.462
52.2        2358.4912  52.3        2363.7224  52.4        2368.9537
52.5        2373.9747  52.6        2378.9957  52.7        2384.2358
52.8        23[illegible]3.4759  52.9        2394.4873  53.         2399.4988
53.1        24[illegible]4.7494  53.2        241[illegible].         53.3        2415.2631
53.4        242[illegible].84[illegible]3  53.5        2425.68[illegible].6  53.6        2431.
53.7        2436.  53.8        2441.  53.9        2446.442
54.         2451.8823  54.1        2456.7226  54.2        2462.
  2
1[illegible]8
.1287       31[illegible].  .116        5[illegible].3.
4.98        .19  29.  135.
.9
  1
.189        51.
  1
1.37
25.
```

```
 27
0.          0.
.1          0.
5.          0.
.5          1.5
.5          4.
.5          10.5
.5          15.
.5          19.3
.5          22.
.5          23.
.5          23.
.5          22.6
.5          21.
.5          19.5
.5          18.
.5          16.7
.5          15.1
.5          12.5
.5          10.5
.5          8.2
.5          7.
.5          6.
.5          5.
.5          4.7
.5          4.
.5          3.5
7.          2.
.15
110
.1287       318[illegible].      .116        503.
4.31        .17          27.         140.
.9
 11
.189        51.
  1
```

```
2.14
25.
 28
 .              0.
1.5             0.
10.             0.
.5              1.
.5              4.5
.5             11.5
.5             22.
.5             29.
.5             35.
.5             37.
.5             36.7
.5             35.8
.5             34.
.5             32.2
.5             30.
.5             27.5
.5             24.6
.5             21.8
.5             19.2
.5             17.
.5             15.
.5             13.
.5             10.7
.5              8.3
.5              6.6
.5              5.5
.5              4.2
4.              2.4
.12
```

# APPENDIX 9

## EXPERIMENTAL DATA

The experimental data has been arranged as follows:

A. Data for the maximum dimensions of air welded pools.

B. Data for the maximum dimensions of underwater pools.

C. Pool contour measurements.

D. Data for temperature distribution with sample thermocouple output tapes.

A. DATA FOR MAXIMUM DIMENSIONS OF AIR WELDED POOLS:

| RUN# | VOLT | AMP | VEL(FT/HR) | Xm(IN) | $X_m^*$ | Ym(IN) | $Y_m^*$ | P | PLATE THICKNESS (IN) |
|---|---|---|---|---|---|---|---|---|---|
| 1 | 24 | 175 | 93.86 | -- | -- | 0.40 | 12.15 | 4.29 | 0.123 |
| 2 | 22 | 170 | 105.23 | 0.56 | 18.90 | 0.26 | 8.85 | 4.03 | 0.122 |
| 3 | 25 | 175 | 99.22 | -- | -- | 0.26 | 8.34 | 4.71 | 0.122 |
| 4 | 23 | 220 | 112.78 | 0.72 | 26.29 | 0.29 | 10.92 | 5.41 | 0.123 |
| 5 | 28 | 175 | 82.55 | 0.64 | 17.14 | -- | -- | 5.12 | 0.126 |
| 6 | 25 | 225 | 130.13 | 0.87 | 36.80 | 0.29 | 12.27 | 6.07 | 0.122 |
| 7 | 27 | 200 | 111.21 | 0.95 | 34.28 | 0.36 | 12.95 | 5.78 | 0.123 |
| 8 | 22 | 185 | 79.09 | 0.73 | 18.64 | 0.33 | 8.46 | 4.42 | 0.121 |
| 9 | 29 | 230 | 116.25 | 1.32 | 49.46 | 0.41 | 15.40 | 7.19 | 0.122 |
| 10 | 24 | 172 | 100.96 | 0.84 | 27.27 | -- | -- | 4.28 | 0.127 |

| RUN# | VOLT | AMP | VEL(FT/HR) | Xm(IN) | $X_m^*$ | Ym(IN) | $Y_m^*$ | P | PLATE THICKNESS (IN) |
|---|---|---|---|---|---|---|---|---|---|
| 11 | 21 | 143 | 84.14 | -- | -- | 0.26 | 7.07 | 3.14 | 0.126 |
| 12 | 24 | 170 | 71.21 | -- | -- | 0.30 | 6.91 | 4.26 | 0.126 |
| 13 | 22 | 175 | 98.18 | 0.56 | 17.76 | 0.27 | 8.51 | 4.02 | 0.126 |
| 14 | 23 | 170 | 90.37 | -- | -- | -- | -- | 3.93 | 0.131 |
| 15 | 26 | 200 | 93.79 | 0.94 | 28.68 | -- | -- | 5.34 | 0.128 |
| 16 | 28 | 210 | 107.27 | 0.88 | 30.47 | 0.35 | 12.14 | 5.95 | 0.130 |
| 17 | 25 | 225 | 110.48 | 1.11 | 39.55 | 0.27 | 9.57 | 5.87 | 0.126 |
| 18 | 25 | 225 | 110.22 | 0.81 | 28.78 | 0.38 | 13.56 | 5.83 | 0.127 |
| 19 | 27 | 245 | 134.00 | 1.29 | 55.99 | 0.34 | 14.68 | 6.85 | 0.127 |

| RUN# | VOLT | AMP | VEL(FT/HR) | Xm(IN) | $X_m^*$ | Ym(IN) | $Y_m^*$ | P | PLATE THICKNESS (IN) |
|---|---|---|---|---|---|---|---|---|---|
| 21 | 32 | 225 | 108.33 | 0.66 | 23.32 | -- | -- | 2.47 | 0.387 |
| 22 | 30 | 250 | 115.33 | 0.86 | 32.32 | 0.44 | 16.46 | 2.62 | 0.381 |
| 23 | 32 | 250 | 130.62 | 1.11 | 47.00 | 0.33 | 13.98 | 2.79 | 0.382 |
| 24 | 30 | 255 | 122.57 | -- | -- | -- | -- | 2.64 | 0.385 |
| 25 | 29 | 250 | 117.03 | 1.04 | 39.21 | 0.33 | 12.52 | 2.50 | 0.386 |
| 26 | 28 | 240 | 118.60 | 0.74 | 28.56 | 0.33 | 12.69 | 2.32 | 0.385 |
| 27 | 30 | 220 | 117.99 | -- | -- | -- | -- | 2.29 | 0.384 |
| 28 | 26 | 240 | 118.89 | 0.96 | 36.80 | 0.32 | 12.11 | 2.14 | 0.388 |
| 29 | 25 | 225 | 121.59 | 0.75 | 29.43 | 0.30 | 11.93 | 1.97 | 0.379 |
| 30 | 26 | 220 | 112.83 | 0.55 | 19.98 | 0.31 | 11.49 | 2.01 | 0.379 |

| RUN# | VOLT | AMP | VEL(FT/HR) | Xm(IN) | $X_m^*$ | Ym(IN) | $Y_m^*$ | P | PLATE THICKNESS (IN) |
|---|---|---|---|---|---|---|---|---|---|
| 31 | 30 | 240 | 121.99 | -- | -- | 0.44 | 17.40 | 2.50 | 0.383 |
| 32 | 27 | 240 | 108.89 | 0.88 | 31.21 | 0.28 | 9.85 | 2.25 | 0.383 |
| 33 | 27 | 230 | 116.89 | -- | -- | 0.40 | 15.19 | 2.14 | 0.386 |
| 34 | 29 | 210 | 107.65 | 0.81 | 28.11 | 0.37 | 13.03 | 2.12 | 0.382 |
| 35 | 26 | 210 | 103.16 | 0.67 | 22.34 | 0.35 | 11.69 | 1.91 | 0.381 |
| 36 | 26 | 190 | 86.15 | 0.47 | 13.06 | 0.33 | 9.33 | 1.70 | 0.387 |
| 37 | 25 | 185 | 88.81 | 0.79 | 22.63 | 0.33 | 9.50 | 1.61 | 0.38 |
| 38 | 21 | 186 | 95.17 | 0.61 | 18.67 | 0.34 | 10.42 | 1.33 | 0.390 |

B. DATA FOR MAXIMUM DIMENSIONS OF UNDERWATER POOL

| RUN# | VOLT | AMP | VEL(FT/HR) | Xm(IN) | $X_m^*$ | Ym(IN) | $Y_m^*$ | P | PLATE THICKNESS (IN) |
|---|---|---|---|---|---|---|---|---|---|
| 41 | 25 | 190 | 117.99 | -- | -- | 0.28 | 10.70 | 4.90 | 0.126 |
| 42 | 31 | 175 | 80.58 | -- | -- | 0.32 | 8.33 | 5.65 | 0.125 |
| 43 | 31 | 169 | 72.67 | 0.75 | 17.63 | 0.34 | 7.96 | 5.32 | 0.128 |
| 44 | 31 | 140 | 93.85 | 0.63 | 19.12 | 0.27 | 8.25 | 4.45 | 0.127 |
| 45 | 27 | 160 | 116.11 | -- | -- | 0.26 | 9.76 | 4.45 | 0.126 |
| 46 | 26 | 190 | 107.94 | 0.59 | 20.61 | 0.26 | 8.94 | 5.14 | 0.125 |
| 47 | 27 | 205 | 112.19 | -- | -- | 0.26 | 9.29 | 5.62 | 0.218 |
| 48 | 32 | 200 | 114.55 | 0.71 | 26.31 | 0.31 | 11.67 | 6.35 | 0.131 |
| 49 | 31 | 215 | 114.70 | 0.74 | 27.47 | 0.31 | 11.54 | 6.61 | 0.131 |

| RUN# | VOLT | AMP | VEL(FT/HR) | Xm(IN) | $X_m^*$ | Ym(IN) | $Y_m^*$ | P | PLATE THICKNESS (IN) |
|---|---|---|---|---|---|---|---|---|---|
| 50 | 32 | 125 | 85.71 | 0.62 | 17.20 | 0.26 | 7.21 | 4.13 | 0.126 |
| 51 | 28 | 155 | 112.89 | -- | -- | 0.24 | 8.77 | 4.31 | 0.131 |
| 52 | 29 | 170 | 108.75 | 0.82 | 28.86 | 0.29 | 10.11 | 4.86 | 0.132 |
| 53 | 30 | 165 | 125.00 | 0.82 | 33.17 | 0.28 | 11.34 | 5.15 | 0.125 |
| 54 | 33 | 180 | 113.75 | 0.69 | 25.40 | 0.29 | 10.72 | 5.90 | 0.131 |
| 55 | 35 | 190 | 145.33 | 0.79 | 37.16 | 0.25 | 12.03 | 6.86 | 0.126 |
| 56 | 34 | 195 | 125.29 | -- | -- | 0.36 | 14.52 | 3.42 | 0.252 |
| 57 | 33 | 205 | 136.43 | 0.83 | 36.64 | 0.30 | 13.38 | 3.51 | 0.251 |
| 58 | 34 | 225 | 174.09 | -- | -- | 0.31 | 17.30 | 3.95 | 0.252 |
| 59 | 37 | 210 | 146.94 | -- | -- | 0.30 | 14.41 | 3.98 | 0.254 |
| 60 | 38 | 220 | 175.89 | -- | -- | 0.32 | 18.37 | 4.30 | 0.253 |
| 61 | 38 | 230 | 182.14 | 0.87 | 51.28 | 0.31 | 18.33 | 4.53 | 0.251 |

C. POOL CONTOUR MEASUREMENTS

| RUN #4 | | RUN #8 | | RUN #13 | |
|---|---|---|---|---|---|
| X (mm) | Y (mm) | X (mm) | Y (mm) | X (mm) | Y (mm) |
| 0.0 | 0.0 | 0.0 | 0.0 | 0.0 | 0.0 |
| 1.5 | 2.0 | 1.4 | 2.9 | 1.1 | 2.8 |
| 2.5 | 2.8 | 2.4 | 3.6 | 2.1 | 3.1 |
| 3.5 | 3.1 | 3.4 | 3.9 | 3.1 | 3.3 |
| 4.5 | 3.6 | 4.4 | 4.2 | 4.1 | 3.4 |
| 5.5 | 3.8 | 5.4 | 4.0 | 5.1 | 3.2 |
| 6.5 | 3.7 | 6.4 | 3.6 | 6.1 | 3.0 |
| 7.5 | 3.5 | 7.4 | 3.4 | 7.1 | 2.8 |
| 8.5 | 3.3 | 8.4 | 3.1 | 8.1 | 2.4 |
| 9.5 | 3.1 | 9.4 | 3.2 | 9.1 | 2.3 |
| 10.5 | 2.8 | 10.4 | 2.9 | 10.1 | 2.1 |
| 11.5 | 2.5 | 11.4 | 3.0 | 11.1 | 1.6 |
| 12.5 | 2.2 | 12.4 | 2.8 | 12.1 | 0.9 |
| 13.5 | 1.8 | 13.4 | 2.7 | 13.1 | 0.5 |
| 14.5 | 1.4 | 14.4 | 2.6 | 14.2 | 0.0 |
| 15.5 | 1.1 | 15.4 | 2.5 | | |
| 16.5 | 0.7 | 16.4 | 2.2 | | |
| 17.5 | 0.4 | 17.4 | 2.0 | | |
| 18.3 | 0.0 | 18.5 | 0.0 | | |

RUN #53

| X (mm) | Y (mm) |
|---|---|
| 0.0 | 0.0 |
| 0.5 | 0.8 |
| 1.5 | 2.0 |
| 2.5 | 2.5 |
| 3.5 | 2.7 |
| 4.5 | 2.8 |
| 5.5 | 2.5 |
| 6.5 | 2.5 |
| 7.5 | 2.2 |
| 8.5 | 2.0 |
| 9.5 | 1.9 |
| 10.5 | 1.7 |
| 11.5 | 1.6 |
| 12.5 | 1.5 |
| 13.5 | 1.5 |
| 14.5 | 1.4 |
| 17.5 | 1.1 |
| 19.5 | 0.5 |
| 21.0 | 0.0 |

RUN #16

| X (mm) | Y (mm) |
|---|---|
| 0.0 | 0.0 |
| 1.8 | 2.4 |
| 3.8 | 2.7 |
| 5.8 | 2.4 |
| 7.8 | 2.6 |
| 9.8 | 2.4 |
| 11.8 | 2.2 |
| 13.8 | 2.1 |
| 15.8 | 2.0 |
| 17.8 | 1.7 |
| 19.8 | 1.2 |
| 21.8 | 0.7 |
| 22.3 | 0.0 |

D. WELDING VARIABLES FOR TEMPERATURE DISTRIBUTION

| RUN# | VOLT | AMP | BEAD LENGTH(IN) | TIME(MIN) | PLATE THICK.(IN) | AMBIENT TEMP. |
|---|---|---|---|---|---|---|
| 100* | 33 | 155 | 6.13 | 0.22 | 0.255 | 73 |
| 101 | 34 | 170 | 1.61 | 0.06 | 0.116 | 43 |
| 102 | 28 | 140 | 4.87 | 0.24 | 0.116 | 43 |
| 103 | 29 | 145 | 5.30 | 0.23 | 0.116 | 43 |
| 104 | 26 | 150 | 5.77 | 0.23 | 0.116 | 43 |
| 105 | 28 | 145 | 6.03 | 0.24 | 0.116 | 43 |
| 106 | 27 | 145 | 4.75 | 0.17 | 0.116 | 43 |
| 107 | 30 | 140 | 4.58 | 0.17 | 0.116 | 43 |
| 108 | 29 | 135 | 4.98 | 0.19 | 0.116 | 43 |
| 109 | 27 | 143 | 5.47 | 0.20 | 0.255 | 43 |
| 110 | 27 | 140 | 4.31 | 0.17 | 0.116 | 43 |
| 111 | 27 | 140 | 4.96 | 0.18 | 0.116 | 43 |

THERMOCOUPLE OUTPUT TAPES

CHART SPEED: 25 mm/sec

VERTICAL SCALE: 1 MILLIVOLT/mm

# RUN NO. 106, T/C NOS. 5,3,4

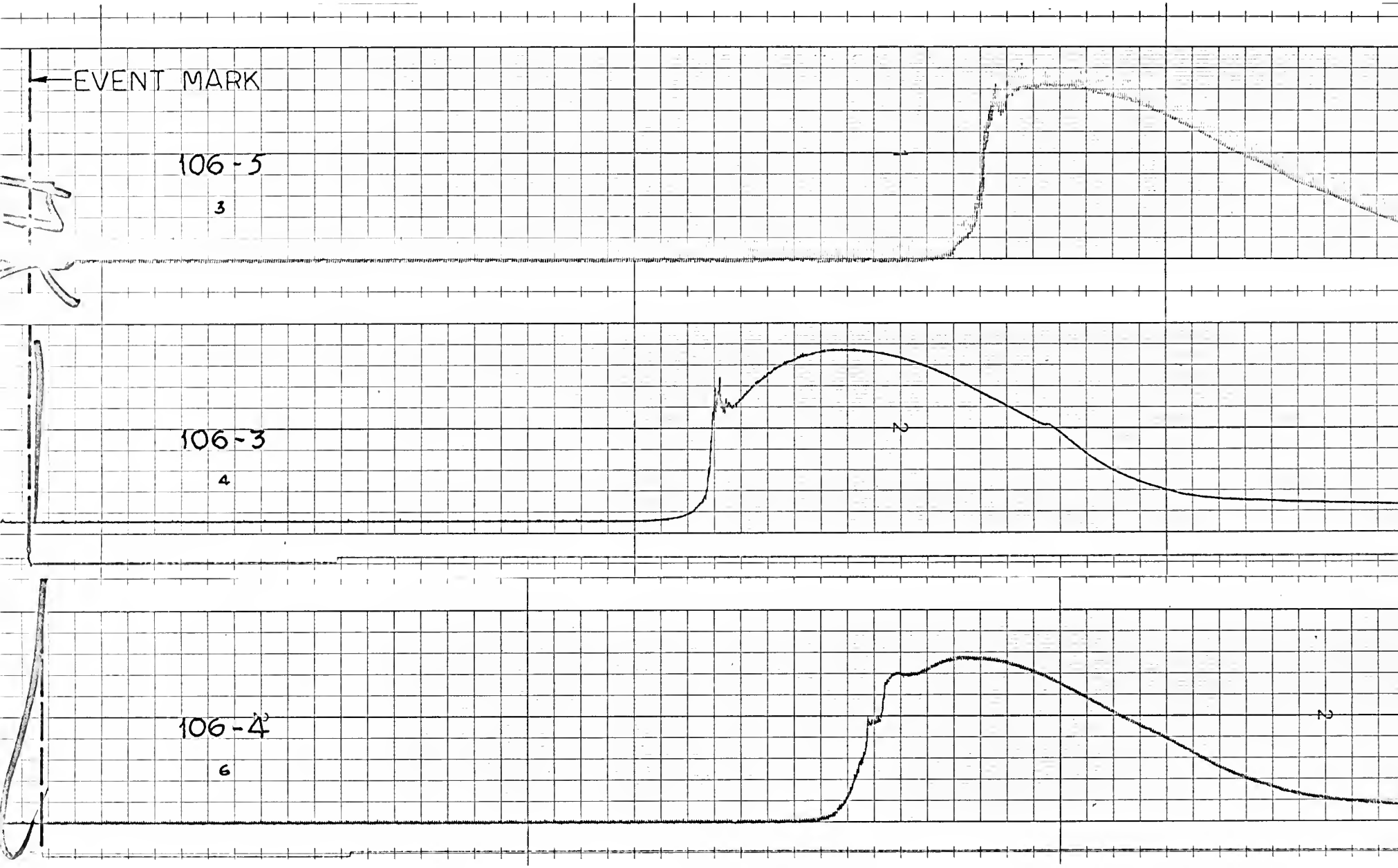

# RUN NO. 104, T/C NOS. 1, 4, 5

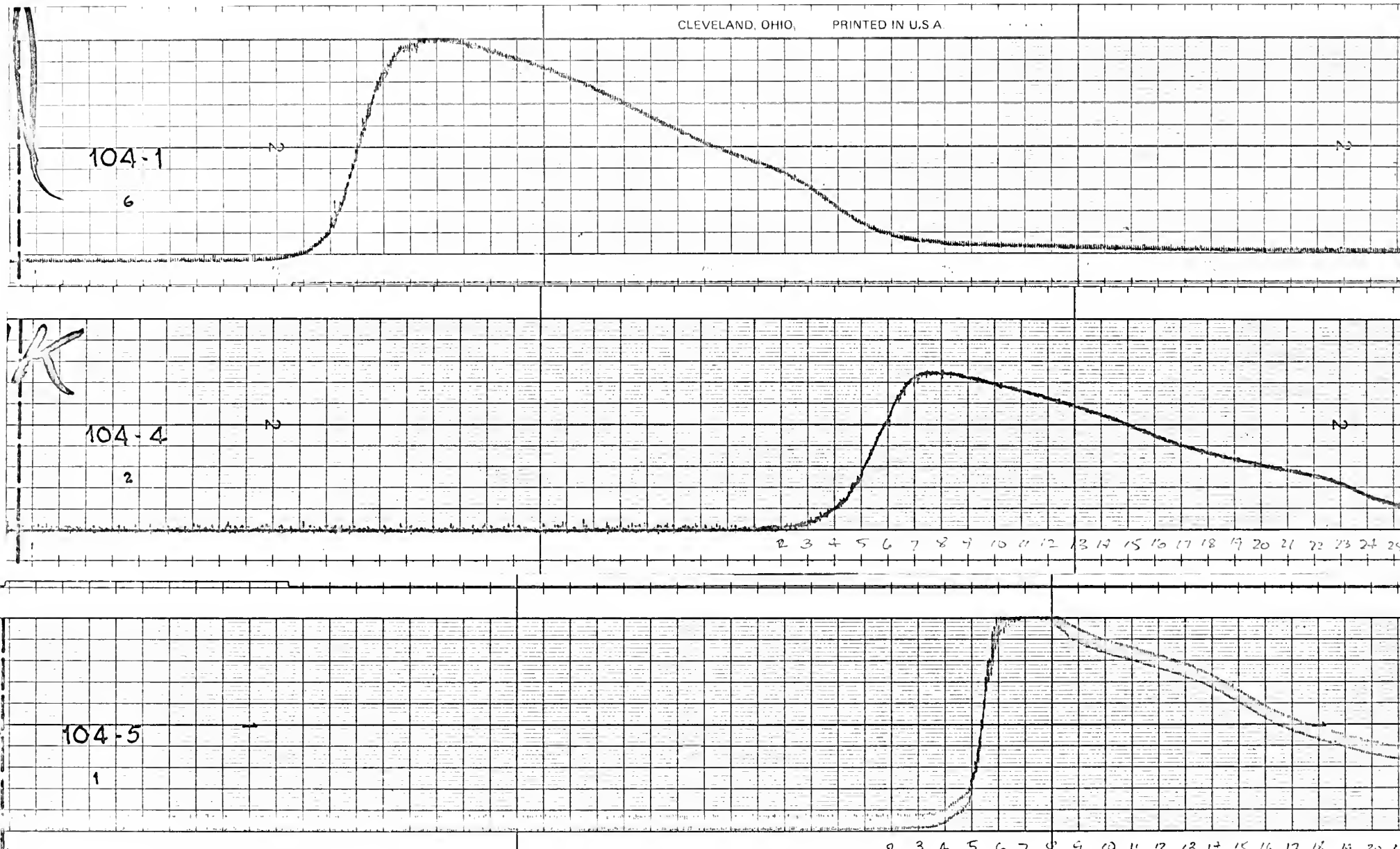

# RUN NO. 108, T/C NO. 1

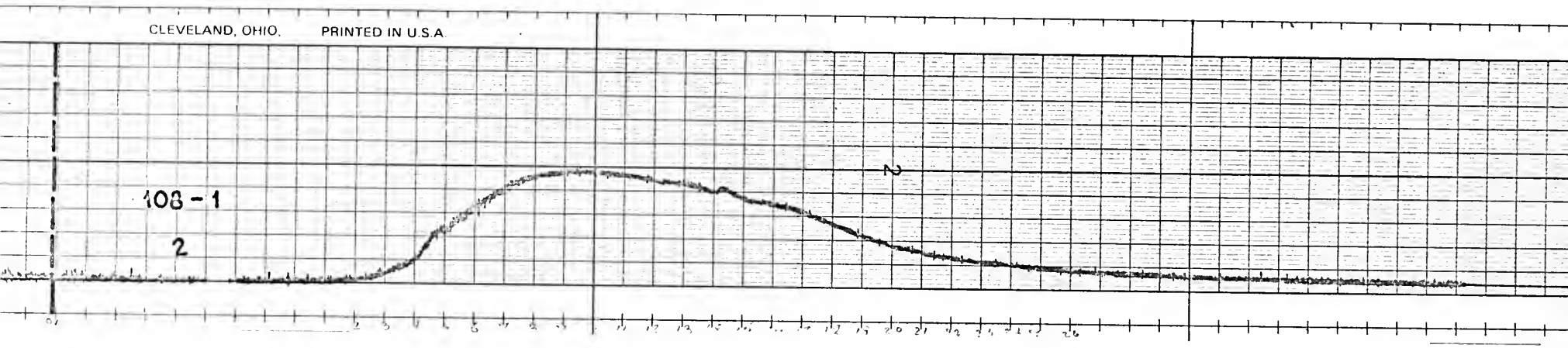


# RUN NO. 110, T/C NO. 11

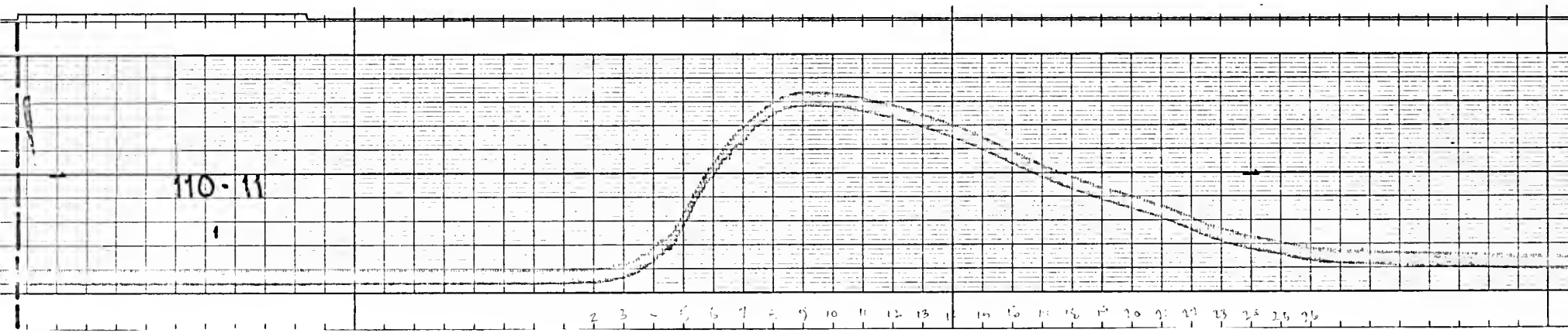

# BIBLIOGRAPHY


1. ADAMS, C, "COOLING RATES AND PEAK TEMPERATURES IN FUSION WELDING," Welding Journal, May 58, p. 210s.

2. AMES, W, NONLINEAR PARTIAL DIFFERENTIAL EQUATIONS IN ENGINEERING, Academic Press, 1965.

3. BARRY, J, "HEAT CONDUCTION FROM MOVING ARCS IN WELDING," Welding Journal, Mar 63, p. 97s.

4. DAVIES, V, CHRISTENSEN, N, GJERMUNDSEN, K, "DISTRIBUTION OF TEMPERATURES IN ARC WELDING," Brit. Weld. J., Feb 65.

5. DORCHU, K, "CONTROL OF COOLING RATES IN STEEL WELD METAL," Weld. J., Feb 68, pp 49s-62s.

6. GREENSPAN, D, INTRODUCTORY NUMERICAL ANALYSIS OF ELLIPTIC BOUNDARY VALUE PROBLEMS, Harper and Row, 1965.

7. GROSH, R, TRABANT, E, HAWKINS, G, "TEMPERATURE DISTRIBUTION IN SOLIDS," Quart. of App. Math., Vol. 13, No. 2, 1955.

8. HIBSHMAN, N, JENSEN, C, "ELECTRIC ARC WELDING UNDERWATER," J. of Amer. Weld. Soc., Oct 33, p. 4.

9. JHAVERI, O, "EFFECT OF PLATE THICKNESS AND RADIATION ON HEAT FLOW IN WELDING," Weld. J., Jan 62, p. 12s.

10. MISHLER, H, RANDALL, M, UNDERWATER JOINING AND CUTTING - PRESENT AND FUTURE, OTC 1251, Vol. II, 1970.

11. NIPPES, E, "THE WELD HEAT-AFFECTED ZONE," Weld. J., Jan 59, p. 1s.

12. PALEY, Z, "HEAT FLOW IN WELDING HEAVY STEEL PLATE," Weld. J., Feb 64, P. 71s.

13. PAVELIC, V, TEMPERATURE HISTORIES IN THIN STEEL PLATE WELDED WITH TUNGSTEN INERT GAS, Ph.D. Thesis, U. of Wisconsin, 1968.

14. ROHSENOW, W.M, DEVELOPMENTS IN HEAT TRANSFER, M.I.T. Press, 1964.

15. ROHSENOW, W.M, CHOI, H, HEAT, MASS, AND MOMENTUM TRANSFER, Prentice Hall, 1961, pp. 211-237.

16. ROSENTHAL, D, MATHEMATICAL THEORY OF HEAT DISTRIBUTION DURING WELDING AND CUTTING, Weld. J., Vol. 20, 1941, pp. 220s-234s.

17. SCHACK, A, INDUSTRIAL HEAT TRANSFER, Wiley and Sons, 1965.

18. SMITH, C, "ANALYTICAL STUDY OF ALUMINUM WELDING," Welding Research Bulletin, No. 12, 1952.

19. STEGNER, K, "EFFECT OF THERMAL CYCLES IN WELDING STEEL," Weld. J., Apr 66, p. 173s.

20. TANBAKUCHI, R, MEASURED METAL TEMPERATURES DURING ARC WELDING, Ph.D. Thesis, U. of Wisconsin, Madison, 1967.

21. TONG, L, BOILING HEAT TRANSFER AND TWO-PHASE FLOW, Wiley and Sons, 1965.

22. VAGI, J, MISHLER, H, RANDALL, M, REPORT ON UNDERWATER CUTTING AND WELDING, Battelle Memorial Institute, Columbus, Ohio, 1969.

23. WAUGH, R, EBERLEIN, O, "UNDERWATER METALLIC ARC WELDING," Weld. J., Oct 64, pp. 531s-534s.

24. WHITE, S, "EXPERIMENTAL DETERMINATION OF DIMENSIONAL HEAT FLOW IN WELDMENTS," Weld. J., Jul 61, p. 317s.

25. ADVANCES IN HEAT TRANSFER, "FILM AND TRANSITION BOILING," Jordan, D.P, Academic Press, N. Y., 1968, pp. 5s-128.

26. UNDERWATER CUTTING AND WELDING MANUAL, NAVSHIPS 250-692-91, Wash., D.C., 1954.

27. WELLS, A, "HEAT FLOW IN WELDING," Weld. J., Vol. 31, 1952, pp. 263s-267s.

Thesis
S6778 Staub 127253
Temperature distribu-
tion in thin plates
welded underwater.